

Copyright Undertaking

This thesis is protected by copyright, with all rights reserved.

By reading and using the thesis, the reader understands and agrees to the following terms:

- 1. The reader will abide by the rules and legal ordinances governing copyright regarding the use of the thesis.
- 2. The reader will use the thesis for the purpose of research or private study only and not for distribution or further reproduction or any other purpose.
- 3. The reader agrees to indemnify and hold the University harmless from and against any loss, damage, cost, liability or expenses arising from copyright infringement or unauthorized usage.

IMPORTANT

If you have reasons to believe that any materials in this thesis are deemed not suitable to be distributed in this form, or a copyright owner having difficulty with the material being included in our database, please contact lbsys@polyu.edu.hk providing details. The Library will look into your claim and consider taking remedial action upon receipt of the written requests.

THE INTERACTION BETWEEN BUILDINGS, GREEN SPACE, AND URBAN THERMAL ENVIRONMENTS IN A HIGH-DENSITY CITY

YU LIU

MPhil

The Hong Kong Polytechnic University

2025

The Hong Kong Polytechnic University

Department of Land Surveying and Geo-Informatics

The Interaction between Buildings, Green Space, And Urban Thermal Environments in A High-Density City

Yu Liu

A thesis submitted in partial fulfilment of the requirements for the degree of Master of Philosophy

November 2024

CERTIFICATE OF ORIGINALITY

I hereby declare that this thesis is my own work and that, to the best of my knowledge
and belief, it reproduces no material previously published or written, nor material that
has been accepted for the award of any other degree or diploma, except where due
acknowledgement has been made in the text.
(Signed)
Yu LIU (Name of student)

Abstract

Rapid urbanization dramatically changed the land surface properties, including the increase of impervious surfaces and encroachment of natural land, and thereby induced substantial thermal environment problems. Buildings and green space within built-up areas are crucial components of urban ecosystems and significantly influence the urban thermal environments. Therefore, investigating the interaction between buildings, green space, and urban thermal environment is crucial for deepening the understanding of urban ecosystems and promoting the mitigation of heat-related environmental problems.

However, due to the complexity of the interactions between buildings, green space, and urban thermal environment, there are still several unresolved issues: (1) The influence of building morphology, particularly three-dimensional building morphology, on vegetation greening has not been fully explored; (2) Previous studies have mostly examined how the size, shape, and complexity of green space affect urban thermal environment, while other important factors like height and green volume, which also play an essential role in cooling, have been overlooked on the macroscale and mesoscale; (3) Combined direct and indirect effect of 2D/3D building and green space on thermal environment have not yet been investigated.

Based on remote sensing data and LiDAR data, herein we analyzed interactions among buildings, green space, and urban thermal environments from both the 2D and 3D perspectives. This study first examined how 2D and 3D urban morphological

indexes influence vegetation greening in Hong Kong by employing Pearson correlation analysis and the boosted regression tree (BRT) model, with a focus on urban-rural differences. Then, we further investigated how 2D/3D building and green space affect urban thermal environment across multiple spatial scales employing stepwise regression and path analysis, both directly and indirectly.

In assessing the impact of 2D and 3D building morphology on vegetation greening trends, results indicated a general increase in vegetation greenness from 2010 to 2020, with a slope of 0.0024, and more pronounced greening observed in rural areas. Although the correlation between building morphology and vegetation greening was relatively weak, it remained statistically significant. The impact varied substantially between urban and rural areas and exhibited strong nonlinearity, with 3D indices exerting a greater influence than 2D indexes. The sky view factor (SVF) was the main driver in urban areas, accounting for 23.60 %, while the landscape shape index (LSI) also contributed a significant amount to rural areas (27.30%). According to marginal trends, mean building height (MBH) and SVF changed from negative to positive results. In contrast, the edge density (ED) and landscape patch index (LPI) shifted in the opposite direction. The inflection points of marginal curves of these indices varied with urban and rural areas. The landscape shape index (LSI) revealed a complex influence that changed from a negative-positive-negative pattern in urban areas and displayed a negative-to-positive pattern in rural areas. Building volume density (BVD) changed from beneficial to detrimental in urban settings, while the pattern for

rural areas was the opposite.

In analyzing the direct and indirect impacts of 2D/3D buildings and green space morphology on the thermal environment, we observed significant spatial heterogeneity and scale differences in summer LST. 2D/3D buildings and green spaces effectively enhance the explanatory power of LST variations. Notably, at the district scale, this enhancement in explanatory power was observed to be 0.038. The explanatory power of 3D indicators was found to exceed that of 2D indicators. Our analysis found that terrain had a direct negative influence on LST and concurrently exerted a stronger indirect negative effect by influencing 2D/3D buildings and green spaces, resulting in a total negative effect ranging from -0.698 to -0.615. 2D buildings not only positively affected LST but also further enhanced LST by influencing 2D/3D green spaces. On the other hand, 3D buildings negatively impacted LST and, at the pixel scale, intensified this negative effect by influencing 2D/3D green spaces. Both 2D and 3D green spaces were found to have a negative effect on LST, with the impact of 3D green space being insignificant at the district scale. The identified complicated interaction between 2D/3D buildings, green space, and urban thermal environment would enhance our understanding of the interaction mechanism of the urban ecosystem, which can also inform 2D/3D urban morphology optimization and UHI mitigation toward sustainable development.

Publications arising from the thesis

[1] **Liu, Y.,** & Weng, Q. (2025). Impacts of 2D/3D building morphology on vegetation greening trends in Hong Kong: An urban-rural contrast perspective. Urban Forestry & Urban Greening, 104, 128624.

Acknowledgements

I would like to take this opportunity to convey my sincere thanks to everyone who has helped and supported me during my MPhil.

First and foremost, I'm extremely grateful to my supervisor, Prof. WENG Qihao, for providing me with the opportunity to study in the Department of Land Surveying and Geo-Informatics at the Hong Kong Polytechnic University. His expertise and patience greatly enriched my graduate school experience. His constructive criticism prompted me to sharpen my thinking and take my research to the next level.

Moreover, I am also grateful to the Board of Examiners (BoE) for my oral examination, and they are Prof. REN Chao and Prof. GAO Meng. I sincerely thank them for their time and constructive comments.

Additionally, I would like to thank the committee members who participated in the oral defense for the confirmation of my registration. They are Prof. DING Xiaoli and Prof. YIN Tiangang. I thank them for their valuable suggestions and kind encouragement.

Finally, I am deeply grateful to my parents and friends, who have always provided me with unconditional support! Their love and constant encouragement are sources of motivation and perseverance for me. Special thanks to the friends in my life for your companionship and support during the ups and downs of this journey. Your understanding and constant encouragement not only helped me stay focused but also brightened my days when challenges seemed overwhelming.

Table of contents

CERTIFICATE OF ORIGINALITY I
ABSTRACTII
PUBLICATIONS ARISING FROM THE THESISV
ACKNOWLEDGEMENTSVI
TABLE OF CONTENTSVII
LIST OF TABLESXI
LIST OF FIGURESXII
NOMENCLATUREXV
CHAPTER 1. INTRODUCTION1
1.1 RESEARCH BACKGROUND1
1.2 RESEARCH OBJECTIVES5
1.3 STRUCTURE OF THE THESIS6
CHAPTER 2. LITERATURE REVIEW7
2.1 Overview
2.2 Urbanization-induced alterations in building, green space, and urban
THERMAL ENVIRONMENTS7
2.3 RELATIONSHIP BETWEEN BUILDING AND GREEN SPACE
2.4 Relationship retween billiding and libran thermal environments 12

2.5 RELATIONSHIP BETWEEN GREEN SPACE AND URBAN THERMAL ENVIRONMENTS 14
2.6 Development in related studies in subtropical high-density regions 15
2.7 URBAN-RURAL DIFFERENCES AND SCALE EFFECTS
2.8 RESEARCH GAPS
CHAPTER 3. METHODOLOGY22
3.1 Overview
3.2 Study area
3.3 Data and pre-processing
$3.4\mathrm{Method}$ for analysis of the impacts of $2D/3D$ building morphology on
VEGETATION GREENING
3.4.1 Overall workflow
3.4.2 Detection of vegetation greening trends from 2010 to 202027
3.4.3 Delineation of urban and rural areas
3.4.4 Calculation of 2D/3D building morphology indexes
3.4.5 Analysis of the impacts of 2D/3D building morphology on vegetation
greening35
$3.5\ Method$ for analysis of the direct and indirect effects of $2D/3D$
BUILDING AND GREEN SPACE ON URBAN THERMAL ENVIRONMENTS
3.5.1 Overall workflow
3.5.2 Land surface temperature inversion based on Landsat 8 OLI images 38
3.5.3 Extraction of 2D/3D buildings, green space structure, and controlling

factors	39
3.5.4 Scale analysis	51
3.5.5 Statistical analysis	52
CHAPTER 4. IMPACTS OF 2D/3D BUILDING MORPHOLOGY O	ON
VEGETATION GREENING	55
4.1 Overview	55
4.2 Results	55
4.2.1 Spatial-temporal patterns of vegetation greening trends	55
4.2.2 Correlation between 2D/3D building morphology and vege	etation greening
trends	59
4.2.3 Impact of 2D/3D building morphology on vegetation green	ning trends61
4.3 DISCUSSION	72
4.3.1 The complexity of building morphology - vegetation green	ing relationship
	72
4.3.2 Differences in urban and rural greening mechanism	75
4.3.3 Policy implications	76
4.3.4 Limitations and future research directions	78
CHAPTER 5. DIRECT AND INDIRECT EFFECTS BETWEEN BU	JILDING,
GREEN SPACE, AND URBAN THERMAL ENVIRONMENTS	81
5.1 Overview	81
5.2 Results	81

5.2.1 Spatial patterns of summer land surface temperature in Hong Kong81
5.2.2 The performances of 2D/3D building and green space in explaining land
surface temperature across different scales83
5.2.3 Direct and indirect effects of 2D/3D building and green space on LST86
5.3 Discussion94
5.3.1 The necessity of introducing both 2D/3D building and green space
morphology indexes in LST-related analysis94
5.3.2 Scale-effect in the relationship between 2D/3D building, 2D/3D green
space, and LST95
5.3.3 Implications of direct and indirect effects of 2D/3D building and green
space on LST97
5.3.4 Limitations and future research directions
CHAPTER 6. CONCLUSIONS100
REFERENCES103

List of tables

Table 3.1 2D/3D building morphology metrics considered in this case study 29
Table 3.2 The explanatory variables used in this study
Table 4.1 Overall vegetation changes trends in built-up environments · · · · · · 58
Table 4.2 Features of overall vegetation changes in urban and rural areas · · · · · · 58
Table 4.3 Correlation between vegetation greening and 2D/3D building morphology
59
Table 5.1 Adjusted determinant coefficients (R ²) of stepwise multiple linear regression
86
Table 5.2 Evaluation indexes of model fit performance of path analysis at different
scales · · · · · 87
Table 5.3 Summary of the direct and indirect effects of variables on LST 93

List of figures

Figure 2.1 Potential interactions between buildings, green space, and urban thermal
environments ······21
Figure 3.1 Hong Kong as seen from GaoFen-1 high-resolution image (a), distribution
of buildings with heights (b), zoomed-in high-resolution image (c, e), and
corresponding building height data (d, f). Data sources: GaoFen-1 high-resolution
image acquired on 22 Feb 2020 from https://www.cresda.com/
Figure 3.2 The overall workflow of first case study ······ 26
Figure 3.3 Spatial distribution of 2D/3D building morphology indexes at 250m scale
32
Figure 3.4 Spatial distribution of 2D/3D building morphology indexes at 500m scale
33
Figure 3.5 Spatial distribution of 2D/3D building morphology indexes at 1000m scale
34
Figure 3.6 The overall workflow of second case study
Figure 3.7 Spatial distribution of NDBI at 30m (a), 300m (b), 600m (c), district (d) 44
Figure 3.8 Spatial distribution of NDVI at 30m (a), 300m (b), 600m (c), district (d) 44
Figure 3.9 Spatial distribution of MNDWI at 30m (a), 300m (b), 600m (c), district (d)
45
Figure 3.10 Spatial distribution of BCR at 30m (a), 300m (b), 600m (c), district (d) 45
Figure 3.11 Spatial distribution of BVD at 30m (a), 300m (b), 600m (c), district (d) 46
Figure 3.12 Spatial distribution of BSVF at 30m (a), 300m (b), 600m (c), district (d)

46
Figure 3.13 Spatial distribution of Mean_BH at 30m (a), 300m (b), 600m (c), district
(d) ······47
Figure 3.14 Spatial distribution of Max_BH at 30m (a), 300m (b), 600m (c), district
(d) ······47
Figure 3.15 Spatial distribution of GCR at 30m (a), 300m (b), 600m (c), district (d) 48
Figure 3.16 Spatial distribution of GVD at 30m (a), 300m (b), 600m (c), district (d) 48
Figure 3.17 Spatial distribution of GSVF at 30m (a), 300m (b), 600m (c), district (d)
49
Figure 3.18 Spatial distribution of Mean_GH at 30m (a), 300m (b), 600m (c), district
(d) · · · · · · 49
Figure 3.19 Spatial distribution of Max_GH at 30m (a), 300m (b), 600m (c), district
(d) · · · · · 50
Figure 3.20 Spatial distribution of DEM at 30m (a), 300m (b), 600m (c), district (d) 50
Figure 3.21 Spatial distribution of Slope at 30m (a), 300m (b), 600m (c), district (d) 51
Figure 4.1 Spatial pattern of vegetation greenness changes trend at 250m (a), 500m
(c), and 1000m (e) scales, and greenness change slope at 250m (b), 500m (d), and
1000m (f) scales
Figure 4.2 Relative contributions (%) of 2D/3D building morphology to vegetation
greening trends in urban and rural areas at 250m scale · · · · · · 62
Figure 4.3 Relative contributions (%) of 2D/3D building morphology to vegetation
greening trends in urban and rural areas at 500m scale

Figure 4.4 The marginal effect of 2D/3D building morphology on the vegetation
greening in urban areas at 250m scale ······ 66
Figure 4.5 The marginal effect of 2D/3D building morphology on vegetation greening
in rural areas at 250m scale 67
Figure 4.6 The marginal effect of 2D/3D building morphology on the vegetation
greening in urban areas at 500m scale ····· 69
Figure 4.7 The marginal effect of 2D/3D building morphology on vegetation greening
in rural areas at 500m scale······71
Figure 5.1 Spatial distribution of summer LST in Hong Kong at 100m (a), 300m (b),
600m (c), and district scale (d)
Figure 5.2 Path analysis of terrain, 2D/3D building/green space, and LST at 300m
scale
Figure 5.3 Path analysis of terrain, 2D/3D building/green space, and LST at 600m
scale
Figure 5.4 Path analysis of terrain, 2D/3D building/green space, and LST at district
scale

Nomenclature

List of abbreviations

Abbreviation	Full Name
UHI	Urban Heat Island
SUHII	Urban Heat Island Intensity
2D	Two-Dimensional
3D	Three-Dimensional
LST	Land Surface Temperature
BRT	Boosted Regression Tree
LCM	Land Change Modeler
MSPA	Morphological Spatial Pattern Analysis
PLAND	Percentage of Landscape
SHDI	Shannon's Diversity Index
AI	Aggregation Index
FAI	Frontal Area Index
SC	Shape Coefficient
PCA	Principal Component Analysis
GWR	Geographically Weighted Regression
SMLR	Stepwise Multiple Linear Regression
RF	Random Forest
CNN	Convolutional Neural Networks

PD Patch Density

EVI Enhanced Vegetation Index

DSM Digital Surface Model

DTM Digital Terrain Model

MK Mann-Kendall

LPI Largest Patch Index

BCR Building Coverage Ratio

LSI Landscape Shape Index

ED Edge Density

BVD Building Volume Density

SVF Sky View Factor

MBH Mean Building Height

FAR Floor Area Ratio

TPU Tertiary Planning Unit

NDBI Normalized Difference Built-Up Index

NDVI Normalized Difference Vegetation Index

MNDWI Modified Normalized Difference Water Index

BCR Building Coverage Ratio

BVD Building Volume Density

BSVF Building Sky View Factor

Mean_BH Mean Building Height

Max_BH Maximum Height of Buildings

GCR Green Space Coverage Ratio

GVD Green Space Volume

GSVF Green Space Sky View Factor

Mean_GH Mean Green Space Height

Max_GH Maximum Green Space Height

SL Slope

LAT Latitude

PA Path Analysis

GFI Goodness of Fit Index

RMSEA Root Mean Square Error of Approximation

RMR Root Mean Square Residual

CFI Comparative Fit Index

NFI Normed Fit Index

NNFI Non-Normed Fit Index

List of variables

Variable	Description	Unit
n	The number of buildings within a spatial unit	/
Sg	The total area of the spatial unit	m^2
Ai	The area of the ith building	m^3
Pi	The perimeter of the ith building	m
Vi	The volume of the ith building	m^3
Hi	The height of the ith building	m
c	The number of floors of ith building	/
θ	The wind direction angle	0
GAi	The area of the ith green space	m^2
GVi	The volume of the ith green space	m^3
GHi	The height of the ith green space	m
Уa	The horizontal project coordinates of point A	/
Уь	The horizontal project coordinates of point B	/
Xa	The vertical project coordinates of point A	/
Xb	The vertical project coordinates of point B	/
τ	Atmospheric transmittance	

Chapter 1. Introduction

1.1 Research background

The rapid urbanization process, changing natural landscapes with built-up environments, has brought many complex changes to urban ecosystems over the past half century (He et al., 2019; Yang and Huang, 2021). Among them, buildings and green spaces have undergone significant variations (Luo et al., 2021). Buildings have expanded outwards and upwards, becoming taller and more densely packed (Frolking et al., 2024; Mahtta et al., 2019). Green space coverage has decreased and fragmentation has increased. These changes have had significant effects on the microclimate and surface energy balance, including lowering albedo and latent heat flux, lowering solar radiation absorption and sensible heat flux, and contributing to many urban thermal issues (Wang et al., 2021; Wang et al., 2016). The worsening of the urban thermal environment has posed a major risk to environmental quality and public health (Wong et al., 2017). For instance, it has been demonstrated that UHI is associated with significant heat-related mortality, particularly when extreme heat events occur (Cuerdo-Vilches et al., 2023; Ho et al., 2023). The heat-related mortality burden is predicted to increase in the future due to the ongoing degradation of the thermal environment (Esper et al., 2024; Masselot et al., 2025; Shahmohamadi et al., 2011). To develop effective strategies to address thermal problems and the associated negative effects, it is necessary to investigate the interactions between buildings, green space, and the thermal environment.

Green spaces are critical components of terrestrial ecosystems. They perform vital functions including a role in carbon sequestration, hydrological regulation, and energy flow maintenance (Ballantyne et al., 2017; Haberl et al., 2007). Recent research demonstrates that vegetation has experienced dynamic transformations. Research has demonstrated that enhanced vegetation greenness significantly contributes to temperature regulation and microclimate mitigation (Baniya et al., 2019; Chen et al., 2021; Zeng et al., 2017). A recent study found that vegetation greening can significantly cool cities (Li et al., 2025). Analyzing vegetation changes over time and influencing factors helps cities develop better green space plans to reduce heat. Compared to natural landscapes, vegetation growth in built-up areas faces more complex challenges and is affected by many different factors (Liu et al., 2023). Although extensive research has examined vegetation responses to natural and anthropogenic factors (Fan et al., 2023; Li et al., 2020), the role of building morphology in influencing greening trends remains understood. Building morphology can influence ambient temperature (Azhdari et al., 2018; Han et al., 2023; Li and Hu, 2022), airflow patterns such as wind speed and direction (He et al., 2022; Zahid Igbal and Chan, 2016), the spatial distribution of light and shading (Tan and Ismail, 2015; Wang et al., 2024; Wu et al., 2024), and humidity levels (Cao et al., 2021; Kamal et al., 2021). The above-mentioned factors strongly influence vegetation growth by regulating physiological processes such as transpiration, photosynthesis, and metabolic activity (Chang et al., 2021; Rawson et al., 1977; Serbin et al., 2015).

Understanding how building morphology affects vegetation growth is crucial for understanding its underlying mechanisms and enhancing its potential to alleviate urban heat.

Building morphology influences urban thermal environments by altering shading and modification of heat capacity, reflection, absorption, and ventilation (Adelia et al., 2019; Kotharkar et al., 2023). The impacts of building morphology on urban thermal environments have been widely studied from horizontal and vertical perspectives (Khoshnoodmotlagh et al., 2021; Yang et al., 2021). For example, Huang et al. (Huang and Wang, 2019) proved that a dispersed and high-rise buildings layout can reduce LST. Chen et al. (Chen et al., 2022) showed that building morphology-LST interaction is seasonal dependent. Green spaces are also vital to alleviate heat by providing canopy shading, absorbing heat, and facilitating heat loss through evaporative processes. From existing knowledge, there is a significant negative connection between heat environments and green space coverage (Basu and Das, 2023; Yang et al., 2017; Yao et al., 2020). The size, shape, connectivity, and complexity of green spaces were also highly correlated with the heat condition (Lin et al., 2023; Maimaitiyiming et al., 2014; Masoudi and Tan, 2019). For instance, Du et al. (Du et al., 2017) showed that the landscape shape index (LSI) of green space has a negative influence on LST and the high complexity of green space could reduce LST. However, heat conditions are simultaneously affected by building and green spaces in practice, and their interaction is generally complex (Yuan et al., 2021; Zhang et al.,

2022). Thus, the effects of buildings or green space on the thermal environment are a combination of direct impacts (e.g., immediate effects of specific factors) and indirect impacts (where an influencing factor affects the thermal environment by influencing other elements). Identifying the direct and indirect impacts of building and green spaces on thermal conditions would inform building and green space optimization toward effective and efficient heat mitigation.

Scale effects are commonly observed in geographic contexts, including both natural and social environments (Šímová and Gdulová, 2012; Turner et al., 1989). Analysis of landscape patterns and driving factors at different scales can lead to distinct assessment results, affecting the scientific understanding and generalization of arguments (Guo et al., 2025; Jia et al., 2024). Some studies have confirmed that the relationship between LST and affecting elements also exhibits scale effects (Chen et al., 2023; Jia et al., 2024). According to Estoque et al. (Estoque et al., 2017), the association between building density and LST appears to strengthen at coarse scales, while at fine scales the connection between green space coverage and LST increases. Consequently, the scale effect is an essential aspect that should be thoughtfully addressed when examining urban thermal environments and their driving factors.

Moreover, effective solutions for the mitigation of the urban thermal environment may benefit from insights gained from multiple spatial scales.

1.2 Research objectives

Hence, the overarching aim of this study is to examine the interaction between buildings, green space, and urban thermal environments.

This study first employs boosted regression tree (BRT) models to quantify the relative importance and marginal effects of 2D and 3D building morphology on vegetation greening in Hong Kong between 2010 and 2020, with a particular focus on urbanrural disparities. Detailed objectives of the first case study are threefold: 1) to characterize the spatiotemporal patterns of vegetation greening and examine urbanrural variations during the 2010–2020 period; 2) to evaluate the relative contributions and marginal effect of 2D and 3D building morphology on vegetation greening; and 3) to compare how these building morphology indexes influences differ between urban and rural settings. The findings are expected to enhance our understanding of how built environment characteristics shape vegetation dynamics over time. Second, this study utilizes stepwise regression and path analysis to assess the direct and indirect impact of both 2D/3D buildings and green space on summer LST at different spatial scales in Hong Kong. Specific objectives of the second case study are: 1) to investigate the differences of spatial patterns in the summer LST across various scales (pixel scales and district scale); 2) to assess the performances of 2D/3D building and green space in explaining LST variations at different scales employing the stepwise regression model; 3) to untangle the direct and indirect impacts of 2D/3D

building and green space on LST across multi-scales using path analysis. This study

would provide scientific support for the design of building and green space structures aimed at efficient climate mitigation and adaptation at both pixel and district scales.

1.3 Structure of the thesis

This thesis is structured into six chapters. In this chapter, the research background, research aim, and specific objectives have been demonstrated. The rest of the thesis comprises the literature review about the interaction of buildings, green space, and urban thermal environments, the methodology for two case studies, the main findings concluded from two case studies, discussion, conclusions, and suggestions for future research. Specifically, the subsequent chapters of this thesis are organized as follows: In Chapter 2, the literature on the relationship between buildings, green space, and urban thermal environments is reviewed. Besides, research gaps are pinpointed. In Chapter 3, this thesis presents the methods for data retrieval and processing regarding the investigation of the impact of 2D and 3D building morphology on vegetation growth, and the analysis of the direct and indirect impact of 2D/3D buildings and green spaces on LST. In Chapter 4, the preliminary results and analysis, and discussion part of the impact of 2D/3D building morphology on vegetation growth are presented. Limitations of the first study and suggestions for future study are also presented. In Chapter 5, this thesis provided the results and discussion of the direct and indirect influences of 2D/3D building and green space on LST. The limitations and recommendations for future research are also discussed. In Chapter 6, this thesis concludes key findings are reported.

Chapter 2. Literature review

2.1 Overview

Previous research on the interaction of buildings, green space, and urban thermal environments is comprehensively examined in this chapter. Urbanization-induced changes in buildings, green space, and urban thermal environments are summarized (Section 2.2). The associations between building and green space, building and LST, and green space and LST are also reviewed in this chapter (Section 2.3, 2.4, 2.5). Development in related studies in subtropical high-density regions is reported (Section 2.6). This chapter also provides an overview of urban-rural differences and scale effects existing in buildings, green space, and urban thermal environments (Section 2.7). Drawing from the review of existing literature, critical research gaps are pinpointed and outlined (Section 2.8).

2.2 Urbanization-induced alterations in building, green space, and urban thermal environments

The world has undergone rapid urban expansion over the last three decades (Antrop, 2004; Streule et al., 2020). Accelerated urbanization is leading to significantly sophisticated and diverse changes to land cover and ecosystems (Oke, 1982). The urbanization process is generally accompanied by the expansion of impervious surfaces, increasing population, and encroachment of natural surfaces (Byomkesh et al., 2012). The largest contributor to the increase in impervious surface is building growth, while green space loss is the dominant change in the natural surface (Li et al.,

Under rapid urbanization, buildings have experienced multi-dimensional changes (Reba and Seto, 2020; Xu and Chi, 2019). The typologies of building evolution in the process of urbanization are primarily categorized as: (1) outward and infilling expansion, and these expansions contribute to increased building density, enhanced connectivity between buildings, and a more compact urban environment (Yang and Zhao, 2022). It is claimed that many urban areas witnessed two dynamic types of urbanization: expansive built-up areas through leapfrog development and infill development, accompanied by substantial population growth (Tian et al., 2022); (2) upward expansion, which results in an increase of high-rise buildings. For example, a recent study has highlighted a significant trend in global urban development, presenting a notable transition from urban expansion towards vertical construction (Frolking et al., 2024); (3) Complexification, the urban development requires a diverse range of functions from buildings, leading to increased complexity in building morphology and structures (Wang et al., 2022).

Dramatic urban development also directly imposes pressures on the shape, morphology, and spatial distribution of green spaces, which includes the encroachment of original green spaces due to outward urban expansion, as well as the fragmentation and lower connectivity caused by the dense distribution of buildings.

By selecting 107 representative cities in China, Wu et al. (Wu et al., 2021) pointed out that newly urbanized areas exhibit an extensive browning impact. According to Zhou

et al. (Zhou and Wang, 2011), the sprawl of built-up areas has resulted in the reduction of green space. Similarly, Nor et al. (Nor et al., 2017) utilized the land change modeler (LCM)-Markov chain models and indicated that the present and future urban expansion can both exert a negative effect on the green space structure. These urbanization-induced land surface changes significantly alter urban ecology and microclimate (Chakraborty and Qian, 2024; Huang et al., 2024). Building materials used in built-up environments (such as concrete, bricks, and asphalt) increase sensible heat flux and altered albedo, which can absorb solar radiation in the daytime and delay heat dissipation at night (Luyssaert et al., 2014; Ouyang et al., 2022). High-density and complex building areas restrict air circulation and weed speed, making it difficult for heat dissipation (Liao et al., 2021; Yuan et al., 2020). Shrinkage of green space reduces the release of moisture and shade through evapotranspiration, decreases latent heat flux, and thereby impairing the cooling effects of green spaces (Oliveira et al., 2011). These changes pose significant challenges to the urban thermal environment, with urban heat islands (UHI) and heat waves being the most emblematic signal (Ferguson and Woodbury, 2007; Livermore et al., 2018; Russo et al., 2014). UHI describes the phenomenon whereby urban areas exhibit higher air and surface temperatures compared to their surrounding rural counterparts (Oke, 1982). Heatwaves are defined as periods during which a region experiences abnormally and uncomfortably temperatures (IPCC, 2021). Furthermore, the UHI and heat waves have mutual effects and tend to intensify each other (Founda and Santamouris, 2017; Li et al., 2015). These urbanization-induced heat problems are increasing the number of people exposed to health-threatening heat (Li and Zha, 2020; Liu et al., 2017). In recent decades, the extent of exposure has increased threefold, significantly exceeding the estimated level in earlier research (Tuholske et al., 2021). Therefore, urbanization-induced thermal problems, such as UHIs and heat waves, are becoming severe threats to the urban climate and human health. Moreover, their adverse effects are projected to intensify in the future (Guo et al., 2017).

2.3 Relationship between building and green space

The expansion of built-up areas during the urbanization process has led to a reduction in overall green space coverage and increased fragmentation of its spatial structure.

Hence, the ecosystem service function and cooling effect of green space on heat mitigation have been significantly weakened.

Firstly, considerable effort has been devoted to investigating the response of green space coverage to the urbanization process (Haaland and Van Den Bosch, 2015; Shahtahmassebi et al., 2021; Zhao et al., 2013). Understanding the relationship between green space and urbanization is crucial for green space management toward the mitigation of the urban thermal environment. For example, taking Kunming as the study area, Zhou et al. (2011) revealed that the rapid growth of built-up areas continuously encroached on the agricultural land, forests, and grasslands from 1992 to 2009 (Zhou and Wang, 2011). Several studies have reported that urban development has been widely associated with the reduction of green space. For instance, Siddique

et al. (2022) suggested that 51.32 km² of green spaces were changed into built-up areas from 1990 to 2020 in Chattogram (Siddique and Uddin, 2022). Moreover, urbanization is expected to increasingly exert a force on green areas with further urban expansion (Zhao et al., 2013). At the same time, it is further suggested that green areas are a stimulus for driving building sprawling explicitly (Koprowska et al., 2020; Zhou et al., 2024).

Moreover, in the previous research, it was established that buildings are significant elements of the regulation of the spatial pattern of urban green areas by correlation and regression analysis methods (Canedoli et al., 2018; Masoudi et al., 2021; Nor et al., 2017). It was noted by Wu et al. (Wu et al., 2019) that the configuration of green space stretched less irregularly during the process of urbanization. However, Zhao et al. (2013) (Zhao et al., 2013) established an expansion and an aggregation of green areas in China. According to landscape ecology theory, fragmentation is the state of dividing consistent ecological land, vegetated land, and habitat into smaller isolated units called patches (Fan and Myint, 2014). Jiao et al. (Jiao et al., 2017) observed that between 1989 and 2013, a period when green space fragmentation became more extensive, trends indicated a declining gradient with the distance from the city center. With the morphological spatial pattern analysis (MSPA), Rogan et al., 2016) evaluated the town-scale forest fragmentation in Massachusetts, United States, and found that urbanization not only caused green space fragmentation but also influenced spatial continuity among patches of green space.

Some studies also indicated that the built-up environment may foster vegetation growth in green spaces (Jia et al., 2018; Zhang et al., 2023). Zhao et al. (Zhao et al., 2016) found that 86% of regions across 32 major Chinese cities experienced vegetation enhancement. According to Jia et al. (Jia et al., 2018), 92.9% of the chosen 377 areas in America have increased vegetation growth. Further, Li et al. (2024) revealed that the built-up land index has a significant influence on vegetation growth, such as percentage of landscape (PLAND) and largest patch index (LPI). However, it is still relatively underexplored how the three-dimensional building morphology index acts on vegetation growth within green space.

2.4 Relationship between building and urban thermal environments

Buildings have a strong influence on the thermal properties of the underlying surfaces by reducing latent heat flux and increasing sensible heat flux, thus creating a fundamental driving factor affecting the urban thermal environment. Much research has been carried out to reveal how buildings affect the thermal environment. It has been suggested that buildings have a considerable effect on air temperature (Lan and Zhan, 2017), land surface temperature (Chen et al., 2020), UHI (Li et al., 2020), extreme heat (Nahlik et al., 2017), and heatwaves (Ji et al., 2022).

Several building morphology indexes have been found to greatly impact the urban thermal environment (Han, 2023; Li and Cheng, 2024). Early studies of building morphology's effect on the thermal environment mainly focus on the 2D perspective.

2D building morphology indicators include the aggregation index (AI), building

density (BD), Shannon's diversity index (SHDI), building landscape patch index (LPI), edge density (ED), contagion index (CI), patch cohesion index (COHESION), and landscape shape index (LSI) (Guo et al., 2015; Li et al., 2011, 2016; Yuan et al., 2021; Zhang et al., 2023). Recently, scholars have concentrated on studying the relationship between 3D building morphology and the urban thermal environment. The selected 3D building morphology indices included mean building height (MBH), sky view factors (SVF), building volume density (BVD), floor area ratio (FAR), frontal area index (FAI), and shape coefficient (SC) (Hu and Wendel, 2019; Huang and Wang, 2019; Qiao et al., 2020; Yuan et al., 2024). Tian et al. (Tian et al., 2019) reported that the volumes of buildings and the cluster spacing have effects on LST. Wu et al. (Wu et al., 2022) proved that 3D building morphology has a great impact on the surface heat island intensity. Huang and Wang (Huang and Wang, 2019) revealed that building heights affected UHI effects by altering wind speed and heat emission. A series of statistical methods have been used in previous research to explore the relationship between urban morphology and urban thermal conditions. Chen et al. (Chen et al., 2014a) conducted cluster analysis, principal component analysis (PCA), and linear regression model to explore key influencing morphology indicators of LST. Yu et al. (Yu et al., 2021) employed a geographically weighted regression (GWR) model to determine the effect of vertical urban morphology on UHIs in the summertime. Many researchers try to use the stepwise multiple linear regression (SMLR) model, which involves the selection of the best candidate set of independent

variables to predict the response variables (Yin et al., 2018; Zhou et al., 2017). However, the SMLR model is unable to estimate individual contributions from variables while the recognition of nonlinear associations between multi-dimensional indicators (Hu et al., 2020). In contrast, the boosted regression trees (BRT), eXtreme gradient boosting (XGBoost), random forest (RF), and convolutional neural networks (CNN) enable the detection of nonlinear relationships (Belgiu and Drăguţ, 2016; Logan et al., 2020; Peng et al., 2021). Shen et al. (Shen et al., 2022) tested the correlation between surface urban heat island intensity (SUHII) and 2D morphology indicators by SMLR and RF models, concluding that the latter was more effective (R² = 0.80) than the SMLR model (R² = 0.75). In addition, Logan et al. (Logan et al., 2020) reviewed both linear and non-linear models and showed that all the non-linear models outperformed their linear counterparts significantly.

2.5 Relationship between green space and urban thermal environments

The cooling effects of green spaces were widely acknowledged by various studies (Asgarian et al., 2015; Cheung et al., 2022; Ren et al., 2016). Green spaces can change the thermal environment with mechanisms like evapotranspiration, canopy shading, and the selective absorption and reflection of solar radiation (Bowler et al., 2010; Wong and Yu, 2005).

In particular, the coverage of green spaces plays a positive impact on its cooling effect (Du et al., 2017). It is reported that the cooling effect of green spaces varies

depending on their spatial morphology (Kong et al., 2014; Li et al., 2013). Some empirical evidence has revealed that the composition and configuration of green spaces are important in shaping the thermal environment (Chen et al., 2014b; Xu et al., 2025). The indexes included total area (TA), percent of landscape (PLAND), patch density (PD), largest patch index (LPI), edge density (ED), area-weighted mean shape index (SHAPE_AM), area-weighted fractal dimension index, landscape shape index (LSI) (Berger et al., 2017; Ke et al., 2021; Zhou et al., 2022; Zhou et al., 2017). Guo et al. (Guo et al., 2019) showed that UHI can be reduced not only by creating and increasing the amount of green spaces but also by optimizing the spatial configuration of these green spaces, which is more effective than the first one. By using a variety of regression methods, Li et al. (Li et al., 2012) identified PLAND as the primary influencing factor of LST. However, much less effort has been devoted to the influence of the 3D green space index on thermal environments.

2.6 Development in related studies in subtropical high-density regions

Urbanization and continuing global warming trends have triggered substantial thermal problems in many regions around the world, especially in subtropical high-density regions (Lau et al., 2019; Shi et al., 2016; Tan et al., 2017). In the subtropical high-density regions, the local climate is typified by excessive warmth, high humidity, and excessive solar radiation, resulting in the retention of excessive heat and moisture (He et al., 2023). The densely distributed high-rise buildings lead to compact and narrow urban settings, which restricts natural ventilation and hinders effective heat

dissipation (He et al., 2022).

Some of these subtropical high-density cities are experiencing severe thermal problems (Giridharan et al., 2004; Tian et al., 2013; Yee and Kaplan, 2022; Zhang and Yuan, 2023). Thermal problems experienced in subtropical high-density cities were more frequent and intense than elsewhere (Aflaki et al., 2017; Fu et al., 2025; Yue et al., 2019). He et al. (He et al., 2023) suggested that Hong Kong experienced a large increase in compound hot-wet events from 1961 to 2020 in the territory. The intensity and occurrence of extreme heat events have been on the rise. Jiang et al. (Jiang et al., 2021) found that the night-time minimum temperatures in Singapore have increased significantly between 1982 and 2018.

Building, green space, and thermal environment relationships in subtropical high-density cities have attracted considerable interest (Giridharan et al., 2007; Giridharan and Emmanuel, 2018; Jia et al., 2024; Xu et al., 2017). Building and green space morphology have been identified as significant factors that affect the heat problem in subtropical high-density cities in prior studies (Chen et al., 2023; Li et al., 2022), with the sky view factor regarded by most studies as the primary influencing factor (Xu et al., 2024).

As in other areas, green space is a favorable element to relieve the heat in subtropical high-density cities (Ng et al., 2012; Ouyang et al., 2024). Green space growth (e.g., more urban trees and street vegetation) is usually unrealistic because there is no spare space in dense cities to increase areas of green space (Tan et al., 2013; Tian et al.,

2012). Numerous investigations have proved that synergistic design of green corridors with the buildings, vertical and rooftop greening, together with the modification of the existing green space spatial pattern, are more applicable for subtropical high-density regions (Li et al., 2023; Tan, 2006). Moreover, the role of green space quantity and the spatial structure of green space in the thermal environment of subtropical high-density cities was investigated by some previous studies (Bai et al., 2024; Guo et al., 2019; Xu et al., 2022). Masoudi et al. (Masoudi et al., 2019) investigated the effect of spatial patterns on the cooling effect of green space in Singapore and Hong Kong. They indicated that patch density (PD), mean Euclidean nearest neighbor distance (ENN_MN), percentage of landscape (PLAND), area-weighted mean shape index (SHAPE AM), and PD are key factors for LST.

Hong Kong, as a typical high-density subtropical city, has attracted plenty of attention to this research field of interaction between buildings, green space, and urban thermal environments. Some studies have been conducted on the spatiotemporal characteristics of UHI, heatwaves, LST, and air temperature in Hong Kong (Chen et al., 2024; Galdies and Lau, 2020; Hua et al., 2021; Li et al., 2023; Liu and Zhang, 2011; Nichol et al., 2009; Wang et al., 2016; Zheng et al., 2023). Overall, scholars have reported that the thermal environment in Hong Kong has degraded due to human activities and climate change. The Hong Kong Observatory collects data showing that the annual average temperature increase of about 0.12 degrees per decade from 1886 to 2015 (The Hong Kong Observatory, 2016). Studies also reveal a great interest in

building morphology and its impact on the thermal environment in Hong Kong (Ren et al., 2020; Wu et al., 2024; Xu et al., 2017). Jia and Wang (Jia and Wang, 2021) argued that urban cooling techniques should include the building form. Li et al. (Li et al., 2023) studied about association of 2D/3D building morphology with air temperature and it was found that SVF was the largest contributor to the variation in air temperature. There have been significant studies about design measures of green space to provide an effective cooling effect in Hong Kong. Tan et al. (Tan et al., 2016) reported that the SVF should be considered during the design of green space in Hong Kong. Kong et al. (Kong et al., 2017) verified that the trees in high-density urban areas were more efficient for reducing LST compared with those in sparse areas.

2.7 Urban-rural differences and scale effects

Spatial heterogeneity both in greening and the urban thermal environment across urban and rural areas was reported in previous studies (Ji et al., 2023; Jia and Zhao, 2020; Yao, 2024). Li et al. (Long Li et al., 2023) discussed a noticeable "V-shaped" distinction in the pattern of greenness variation between the urban and rural regions. Considerable differences in vegetation density between urban and rural regions also created notable temperature differences, which formed the core of the UHI effect (Chen et al., 2021; Gallo and Tarpley, 1996; Heinl et al., 2015). In addition, the urban and rural areas are very different in terms of land surface characteristics, climatic conditions, vegetation composition, community or built environment configuration, and human activities (Jia et al., 2021; Wang et al., 2024). These differences could lead

to many distinct interactions between buildings, green infrastructure, and the thermal environment. Therefore, they necessitate practice-specific planning and management strategies tailored to urban, and rural environments.

The statistical distributions of geographic processes and variables (such as mean, variance, and relationships among multi-variables), the spatial patterns of geographic phenomena (spatial heterogeneity, spatial correlations among different variables), and the relationships among evolutionary processes and their influencing factors may all exhibit scale effects. Zhang et al. (Zhang et al., 2023) stated that the building density index is the most influential factor for LST at the block scale in Chinese megacities. Han et al. (Han et al., 2023) presented that 2D indicators showed a stronger impact on LST in warmer seasons, while Ezimand et al. (Ezimand et al., 2021) argued that 3D urban structures can better explain the changes in LST than 2D structures. This inconsistency in the literature suggests the need for multi-scale studies with different indicators to provide more evidence that supports drawing general conclusions.

2.8 Research gaps

Many studies have analyzed the relationship between buildings, green space, and the urban thermal environment at various scales using different approaches. However, due to the complex interactions of buildings, green space, and urban thermal environment, there remain some issues that need to be addressed:

(1) The effect of building morphology, especially that of 3D buildings, on vegetation greening in green space remains underexplored. Previous studies have

only examined the relationship between vegetation greening and 2D building morphology (L. Zhang et al., 2022; Zhao et al., 2016; W. Zhou et al., 2023). For example, Li et al. (Li et al., 2024) analyzed the nonlinear effects of horizontal built-up land patterns on vegetation growth in Kunming. However, 3D building morphology significantly influences local microclimates (Salvati et al., 2019; Yang et al., 2023), an aspect that remains largely neglected in current research on vegetation greening.

- (2) Moreover, while urban and rural areas differ greatly in their building and vegetation contexts, the differences in the influence of 2D/3D building indexes on vegetation greening across urban and rural settings have not been studied.
- (3) The individual influence of buildings and green space morphology on the thermal environment has been investigated extensively. After summarizing the available literature, we concluded the potential interaction between buildings, green space, and urban thermal environment (Figure 2.1). However, we found that there is a lack of research on direct and indirect interaction between buildings, green space, and urban thermal environments from horizontal and vertical perspectives, especially at multiple scales (like pixel scale and district scale).
- (4) 3D green space landscape pattern was ignored in macroscale and mesoscale analysis. Only a few studies have examined 3D green space patterns based on onsite measurement data, whose limited spatial coverage and representativeness hinder a thorough understanding of the relationship between buildings, green space, and thermal environments. Previous macroscale and mesoscale analysis

have mainly centered on the effects of two-dimensional (2D) features of green spaces on the urban thermal environment, while other important factors like height, which also serve a significant function in cooling, have been overlooked.

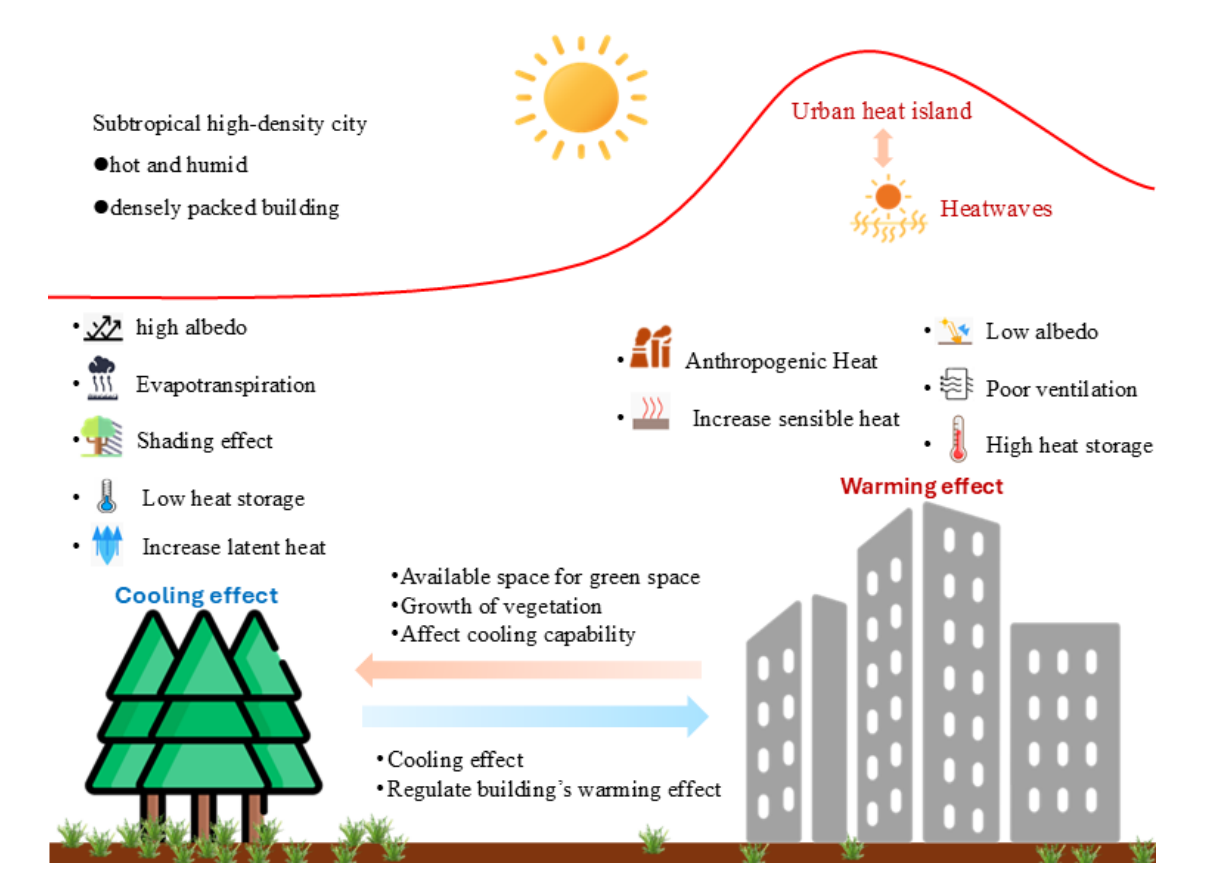


Figure 2.1 Potential interactions between buildings, green space, and urban thermal environments

Chapter 3. Methodology

3.1 Overview

This chapter presents the study areas and outlines the data sources, along with the methods for data retrieval and processing. It also gives a full introduction and description of the research methods, which are categorized into five categories: (1) Study area (Section 3.2); (2) Data and pre-processing (Section 3.3); (3) Method for the analysis of the impact of 2D/3D building morphology on vegetation greening (Section 3.4); (4) Method for the analysis of the direct and indirect effects between building, green space, and urban thermal environments (Section 3.5).

3.2 Study area

Located on the southern seaboard of China (22°08′-22°35′, 113°49′-114°31′), Hong Kong occupies an area of about 1106 km² (Figure 3.1). Hong Kong is subject to a subtropical monsoon climate, with temperate winters and summers that are typically hot, humid, and high precipitation. Hills cover more than 80% of the total area, leaving only 20% of the space available to accommodate over seven million residents. Hong Kong has experienced rapid urbanization within the context of limited land resources since the mid-19th century. This has led to the development of densely packed high-rise structures and complex building morphology, which substantially changes the local microclimate in Hong Kong. Moreover, with Hong Kong entering a mature phase of urban development, large-scale urban expansion has barely expanded since 2010. Instead, there are areas where existing buildings have remained

unchanged, with relatively fixed green space. Moreover, high-density impervious surfaces, densely populated buildings, and highly concentrated populations resulted in drastic changes in the surface structure and properties in Hong Kong. As a consequence, these factors cause a more prominent UHI effect and increased surface temperatures in Hong Kong. Therefore, Hong Kong is a beneficial area for studying the impact of buildings, green space, and urban thermal environment. By this measure, the study provides insight into other cities, particularly those that are increasingly high-density and quickly developing.

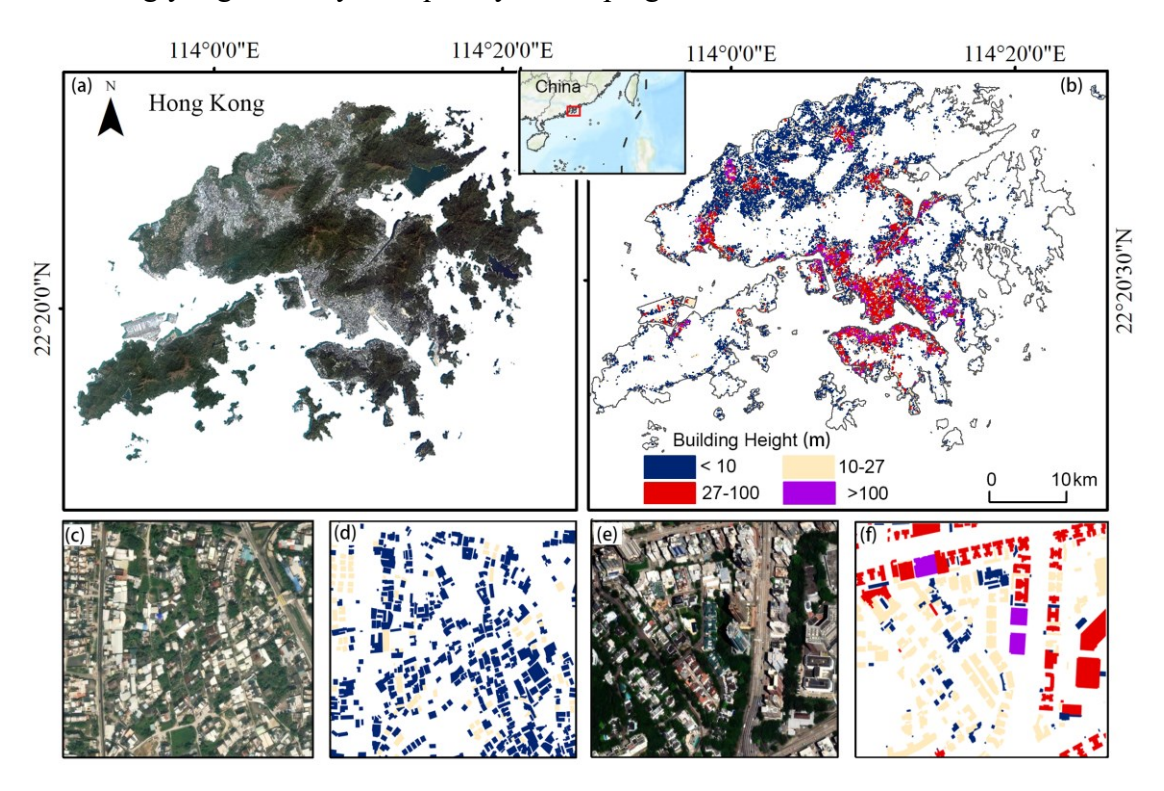


Figure 3.1 Hong Kong as seen from GaoFen-1 high-resolution image (a), distribution of buildings with heights (b), zoomed-in high-resolution image (c, e), and corresponding building height data (d, f). Data sources: GaoFen-1 high-resolution image acquired on 22 Feb 2020 from https://www.cresda.com/.

3.3 Data and pre-processing

This study analyzed Hong Kong vegetation greening trends from 2010 to 2020 using 16-day composite Enhanced Vegetation Index (EVI) data acquired from the MODIS Terra Vegetation Index Version 6 product with three spatial resolutions: 250 m (MOD13Q1), 500 m (MOD13A1), and 1,000 m (MOD13A2). The EVI has been proven more effective than others in capturing vegetation dynamics because it reduces the effects of cloud cover, atmospheric aerosols, and signal saturation (Huete et al., 2002). In this study, annual average EVI was calculated platform using monthly max composite during the growing season (June 1 to September 30 each year) for the period 2010–2020, based on the work of Ru et al. (Ru et al., 2018). Data acquisition was carried out based on the Google Earth Engine (GEE) platform with lowconfidence pixels being excluded utilizing the quality assessment (QA) layer. Building height data in 2010 and 2020 were generated using building footprint data, digital surface models (DSM), and digital terrain models (DTM) obtained from the Hong Kong Common Spatial Data Infrastructure (CSDI) platform (https://www.csdi.gov.hk/zh-hk). DSM and DTM data were generated by the light detection and ranging (LiDAR) data of 2010 and 2020. Then, by subtracting the DTM from the DSM, the first layer called normalized DSM (nDSM) will be generated for the height of the above-ground feature. Next, the building heights were determined for 2010 and 2020 by executing the zonal statistical analysis by overlaying the normalized DSM (nDSM) with the building footprint data. Finally, to avoid the

influence of changes in built-up and vegetation coverage, only areas that did not make any changes in building footprint and height during the period of 2010–2020 were selected as the unit of analysis.

Urban and rural areas in 2010 were delineated using the Global Urban Boundary (GUB) dataset, which is derived from the 30 m-resolution Global Artificial Impervious Area (GAIA) product (Gong et al., 2020). To match the spatial resolution of the EVI data, all datasets were resampled into 250 m, 500 m, and 1,000 m.

The following scenes of Landsat 8 Collection 2 Tier 1 remote sensing data were used to derive LST: row 44/column122, row 45/column122, and row 45/column121. Due to substantial cloud contamination in images during the summer in Hong Kong, the number of available images is limited. Therefore, this study selected median value composite images acquired from Google Earth Engine (GEE)

(https://earthengine.google.com/) platform date from 1 June to 30 September 2019, 2020, 2021 was to represent the summer land surface temperature in 2020. These images have a spatial resolution of 30 meters (bands 10 and 11 have a resolution of 100 meters). All data were projected in the UTM coordinate system based on the WGS84 datum. All selected pixels used for the inversion of land surface temperature had a cloud cover of less than 10%.

Green space coverage and height data in 2020 were extracted from the light detection and ranging (LiDAR) provided by the Hong Kong Civil Engineering and Development (https://www.cedd.gov.hk/eng/home/index.html). By subtracting the

DTM from the DSM, the normalized DSM (nDSM) layer was created to represent the height of the above-ground feature. Then, the vegetation height data in 2020 was generated by overlaying the green space coverage and nDSM data.

3.4 Method for analysis of the impacts of 2D/3D building morphology on vegetation greening

3.4.1 Overall workflow

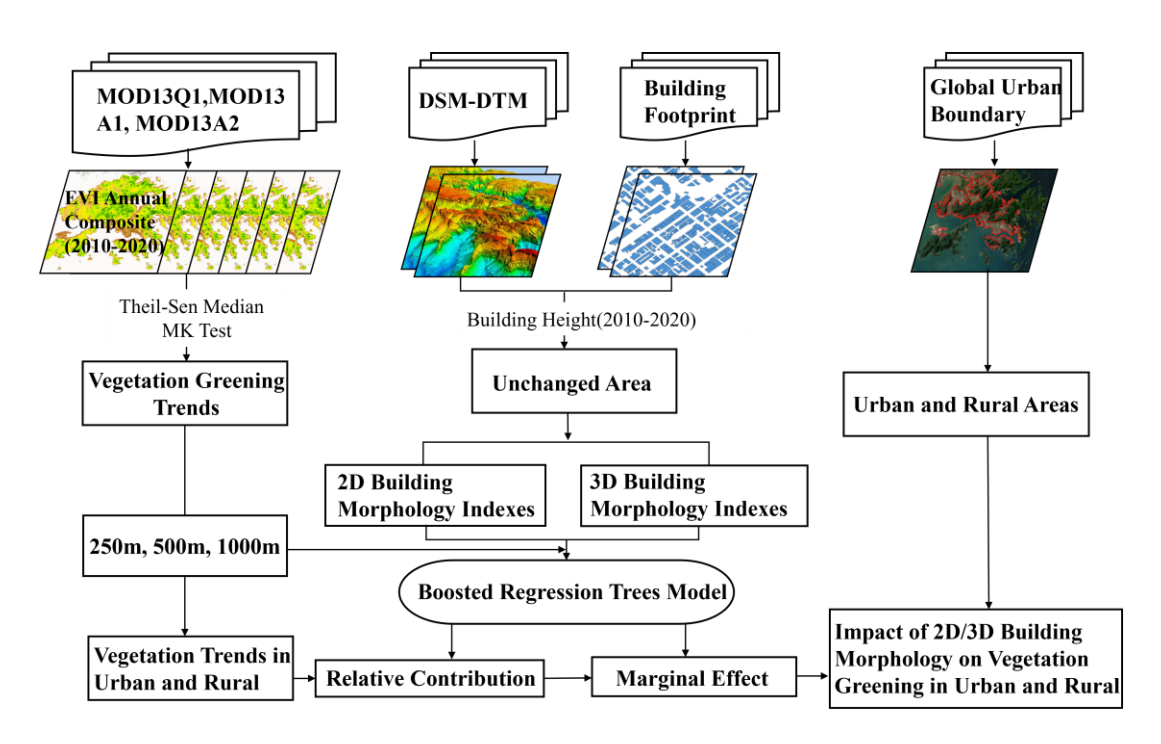


Figure 3.2 The overall workflow of the first case study

The first case study aimed to investigate the influence of 2D and 3D building morphology on vegetation greening trends across urban and rural areas in Hong Kong. The overall research workflow is presented in Figure 3.2. Initially, vegetation greening trends between 2010 and 2020 were derived. To minimize the effects of land cover changes on vegetation dynamics, areas that exhibited no variation in building

height over the study period were selected. Subsequently, static 2D and 3D building morphology indicators were calculated based on 2020 data. Finally, correlation and nonlinear analyses were conducted to assess the relationships between building morphology and vegetation greening across urban and rural areas.

3.4.2 Detection of vegetation greening trends from 2010 to 2020

In this study, vegetation greening trends from 2010 to 2020 were assessed using the Theil–Sen median method combined with the annual composite EVI data. The Theil–Sen approach is a robust nonparametric statistical method widely used for detecting monotonic trends in long-term geospatial time series. Theil–Sen median method computes the median of all possible pairwise slopes between data points, thereby reducing sensitivity to outliers. The mathematical formulation of the Theil–Sen estimator is given as follows:

$$EVI_{slope} = Median\left(\frac{EVI_b - EVI_a}{b - a}\right), 2010 < b < a < 2020$$
 (1)

where EVI_{slope} is the Theil-Sen median, EVI_b and EVI_a represent the average growing season EVI values of the years a and b. $EVI_{slope} > 0$ means a greening trend, and $EVI_{slope} < 0$ means a browning trend in vegetation.

The Mann–Kendall (MK) test was used to test the significance of the vegetation greening and browning trends. The MK test is one of the most commonly used methods for trend analysis in time series data. The test statistics are computed as follows:

$$S = \sum_{a=1}^{n-1} \sum_{b=a+1}^{n} sgn(EVI_b - EVI_a)$$
 (2)

$$sgn(EVI_b - EVI_a) = \begin{cases} +1, EVI_b - EVI_a > 0\\ 0, EVI_b - EVI_a = 0\\ -1, EVI_b - EVI_a < 0 \end{cases}$$
(3)

$$Var(S) = \frac{n(n-1)(2n+5)}{18} = \sigma^2$$
 (4)

$$Z = \begin{cases} \frac{S-1}{\sqrt{Var(S)}}, S > 0\\ 0, S = 0\\ \frac{S-1}{\sqrt{Var(S)}}, S < 0 \end{cases}$$
 (5)

where n represents the length of the EVI time series; σ is the standard deviation of the test statistic; a trend is considered statistically significant at the 0.05 level if |Z|>1.96.

3.4.3 Delineation of urban and rural areas

A binary approach was adopted for mapping urban and rural areas. The delineation was based on the Global Urban Boundary (GUB) dataset (Li et al., 2020). This was derived from the 30 m Global Artificial Impervious Area (GAIA) data, which was created using Landsat time series imagery and a machine learning algorithm. The overall accuracy of the GAIA is over 90%, so this dataset can be used reliably for global impervious surface mapping. The GUB dataset presents strong agreement with other maps made through other remote sensing approaches and manual analysis that shows it can also be used effectively for identifying urban-rural boundaries. The GUB dataset delineates urban areas as the proportion of impervious surface coverage within a given neighborhood distance exceeds 20%. Rural areas are the regions that fall outside the delineated definition of city boundaries. The GUB dataset shows great accuracy in delimiting urban extents, specifically when compared with high-resolution Google Earth images. Comparatively, other datasets (e.g., NTL-derived

urban extent) are less accurate and provide less precise urban boundary delineations, especially in areas of transition that are situated along the urban edge. Due to such advantages, GUB has been used in numerous studies on urban-rural mapping (Ji et al., 2023). This study defined urban areas as pixels located within the boundaries of the GUB dataset, while rural areas were those situated outside these delineated urban extents.

3.4.4 Calculation of 2D/3D building morphology indexes

Table 3.1 2D/3D building morphology metrics considered in this case study

Dimension	Metrics	Abbreviations	Formula	Description
2D	Largest patch index	LPI	$LPI = \frac{\max{(A_i)}}{S_g} \times 100$	Measures the percentage of the total grid area comprised of the largest patch
	Building coverage ratio	BCR	$BCR = \frac{1}{S_g} \sum_{i=1}^{n} A_i$	Measures the ratio between the total area of buildings within a grid and the total grid area
	Landscape shape index	LSI	$LSI = \frac{E}{\min E}$	Measures the degree of landscape shape complexity
	Edge density	ED	$ED = \frac{\sum_{i=1}^{n} P_i}{A}$	Measures the total lengths of all building patch edges within a grid
3D	Building volume density	BVD	$BVD = \frac{1}{S_g} \sum_{i=1}^{n} V_i$	Measures the ratio between the total volume of the buildings in a grid and the total grid area
	Sky view factor	SVF	$SVF = 2\pi \left[1 - \frac{\sum_{i=1}^{n} \sin \alpha_i}{n} \right]$	α is the vertical angle of the horizon in the direction j
	Mean building height	MBH	$MBH = \frac{\sum_{i=1}^{n} H_i}{n}$	Measures the mean height of the buildings in a grid
	Floor area ratio	FAR	$FAR = \frac{\sum_{i}^{n} (c \times A_{i})}{S_{g}}$	Measures the total building floor area compared to the land area it occupies in a grid

Note: n is the number of buildings within a grid; Sg is the total area of the grid; Ai, Pi, Vi, Hi,

c are the area, perimeter, volume, height, and the number of floors for the ith building, respectively; θ is the wind direction angle.

A range of indicators has been proposed to characterize building morphology. In this study, there were selected four 2D building morphology indexes and four 3D building morphology indexes to represent building morphology. 2D building morphology indexes included the largest patch index (LPI) (Yuan et al., 2021), building coverage ratio (BCR) (Zeng et al., 2022), landscape shape index(LSI) (Liu et al., 2017), and edge density (ED) (Zhou et al., 2011). For the 3D building morphology, the indicators chosen were the building volume density (BVD), sky view factor (SVF) (Daramola and Balogun, 2019), mean building height (MBH) (Alexander, 2021), and floor area ratio (FAR) (Chen et al., 2022). These indicators were selected due to three main criteria: (1) the ability to describe building morphology from several directions, (2) the representativeness and commonness of indicators found in existing literature, and (3) a relatively low degree of redundancy (Li and Wu, 2004; Li et al., 2012). BCR is frequently used to measure building density. It is widely reported that BCR had a considerable impact on the microclimate conditions (Rhee et al., 2014; Zhang et al., 2022). LPI, LSI, and ED are commonly used to estimate spatial features such as landscape connectivity, shape complexity, and fragmentation. The variations in these metrics were strongly associated with the distinctions in thermal environments and air flow (Han et al., 2023). SVF contributes largely to the 3D urban environment analysis since it substantially affects solar radiation, wind flow, and thermal environment (Li

and Hu, 2022). Furthermore, BVD, MBH, and FAR were also commonly used to estimate the spatial characteristics of building volume and height. These metrics have been identified as pivotal determinants of environmental variables such as air temperature, land surface temperatures, wind dynamics, and relative humidity (Cao et al., 2021). The definitions and abbreviations of all selected building morphology indicators are presented in Table 3.1. The spatial patterns of 2D and 3D building morphology indexes across scales are presented in Figure 3.3-3.5.

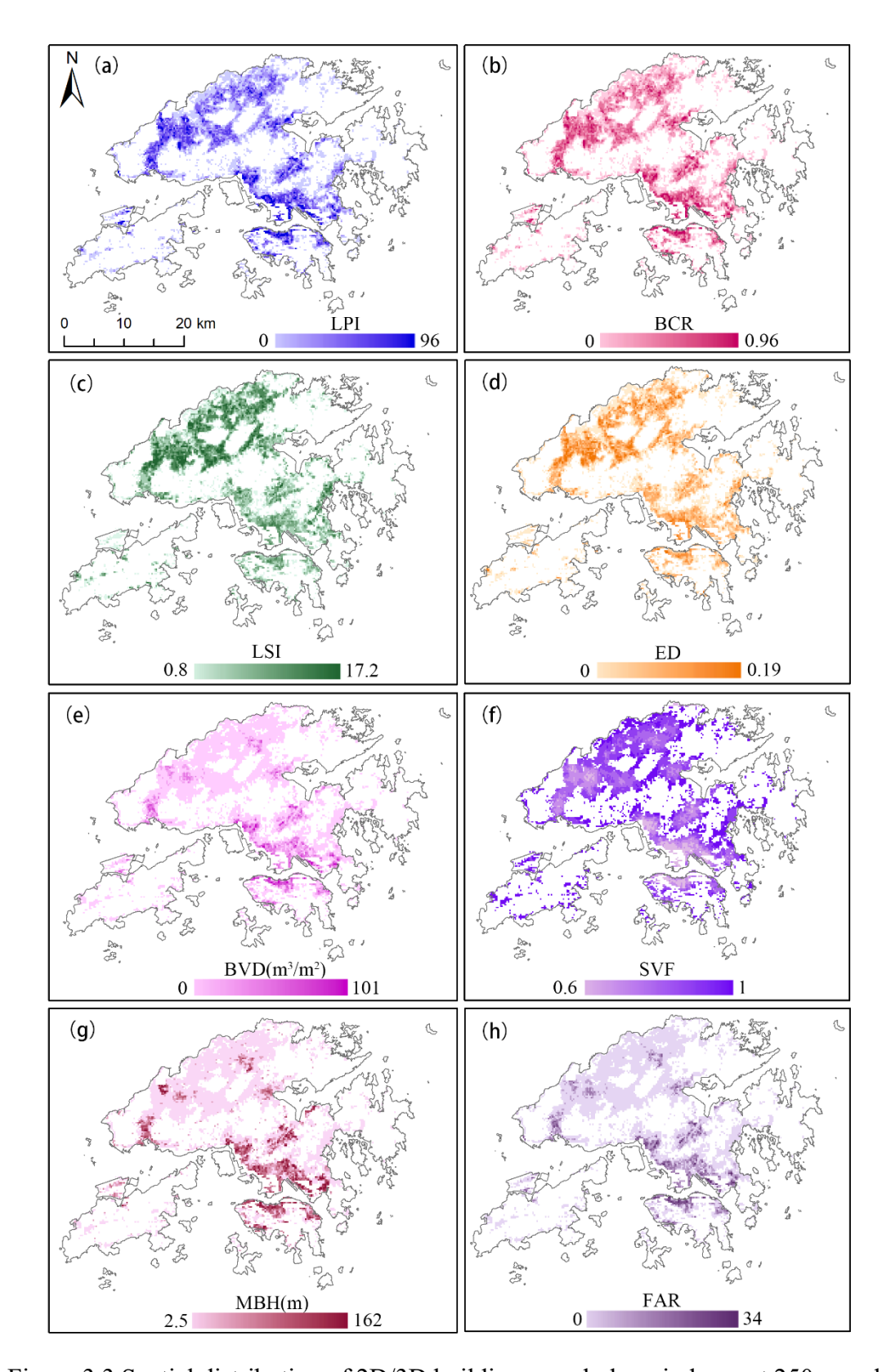


Figure 3.3 Spatial distribution of 2D/3D building morphology indexes at 250m scale

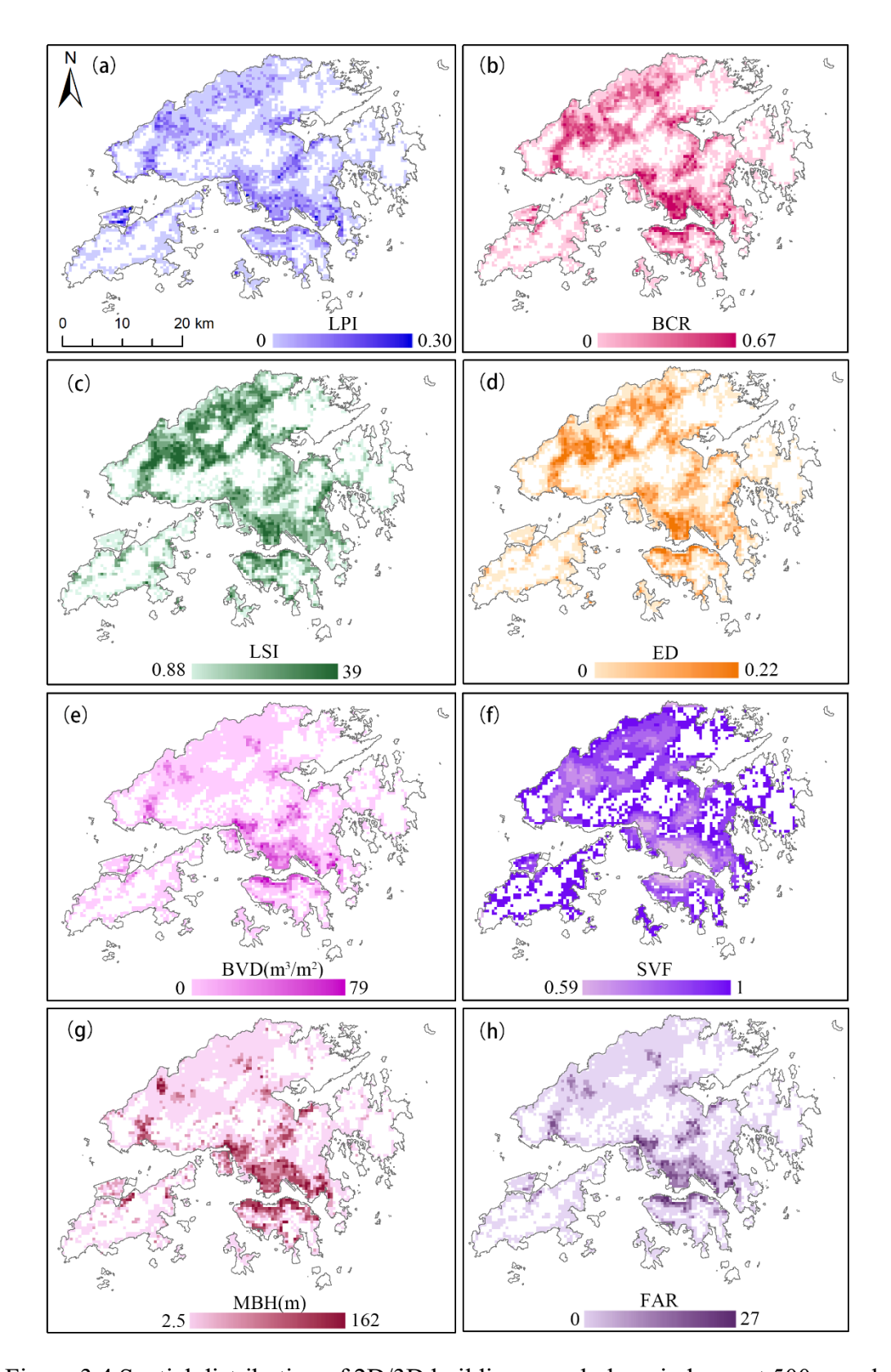


Figure 3.4 Spatial distribution of 2D/3D building morphology indexes at 500m scale

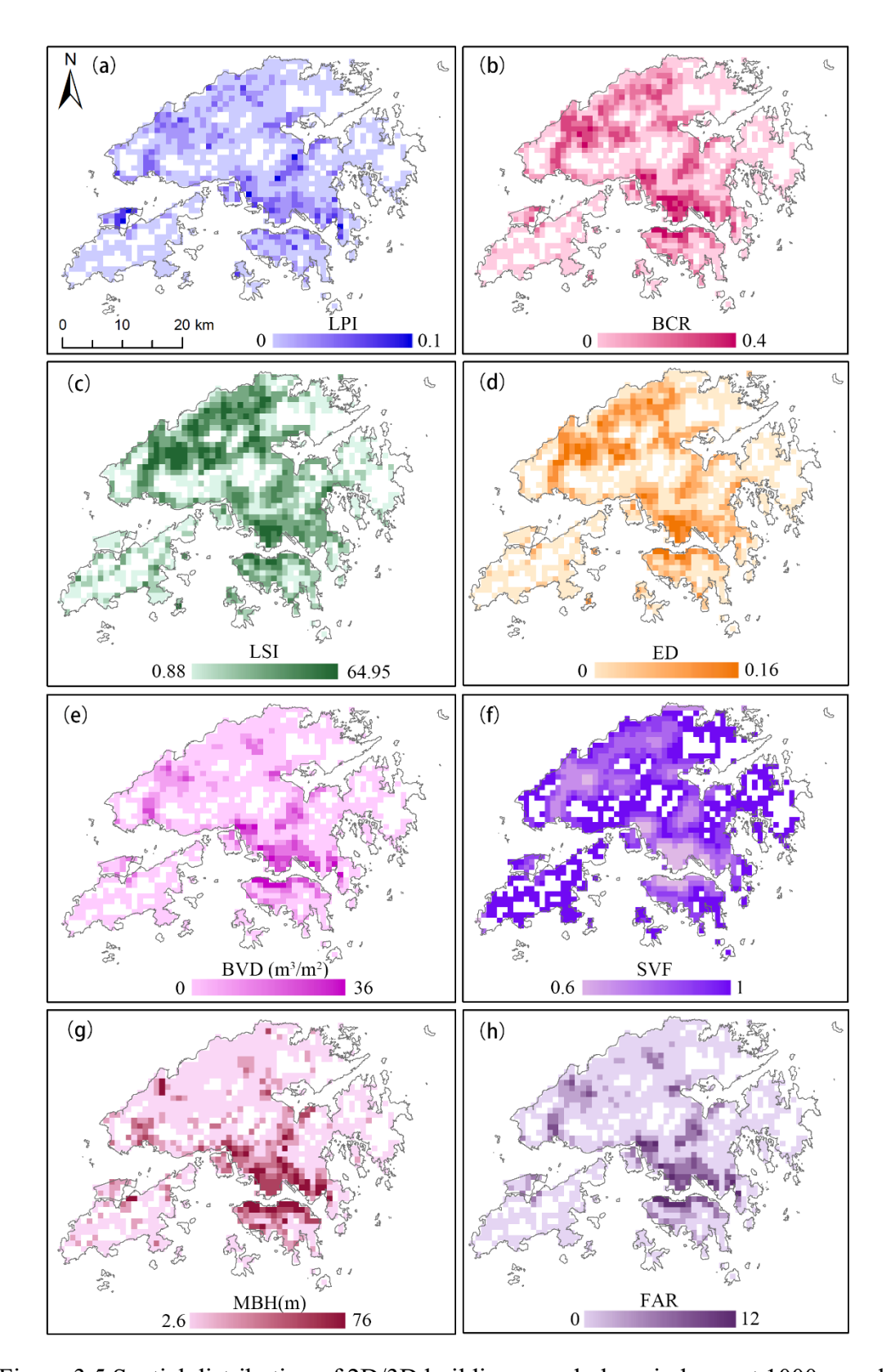


Figure 3.5 Spatial distribution of 2D/3D building morphology indexes at 1000m scale

3.4.5 Analysis of the impacts of 2D/3D building morphology on vegetation greening

This study combined traditional statistical techniques with advanced machine learning methods to investigate the influence of 2D/3D building morphology on vegetation greening. Initially, Pearson correlation analysis was conducted to assess the linearity between 2D/3D building morphology metrics and vegetation greening trends. This coefficient denotes the degree and direction of correlation between building morphology and vegetation greening (Pearson, 1908). Second, the boosted regression tree (BRT) model was applied to investigate the effects of 2D and 3D building morphology on vegetation greening trends in Hong Kong. BRT is a machine learning method that combines the traditional regression tree technique with boosting that improves model robustness and predictive accuracy (De'ath, 2007). Unlike standard linear regression, BRT uses recursive binary splitting to accommodate any interactions between observers and forms several regression trees to explain complicated and nonlinear relationships. Model output results consist of the relative contribution curve and the marginal effect curve. Relative contribution expresses how each morphological variable contributes to greening trends. Marginal effect demonstrates how the impact of each variable varies as a function of their magnitude. In the marginal effect curves generated by the BRT model, the relative influence value of zero indicates no effect, values below zero indicate negative effects, and values above zero are positive associations. One of the key strengths of BRT is its ability to be flexible enough to handle different types of data without making prior assumptions

about interaction between classes or other variables, while delivering estimates that can be easily interpreted, such as variable importance, marginal response (Pouteau et al., 2011). That is why BRT has been widely used in urban ecological studies (Han et al., 2022; Hu et al., 2020). To reduce the noise introduced by changes in the building and vegetation coverages, spatial analysis tools were used to detect all areas where the building footprint and orientation height were the same in the period between 2010 and 2020. The dependent variables were set as the vegetation greening slope in every unchanging spatial unit. The independent variables were set as eight static 2D/3D building morphology indexes found within each unchanging unit. After much debugging and optimization, the final parameters for the BRT model were set: learning rate = 0.005, bag fraction = 0.5, and tree complexity = 5. For model training, we employed a 50% random sampling strategy of the dataset while implementing 10-fold cross-validation to ensure robust performance evaluation.

.

3.5 Method for analysis of the direct and indirect effects of 2D/3D building and green space on urban thermal environments

3.5.1 Overall workflow

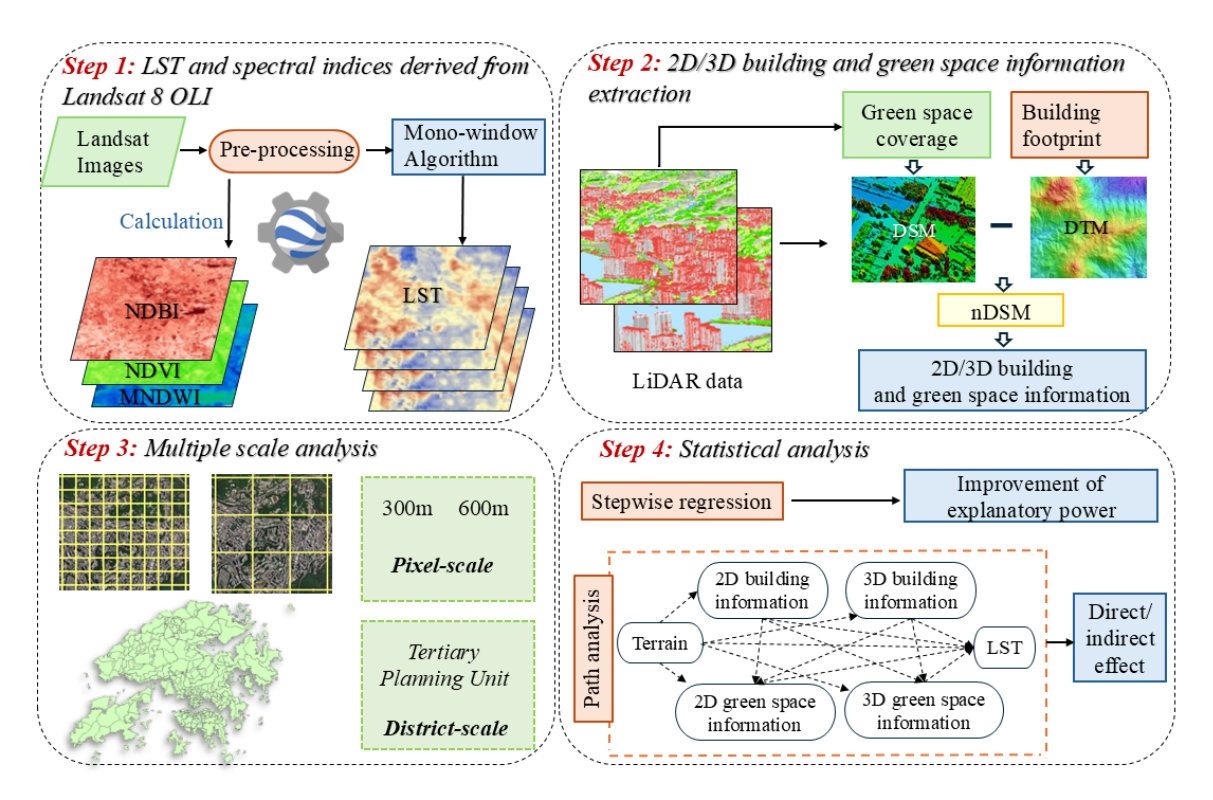


Figure 3.6 The overall workflow of the second case study

This study utilizes stepwise regression and path analysis to assess the direct and indirect influence of 2D/3D buildings and green space on summer land surface temperatures across pixel and district scales in Hong Kong in 2020 (Figure 3.6). The first step is the LST inversion and spectral indices extraction by using the Landsat 8 OLI images based on the GEE platform. The second step is the extraction of 2D/3D building and green space features based on the LiDAR-derived green space data, building footprint, and surface elevation data (DSM/DTM). The third step is the generation of multiple scales: pixel scales and tertiary planning unit (TPU) scales.

Finally, stepwise regression and path analysis are used to explore the interaction between buildings, green space, and LST.

3.5.2 Land surface temperature inversion based on Landsat 8 OLI images

With the development of remote sensing techniques, LST has been largely adopted as an indicator for the thermal environment due to its large coverage area and cheaper acquisition costs than air temperature data (Chang et al., 2025; Fu and Weng, 2016; Weng et al., 2014). Hence, this study chose the LST to represent the thermal environment.

Land surface temperature inversion algorithms are mainly divided into three categories according to different thermal infrared remote sensing data: single-channel algorithms, multi-channel algorithms, and split-window algorithms. Single-channel algorithms include the radiative transfer equation method (Sobrino et al., 2004), the Jiménez-Muñoz single-channel algorithm (Jimenez-Munoz et al., 2009), and the Qin Zhihao single-window algorithm (Qin et al., 2001). Multi-channel algorithms mainly include the gray body emissivity method (Barducci and Pippi, 1996), the day/night method (Jimenez-Munoz et al., 2009), and the temperature emissivity separation method (Gillespie et al., 1998). Among them, split-window algorithms are primarily used for surface temperature inversion with NOAA-AVHRR data, TERRA-MODIS data, Landsat-TIRS data, and ASTER data. Therefore, the split-window algorithm was selected for LST retrieval (unit: °C). The formula is as shown in equations (7)–(9):

$$T_s = \{a(1-C-D) + [b(1-C-D) + C + D] * T_{10} - DT_a\}/C$$
 (7)

$$C = \tau \varepsilon$$
 (8)

$$D = (1 - \tau)[(1 - \varepsilon)\tau] \tag{9}$$

where T_s is the derived LST value (°C), The coefficients a and b are defined with values a = -67.355351 and b = 0.458606. C and D represent intermediate variables. T_{10} is the brightness temperature of the 10th band of TIRS. T_a is the average atmospheric action temperature. τ is the atmospheric transmittance. ε is the land surface emissivity.

3.5.3 Extraction of 2D/3D buildings, green space structure, and controlling factors

Drawing on previous research, a total of 16 factors were selected as explanatory variables of summer land surface temperature in this study, including spectral information, 2D/3D building morphology information, 2D/3D green space structure information, and terrain and location information. 2D/3D building morphology information includes building coverage ratio (BCR) (Song et al., 2020), building volume density (BVD) (Azhdari et al., 2018; Zhou et al., 2022b), building sky view factor (BSVF) (Li et al., 2021), mean building height (Mean_BH) (C. Chen et al., 2022), and maximum height of buildings (Max_BH) (Chen et al., 2022). 2D/3D green space structure information includes green space coverage ratio (GCR) (Yao et al., 2020), green space volume (GVD) (Handayani et al., 2018; Hecht et al., 2008), green space sky view factor (GSVF) (Chiang et al., 2023), mean green space height (Mean_GH) (Alexander, 2021), and maximum height of green space (Max_GH)

(Alexander, 2021). In this study, these indices were carefully selected for three key characteristics: they can (1) explain building morphology and green space structural attributes from several perspectives comprehensively, (2) serve widespread and stable representation in urban environmental studies, (3) have been firmly recognized as major contributing factors in previous studies (Wang et al., 2025b; Yuan et al., 2024). BCR stands for building density and has been reported as positively correlated with LST in the previous (Song et al., 2020). BVD refers to the degree to which the building utilizes vertical space. It can influence LST by changing wind environments, shade conditions, and land surface roughness (Wu et al., 2025). BSVF shows the extent to which the sky is covered by the building, affecting shade and heat dissipation (Gong et al., 2018; Wang et al., 2025a). Mean BH and Max BH represent vertical structure features of the building environment from average height and maximum height perspectives. It can influence the ventilation condition and shading conditions (Chen et al., 2022). GCR is the density of green space, and it shows the negative impact on LST. GVD is the density of green space volume (Jia et al., 2024). GSVF delineates the degree to which the sky is obstructed by green space (Chiang et al., 2023). GVD and GSVF are associated with evapotranspiration and shading conditions. Mean GH and Max GH reflect vertical structure features of green space from the average height and maximum height perspectives and can impact the shading effect of green space (Alexander, 2021).

Spectral information includes normalized difference built-up index (NDBI), normalized difference vegetation index (NDVI), and modified normalized difference

water index (MNDWI). Terrain and location information includes elevation terrain model (DEM), slope (SL), and latitude (LAT). We chose spectral information and terrain and location information as controlling factors in the regression model to figure out whether 2D/3D building and green space indexes are conducive to increasing the explanatory power of LST variation compared to factors that are already widely recognized as having a significant influence on LST. Selected indexes for spectral, terrain and location information are commonly used and have been identified as basic impact factors in previous LST-related research. Table 3.2 provides a detailed description of the selected indexes in this study, and the spatial maps of those indexes are shown in Figure 3.7-21.

Table 3.2 The explanatory variables used in this study

Dimension	Metrics	Abbreviations	Formula	Description
Spectral information	Normalized difference built-up index	NDBI	$NDBI = \frac{(SWIR - NIR)}{(SWIR + NIR)}$	Quantifies built-up areas in satellite images
	Normalized difference vegetation index	NDVI	$NDVI = \frac{(\text{NIR} - \text{R})}{(NIR + R)}$	Quantifies vegetation coverage, density, and growth condition
	Modified normalized difference water index	MNDWI	$MNDWI = \frac{(SWIR - NIR)}{(SWIR + NIR)}$	Quantifies water coverage, density, and quality
2D/3D building information	Building coverage ratio	BCR	$BCR = \frac{1}{S_g} \sum_{i=1}^{n} BA_i$	Measures the ratio between the total area of buildings within a spatial unit and the area
	Building volume density	BVD	$BVD = \frac{1}{S_g} \sum_{i=1}^{n} BV_i$	Measures the ratio between the total volume of the buildings in a spatial unit and the area
	Building sky view factor	BSVF	$SVF = 2\pi \left[1 - \frac{\sum_{i=1}^{n} \sin \alpha_j}{n} \right]$	α is the vertical angle of the horizon in the direction j
	Mean building height	Mean_BH	$MBH = \frac{\sum_{i=1}^{n} BH_i}{n}$	Measures the mean height of the buildings in a spatial unit
	Maximum height of buildings	Max_BH	$MAX_BH = \max(BH_i)$	Measures the maximum height of the buildings in a spatial unit
2D/3D green space information	Green space coverage ratio	GCR	$GCR = \frac{1}{S_g} \sum_{i=1}^{m} GA_i$	Measures the ratio between the total area of green space within a spatial unit and the area
	Green space volume	GVD	$GVD = \frac{1}{S_g} \sum_{i=1}^{m} GV_i$	Measures the ratio between the total volume of the green space in a spatial unit and the area
	Green space sky view factor	GSVF	$GSVF = 2\pi \left[1 - \frac{\sum_{i=1}^{m} \sin \alpha_j}{m} \right]$	α is the vertical angle of the horizon in the direction j
	Mean green space height	Mean_GH	$MGH = \frac{\sum_{i=1}^{m} GH_i}{m}$	Measures the mean height of the green space in a spatial unit
	Maximum green space	Max_GH	$MAX_GH = \max(GH_i)$	Measures the maximum height of the green space in a spatial unit

height

	Digital elevation model	DEM	-	Measures the height of the land's surface over a spatial unit
Terrain and location	Slope	SL	Slope $= \operatorname{Arctan} \left(\frac{DTM_a - DTM_b}{\sqrt{(y_{a-}y_b)^2 + (x_{a-}x_b)^2}} \right)$	Measures the steepness or incline of a terrain surface in a spatial unit
	Latitude	LAT	-	-

Note: n is the number of buildings within a spatial unit; m is the number of green space pixels within a spatial unit; Sg is the total area of the spatial unit; BAi, BVi, BHi, are the area, volume, and height for the ith building, respectively; GAi, GVi, GHi, are the area, volume, and height for the ith green space pixel; θ is the wind direction angle. a and b are the pixels needed to calculate the slope; y_a , y_b and x_a , x_b are the horizontal and vertical project coordinates.

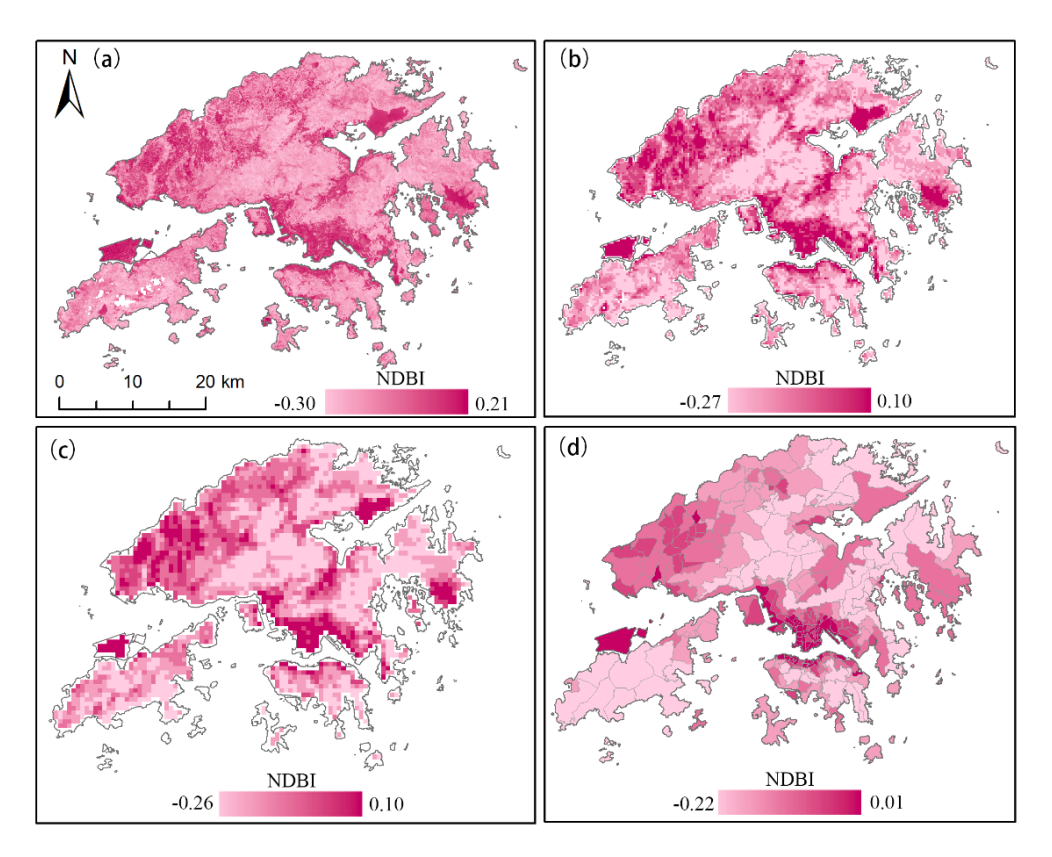


Figure 3.7 Spatial distribution of NDBI at 30m (a), 300m (b), 600m (c), district (d)

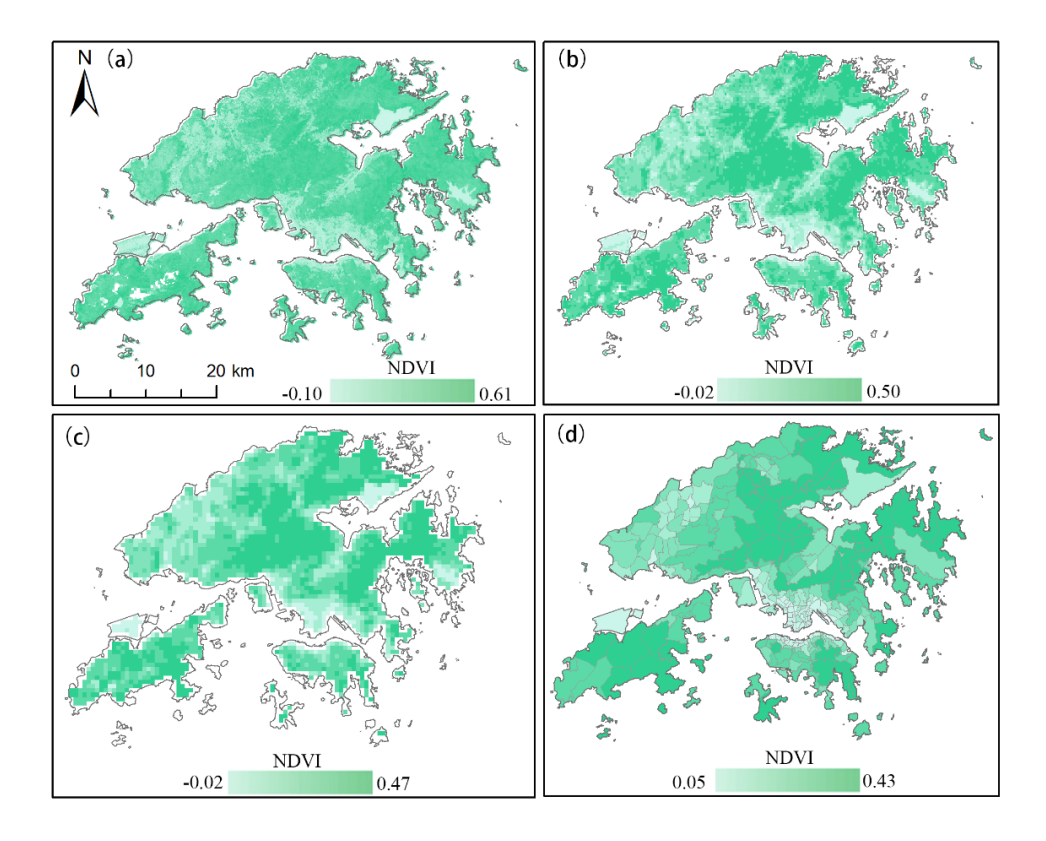


Figure 3.8 Spatial distribution of NDVI at 30m (a), 300m (b), 600m (c), district (d)

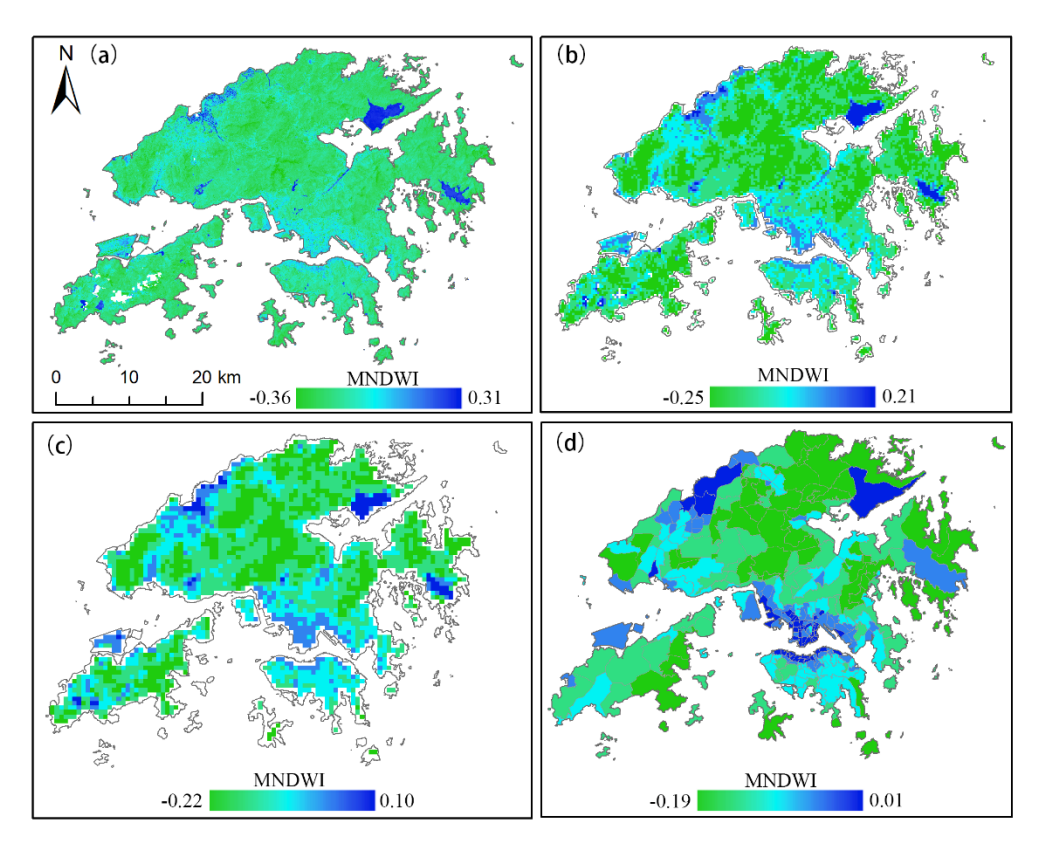


Figure 3.9 Spatial distribution of MNDWI at 30m (a), 300m (b), 600m (c), district (d)

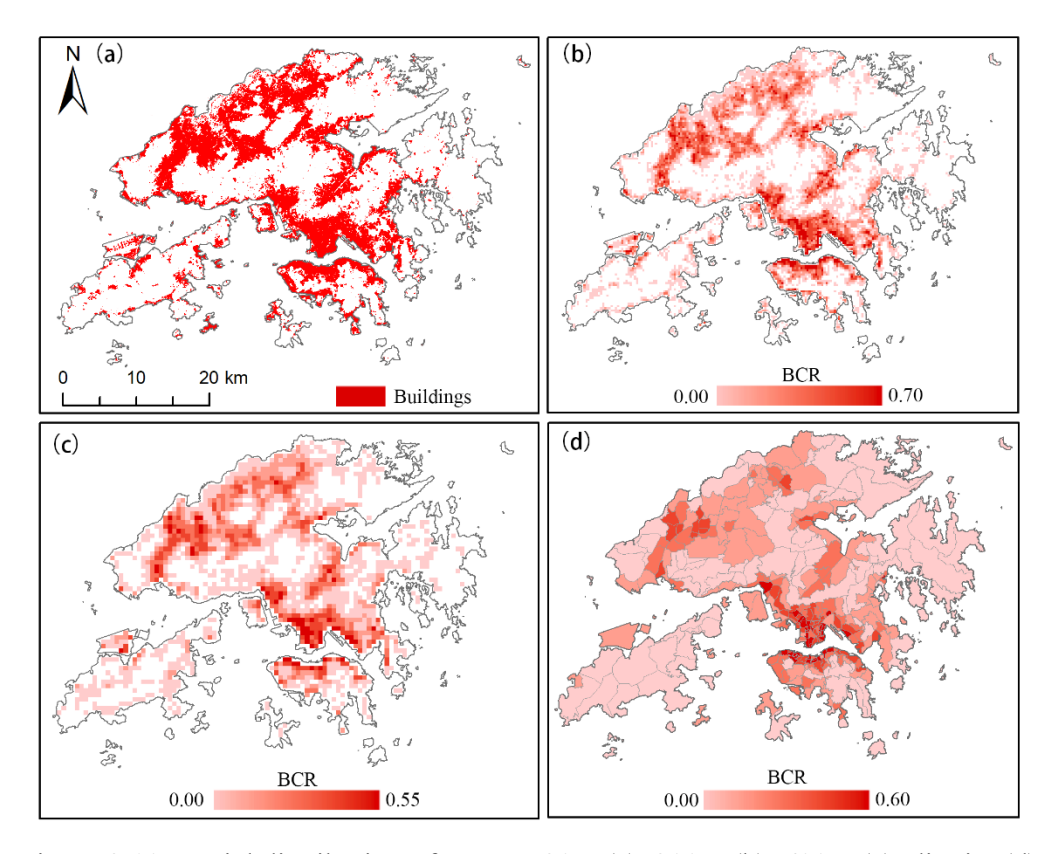


Figure 3.10 Spatial distribution of BCR at 30m (a), 300m (b), 600m (c), district (d)

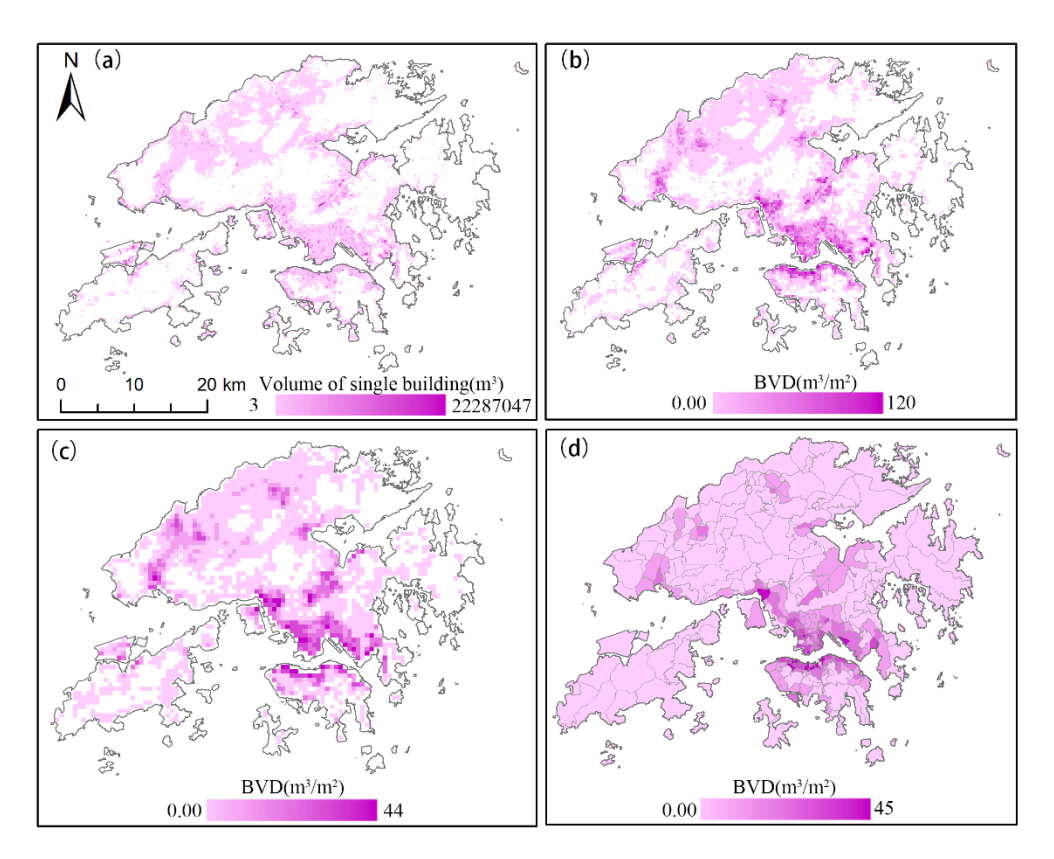


Figure 3.11 Spatial distribution of BVD at 30m (a), 300m (b), 600m (c), district (d)

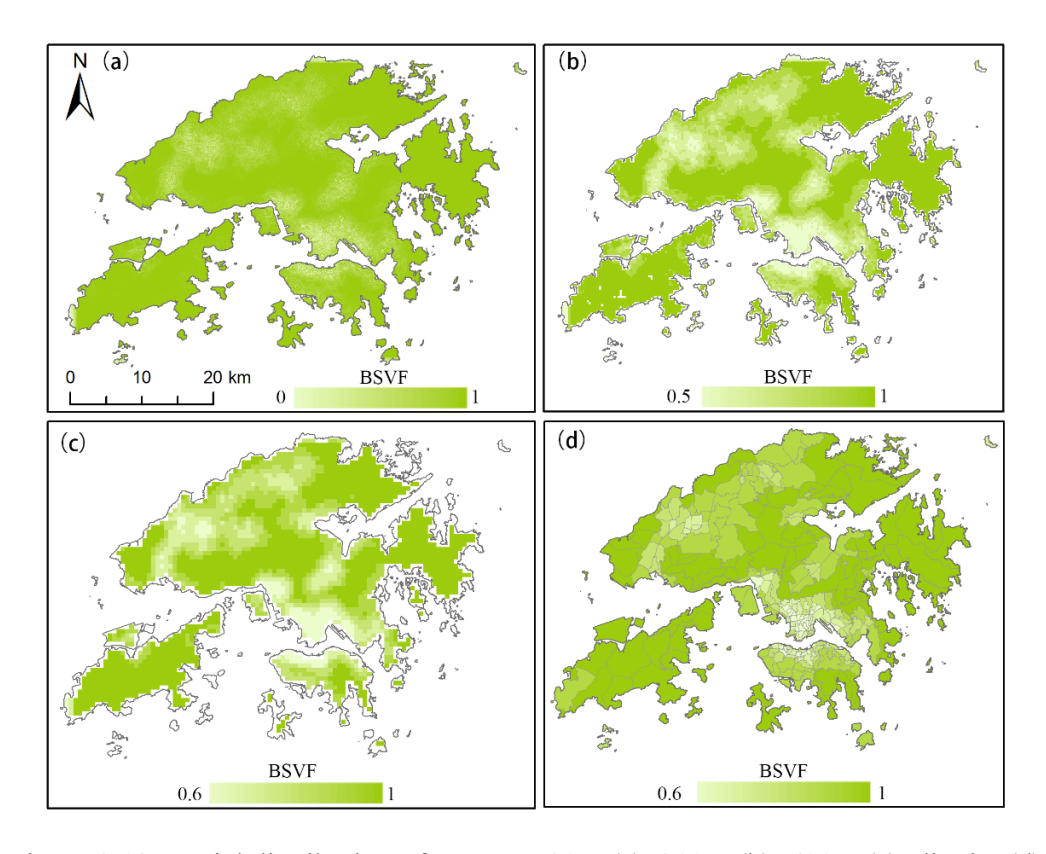


Figure 3.12 Spatial distribution of BSVF at 30m (a), 300m (b), 600m (c), district (d)

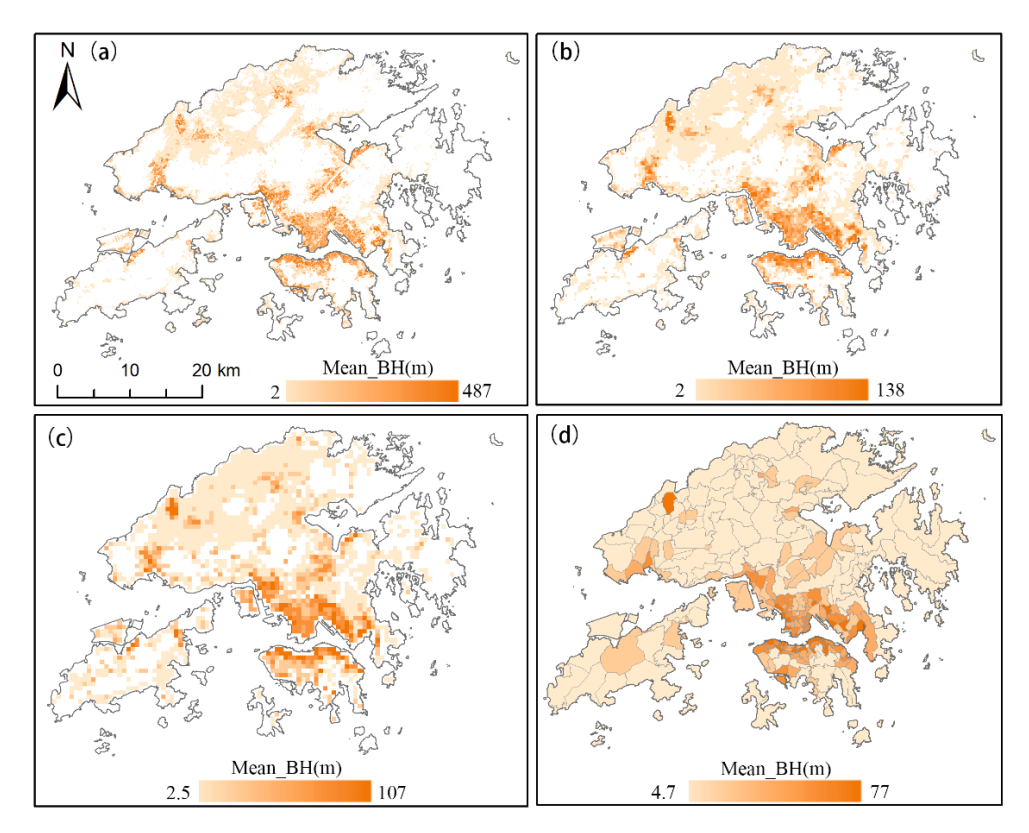


Figure 3.13 Spatial distribution of Mean_BH at 30m (a), 300m (b), 600m (c), district (d)

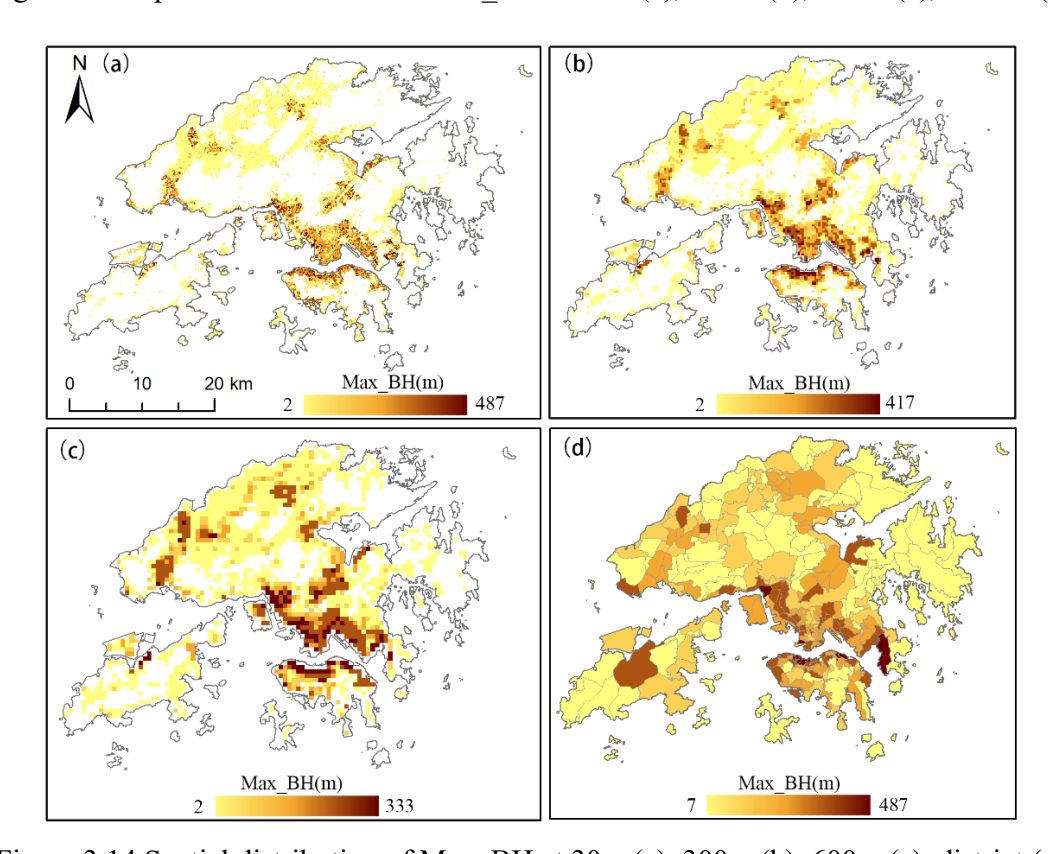


Figure 3.14 Spatial distribution of Max_BH at 30m (a), 300m (b), 600m (c), district (d)

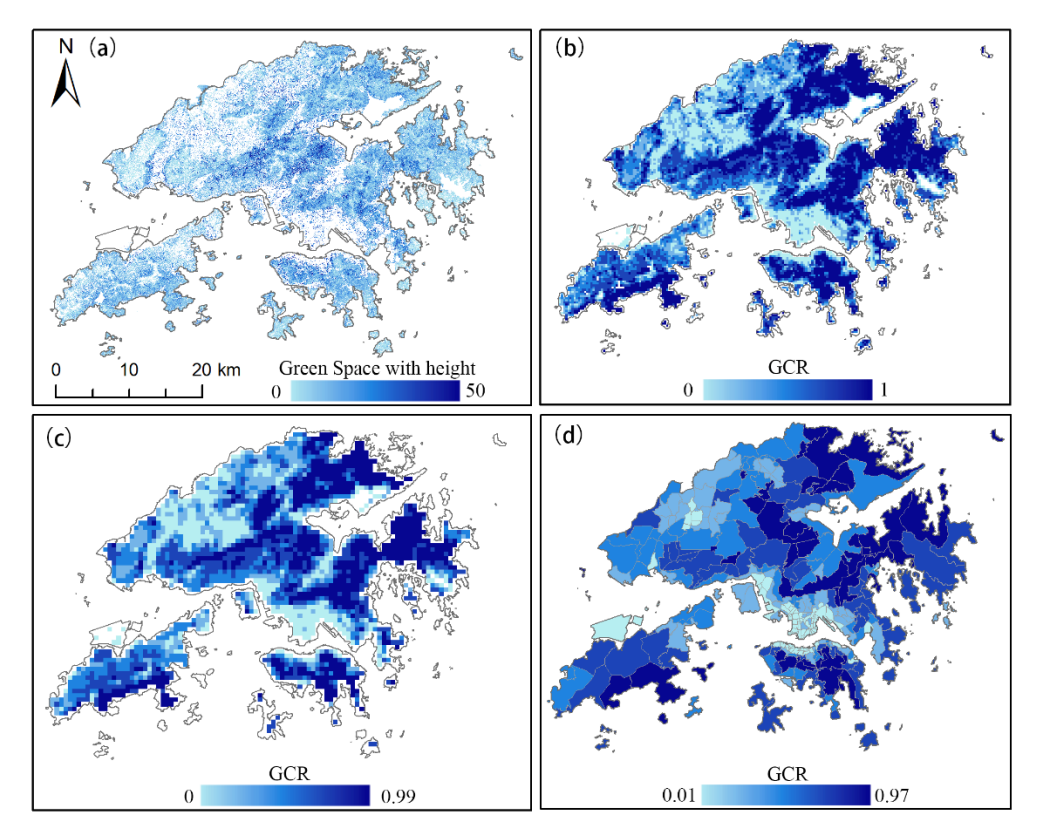


Figure 3.15 Spatial distribution of GCR at 30m (a), 300m (b), 600m (c), district (d)

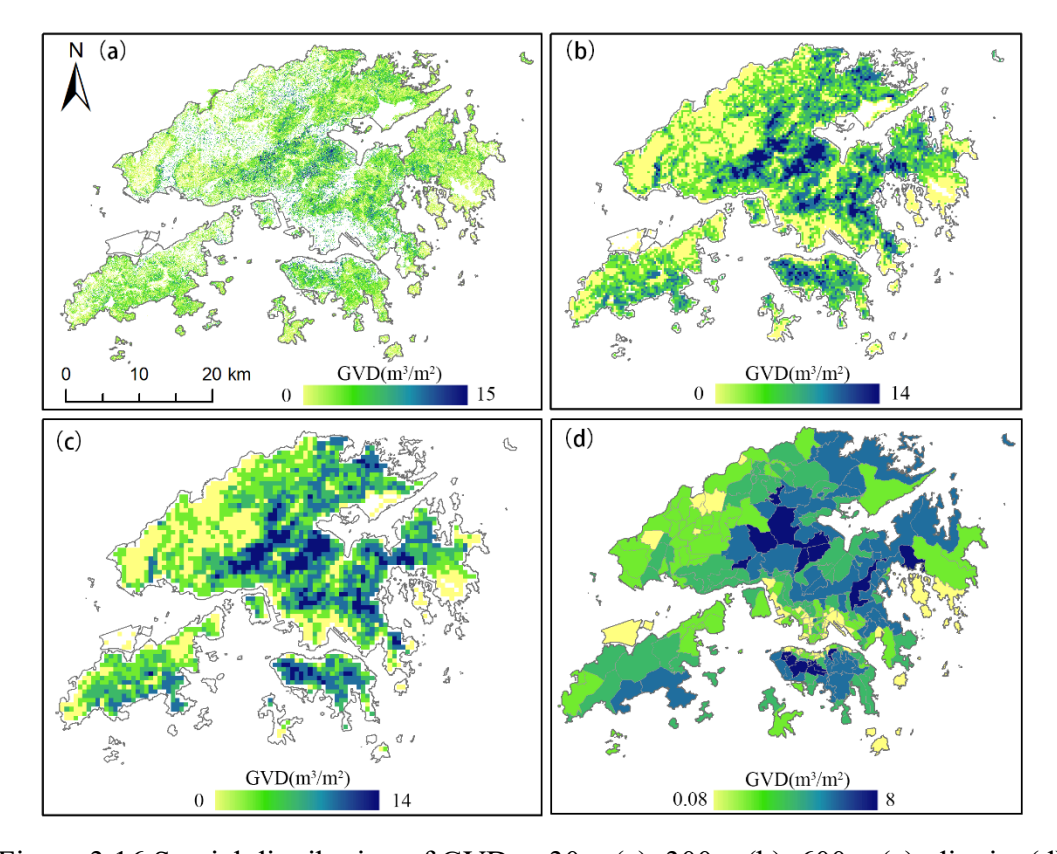


Figure 3.16 Spatial distribution of GVD at 30m (a), 300m (b), 600m (c), district (d)

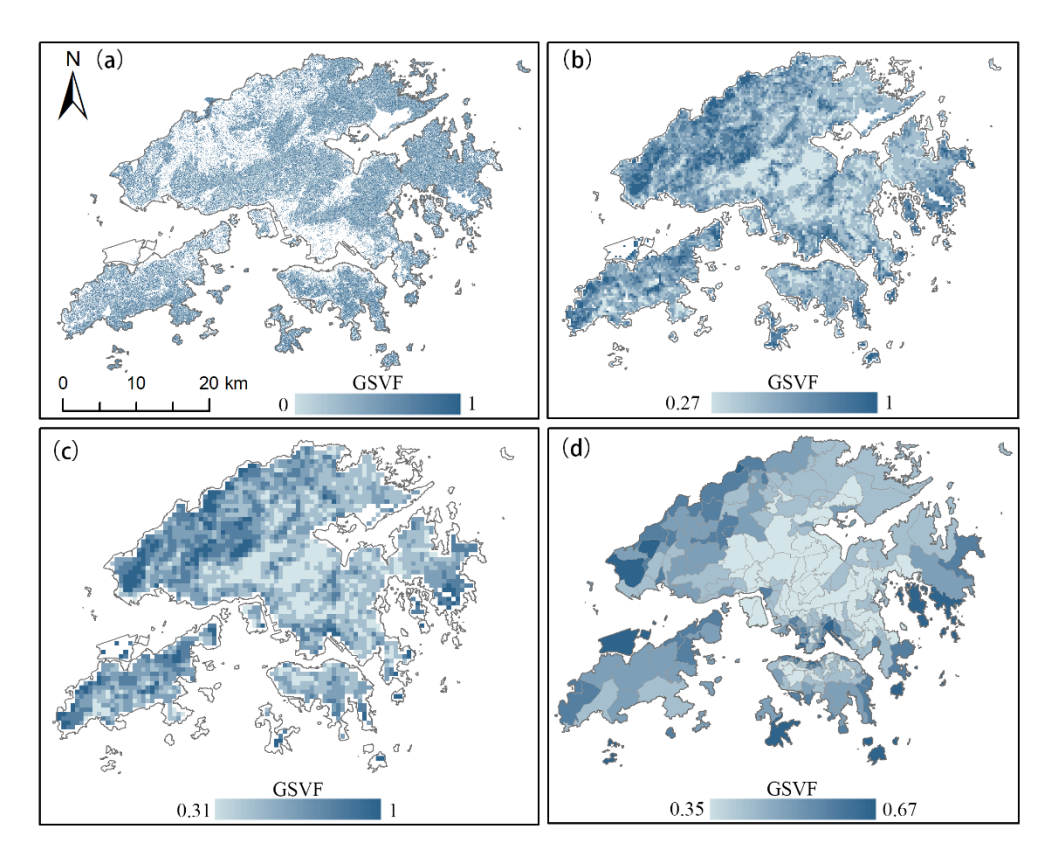


Figure 3.17 Spatial distribution of GSVF at 30m (a), 300m (b), 600m (c), district (d)

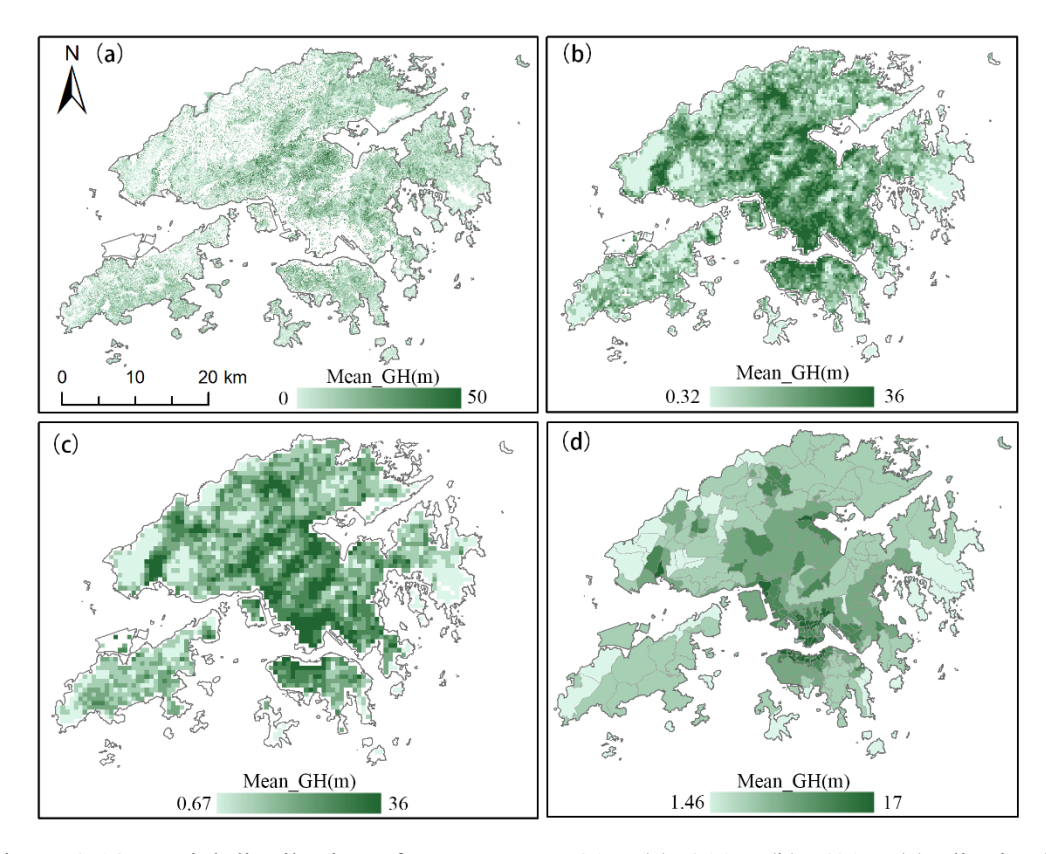


Figure 3.18 Spatial distribution of Mean_GH at 30m (a), 300m (b), 600m (c), district (d)

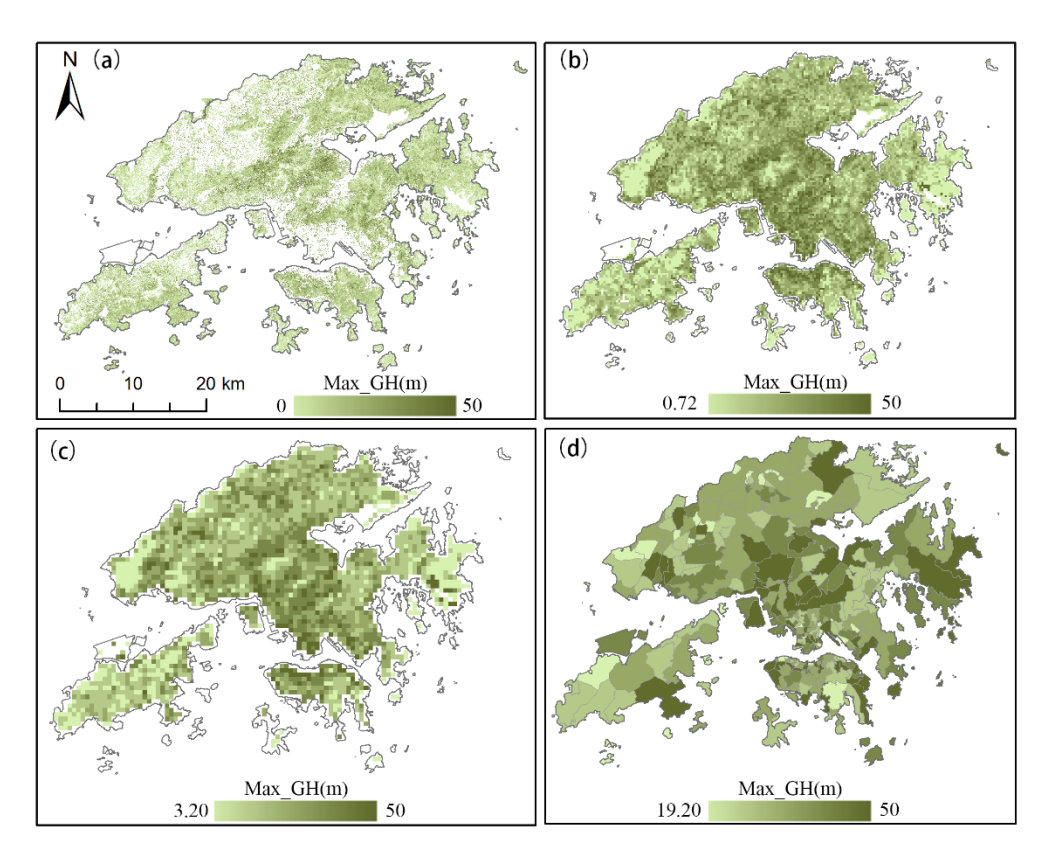


Figure 3.19 Spatial distribution of Max_GH at 30m (a), 300m (b), 600m (c), district (d)

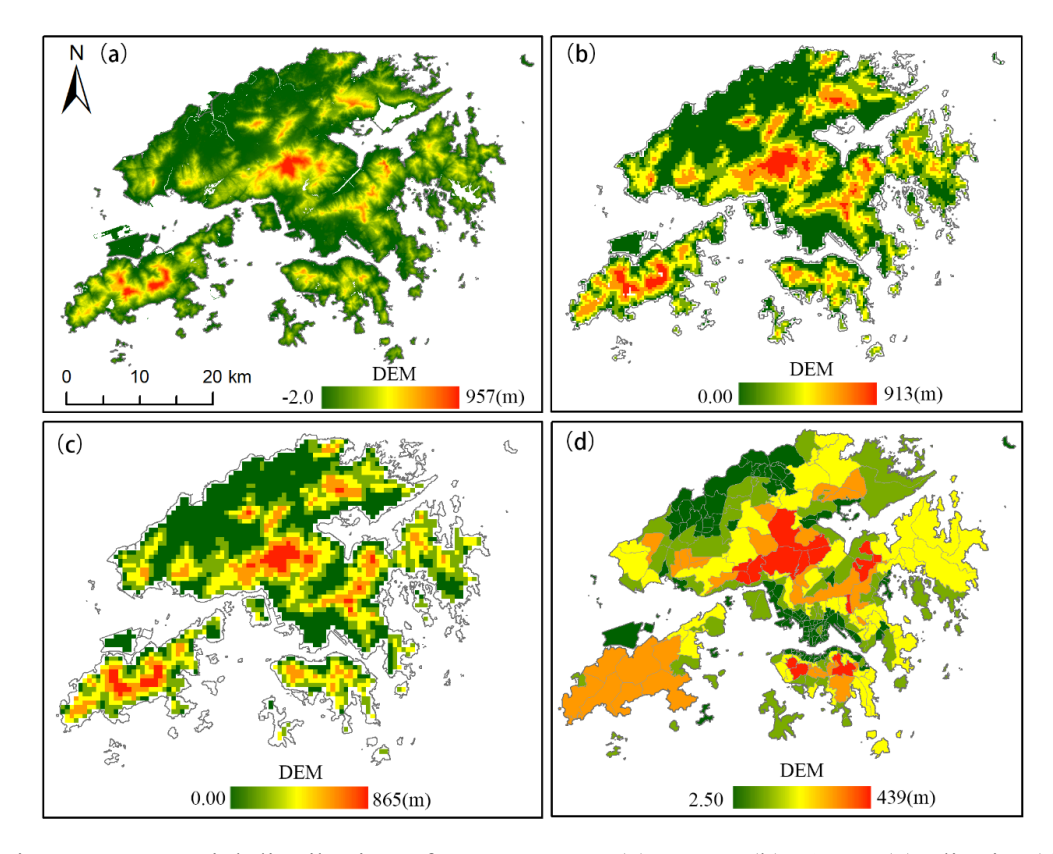


Figure 3.20 Spatial distribution of DEM at 30m (a), 300m (b), 600m (c), district (d)

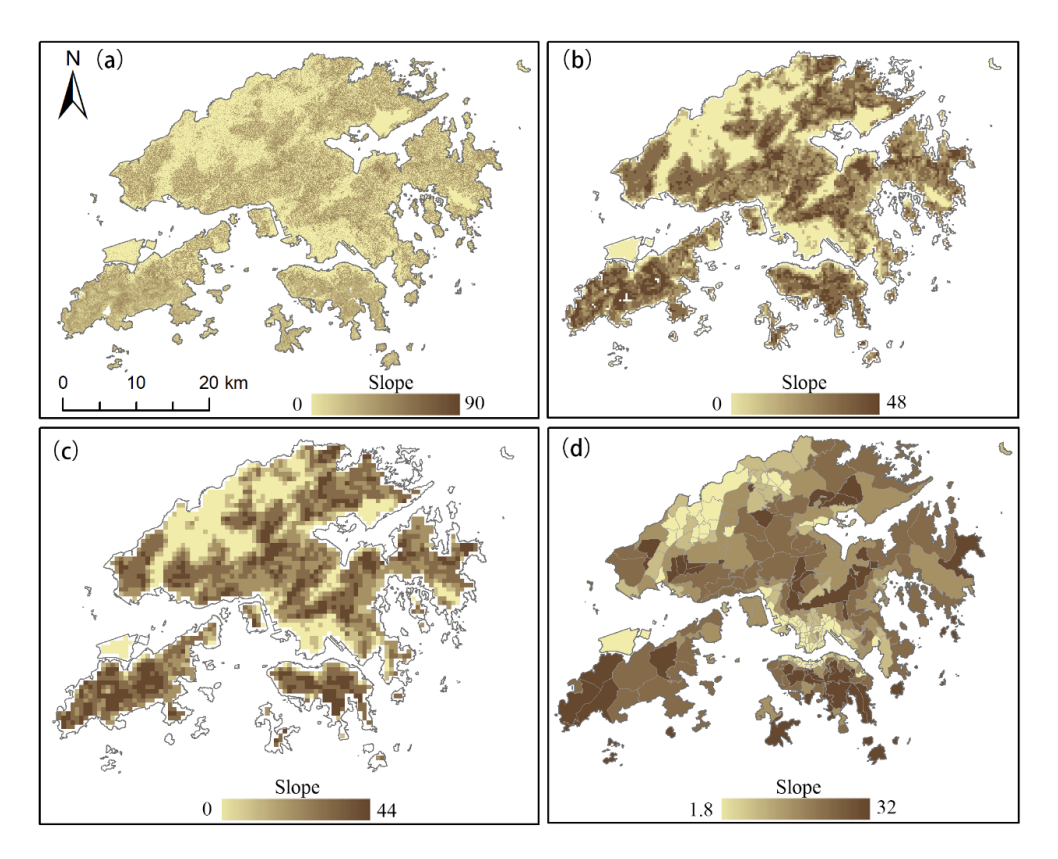


Figure 3.21 Spatial distribution of Slope at 30m (a), 300m (b), 600m (c), district (d)

3.5.4 Scale analysis

To analyze whether research findings are influenced by the spatial scales and support multi-scale urban planning, a multi-scale analysis was carried out by utilizing the pixel scales and district scale to examine the performances of 2D/3D building and green space in improving the explanatory power of LST variations and the direct and indirect impacts of 2D/3D building and green space on LST. We created 300m×300m and 600m×600m fishnets to conduct the analysis at pixel scales and employed the vector data of tertiary planning units provided by the Hong Kong government to represent the district scale. We chose these three scales for the following reasons: (1) the initial spatial resolution of the derived LST was 100 m, scales based on multiples of initial spatial resolution can help to maximize data accuracy and reduce data errors;

(2) original 100m grid size may introduce more noise in the data due to higher surface heterogeneity; (3) if the spatial is too large, the number of samples will be limited and lead to biased and unreliable results; (4) several local studies have indicated that buildings within 300m presented strongest autocorrelation in Hong Kong (Lau et al., 2015; Zheng et al., 2018). Based on this, we further extended the analysis to a 600m scale; (5) since policy and planning decisions are often made based on administrative boundaries, this study also conducted analysis at the district scale to better support decision-making. LST in each analysis unit across different spatial scales was represented by the average summer LST in 2020. The explanatory variables shown in Table 3.2 in each unit at different scales were calculated using ArcGIS Pro.

3.5.5 Statistical analysis

A stepwise multiple linear regression model was utilized to examine the ability of 2D/3D building and green space indexes to improve the explanatory power of LST variations across different scales. The stepwise multiple linear regression model is an advanced version of the traditional multiple linear regression. It combines the forward and backward selection approach to identify the best-fitting model while avoiding collinearity (Efroymson, 1960). Given the potential collinearity among the proposed multiple independent variables (Table 3.2), and to ensure the best goodness of model fitting, the stepwise multiple linear regression model is considered the most suitable regression model for evaluating the capability of 2D/3D building and green space morphology in improving explanatory power of LST variation. The dependent

variable of stepwise multiple linear regression in each spatial unit was average summer LST. The independent variables were the proposed spectral indexes, 2D/3D building structures, 2D/3D green space structures, and terrain in each spatial unit. We perform the stepwise multiple linear regression with the "MASS" package of R. First, we only included spectral indexes and terrain as independent variables and recorded the Adjusted R² for the fitted model. Then, we added the 2D building structure, 2D green space structures, 3D building structures, 3D green space structures, 2D/3D building structures, 2D/3D green space structures gradually to evaluate the performance of the 2D/3D building and green space structures in improving the explanatory power of LST variations, which was represented by the improved Adjusted R².

Furthermore, the path analysis (PA) method was conducted at each spatial scale to investigate the direct and indirect impacts of the 2D/3D building and green space on summer LST. Unlike traditional regression models, path analysis allows the detection of the direct and indirect impacts of independent variables on dependent variables and the investigation of interactions between independent variables (Wright, 1934). Path analysis consists of the construction of a hypothetical model and the analysis of the built hypothetical model. The created prior causal conceptual structure is shown in Figure 3.22. First, we selected the BCR to represent the 2D building structure, BVD to represent the 3D building structure, GCR to represent the 2D green space structure, and GVD to represent the 3D green space structure for their higher standardized

coefficient. We calculated the average of DEM and slope to represent the terrain.

Next, we assumed that both the terrain, 2D building structure, 3D building structure,

2D green space structure, and 3D green space structure directly impact the LST. Then,

we hypothesized that terrain can indirectly affect the LST by influencing the 2D/3D

building and green space structure. Finally, we hypothesized that 2D building

structures and 3D building structures indirectly affect LST by influencing 2D and 3D

green space structures.

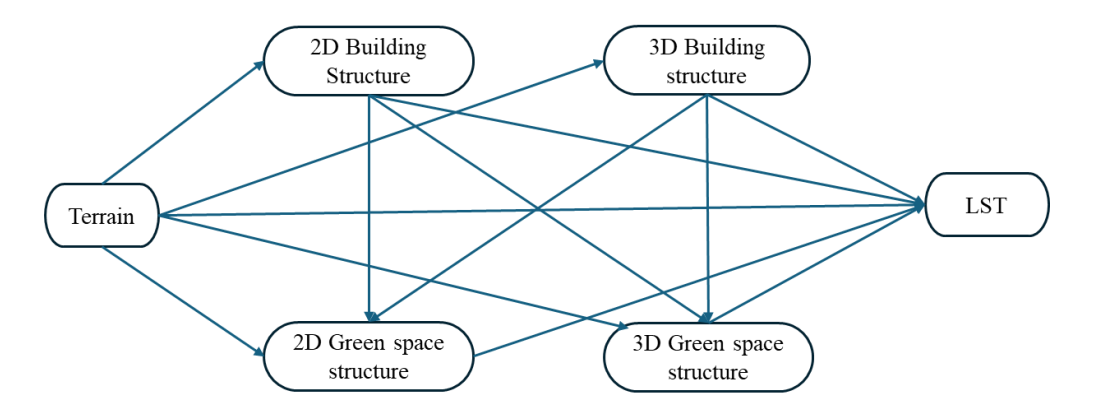


Figure 3.22 The created prior causal conceptual structure of path analysis

Chapter 4. Impacts of 2D/3D building morphology on vegetation greening

4.1 Overview

In this chapter, we present the preliminary results and analysis (Section 4.2), and discussion (Section 4.3) part of the impact of 2D/3D building morphology on vegetation growth. Further, we provide the spatiotemporal patterns of vegetation greening trends from 2010 to 2020 (Section 4.2.1), the correlation between 2D/3D building morphology and vegetation greening (Section 4.2.2), and the relative contribution and marginal effects of 2D/3D building morphology on vegetation greening trends (Section 4.2.3). In the Discussion part, we discuss the complexity of the building morphology - vegetation greening relationship (Section 4.3.1), distinctions in urban and rural greening mechanisms (Section 4.3.2), and limitations and future research directions (Section 4.3.3).

4.2 Results

4.2.1 Spatial-temporal patterns of vegetation greening trends

Overall, a widespread increase in vegetation greening was observed across Hong Kong between 2010 and 2020, with approximately 69.10% of the area exhibiting a positive greening trend. This trend was more evident than that observed in urban regions across all three spatial scales. As the scale increases, the trend of vegetation greening becomes more apparent.

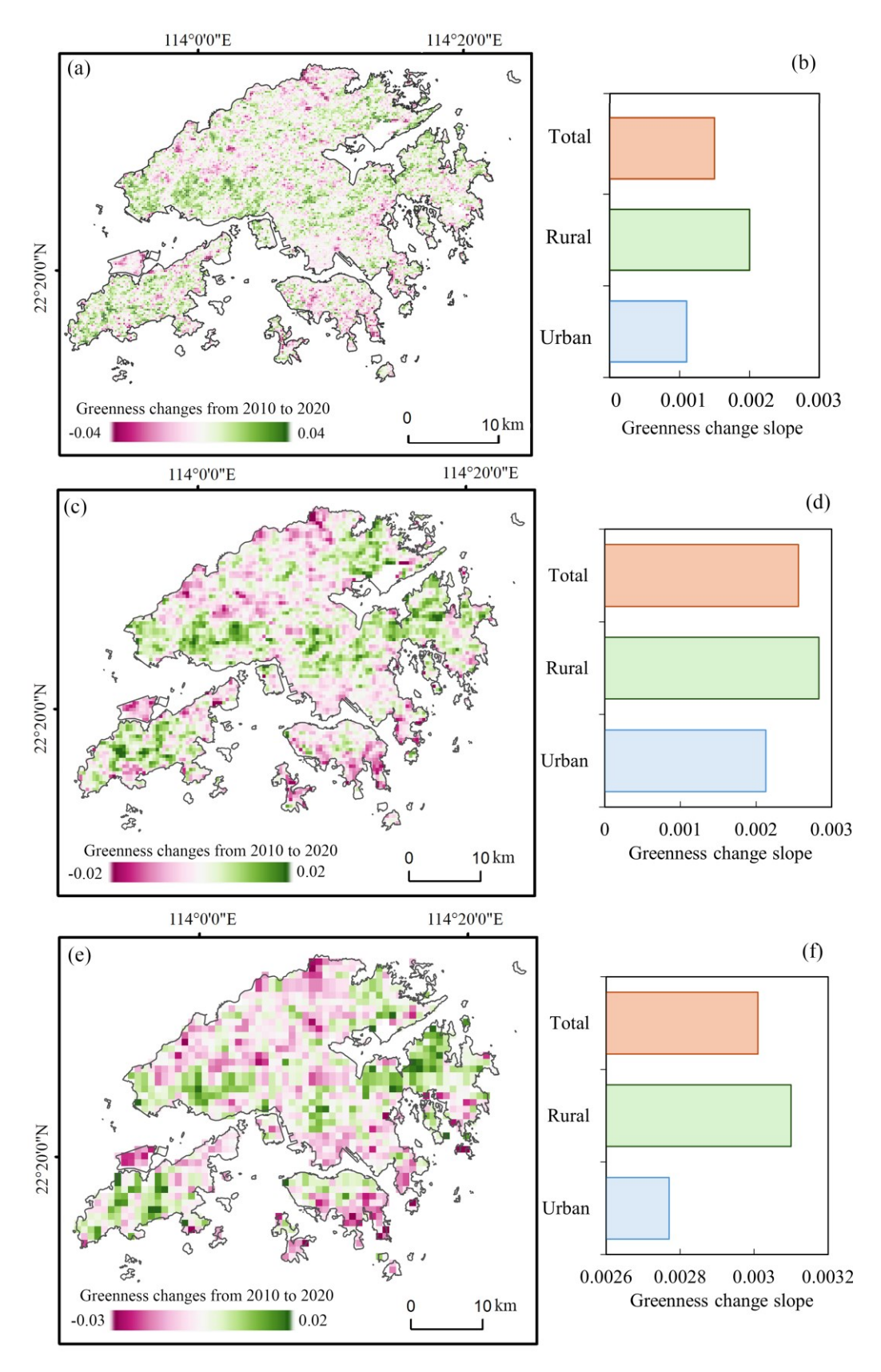


Figure 4.1 Spatial pattern of vegetation greenness changes trend at 250m (a), 500m (c), and 1000m (e) scales, and greenness change slope at 250m (b), 500m (d), and

Specifically, at the 250m scale, the overall EVI trend exhibited a positive slope of 0.0015. Areas exhibiting significant greening and significant browning accounted for 11.89% and 4.30% of the total area, with mean slopes of 0.0078 and -0.0083, respectively. Areas exhibiting non-significant greening and non-significant browning comprised 52.23% and 31.42% of the total area, respectively, reflected by average EVI slopes of 0.0034 and -0.0027 (Table 4.1). At the 500m scale, the study area exhibited an overall positive vegetation trend (mean slope = 0.0026), characterized by marked spatial heterogeneity. 19.57% of the area demonstrated statistically significant greening (mean slope = 0.0068), contrasting with 1.58% showing significant browning (mean slope = -0.0073). More extensive but less pronounced changes were observed in non-significant vegetation changes, where 59.48% of pixels displayed greening tendencies (mean slope = 0.0029) and 19.38% exhibited browning trends (mean slope = -0.0019). Vegetation trend analysis at the 1km spatial scale also demonstrated an overall enhancement in greenness (mean EVI slope = 0.0030). 19.63% of the study area showed statistically significant improvement (mean slope = 0.0076) and 1.15% exhibited notable degradation (mean slope = -0.0067). 58.88% of pixels displayed non-significant greening trends (mean slope = 0.0034) and 20.20% showed insignificant browning trends (mean slope = -0.0017).

Table 4.1 Overall vegetation changes trends in built-up environments

Scale	Classification	Criterion	Percentage (%)	Averaged Slope	
	Significant greening	Z >1.96, slope>0	11.89	0.0078	
MOD13Q1 (250m)	Significant browning	Z >1.96, slope<0	4.30	-0.0083	
	No change	slope=0	0.16	0	
	Not significant greening	Z <1.96, slope>0	52.23	0.0034	
	Not significant browning	Z <1.96, slope<0	31.42	-0.0027	
	Significant greening	Z >1.96, slope>0	19.57	0.0068	
MODIANI	Significant browning	Z >1.96, slope<0	1.58	-0.0073	
MOD13A1	No change	slope=0	0.04	0	
(500m)	Not significant greening	Z <1.96, slope>0	59.48	0.0029	
	Not significant browning	Z <1.96, slope<0	19.38	-0.0019	
	Significant greening	Z >1.96, slope>0	19.63	0.0076	
MOD13A2	Significant browning	Z >1.96, slope<0	1.15	-0.0067	
	No change	slope=0	0.14	0	
(1000m)	Not significant greening	Z <1.96, slope>0	58.88	0.0034	
	Not significant browning	Z <1.96, slope<0	20.20	-0.0017	

Substantial differences in both the average EVI slope and the proportion of vegetation greening and browning were observed between urban and rural areas (Table 4.2). At the 250m scale, urban areas exhibited a greening extent of 62.71%, with a corresponding mean slope of 0.0035, while browning occupied 37.22% with an average negative trend of -0.0031. Rural areas exhibited a higher proportion of vegetation greening (65.38%) and a greater degree of greening, as reflected by a mean EVI slope of 0.0050. Conversely, the proportion of browning was relatively smaller (34.60%), yet its average slope was slightly higher (-0.0037). At the 500m scale, in urban areas, greening trends covered 80.56% of the area with a mean slope of 0.0049, while browning occupied 19.44% (average slope: -0.0046). In rural areas, the percentage of greening was 78.09% with higher slope values in contrast to urban areas (0.0065), and the browning percentage was 20%, showing a greater degree of

browning compared to urban areas. At the 1000m scale, urban areas exhibited 80.56% vegetation greening with a slope of 0.0057, whereas vegetation browning made up 19.44% with a browning slope of -0.0033. In contrast, rural regions displayed 78.26% greening (0.0069) in contrast to urban areas, and 21.45% browning with a browning slope of -0.0054.

Table 4.2 Features of overall vegetation changes in urban and rural areas

Scale	Greenness and its changes indexes	Urban	Rural
	Averaged slope of greening	0.0035	0.005
MOD13Q1	Averaged slope of browning	-0.0031	-0.0037
(250m)	Percentage of greening (%)	62.71	65.38
	Percentage of browning (%)	37.22	34.60
	Averaged slope of greening	0.0049	0.0065
MOD13A1	Averaged slope of browning	-0.0046	-0.0070
(500m)	Percentage of greening (%)	80.56	78.09
	Percentage of browning (%)	19.44	21.85
	Averaged slope of greening	0.0057	0.0069
MOD13A2	Averaged slope of browning	-0.0033	-0.0054
(1000m)	Percentage of greening (%)	79.17	78.26
	Percentage of browning (%)	20.83	21.45

4.2.2 Correlation between 2D/3D building morphology and vegetation greening trends

As shown in Table 4.3, the Pearson correlation analysis revealed a relatively low yet statistically significant relationship between 2D/3D building morphology and vegetation greening trends at the 250 m and 500 m spatial resolutions, with correlation coefficients ranging from -0.20 to 0.10. The correlation results at the 1000m scale were not presented because most of the indexes were not significantly correlated with the vegetation greening trends. Furthermore, at the 250m scale, 2D building morphology exhibited a stronger correlation with vegetation greening compared to 3D

morphology, as indicated by higher mean absolute correlation coefficients of 0.19 and 0.12, respectively. Specifically, the SVF demonstrated a low positive correlation with vegetation greening trends, reflected by a correlation coefficient of 0.10. In contrast, BCR, LPI, LSI, ED, BVD, and FAR were negatively correlated with greening, whereas MBH was not significantly related to vegetation greening trends. At the 500m scale, the correlation between 2D building morphology and vegetation greening remained stronger than that of 3D morphology. However, the correlation degree with 2D morphology indexes declined compared to the 250 m scale, while the correlation with 3D morphology indexes increased. Similarly, the SVF showed a positive correlation with vegetation greening, while variables such as BCR, LPI, LSI, ED, BVD, and FAR were negatively correlated with vegetation greening.

Table 4.3 Correlation between vegetation greening and 2D/3D building morphology

Scale	2D building	Correlation	3D building	Correlation
	morphology	coefficient	morphology	coefficient
	BCR	-0.21**	BVD	-0.17**
	LPI	-0.16**	SVF	0.17**
MOD13Q1	LSI	-0.17**	MBH	-0.13**
(250m)	ED	-0.20**	FAR	-0.17**
	Average absolute	0.19	Average absolute	0.16
	value of 2D metrics		value of 3D metrics	
	BCR	-0.17**	BVD	-0.11**
	LPI	-0.11**	SVF	0.18**
MOD13A1	LSI	-0.15**	MBH	-0.08
(500m)	ED	-0.15**	FAR	-0.11**
	Average absolute	0.15	Average absolute	0.13
	value of 2D metrics		value of 3D metrics	

Note: ** means the level of significance at 0.01.

4.2.3 Impact of 2D/3D building morphology on vegetation greening trends 4.2.3.1 Relative contribution of 2D/3D building morphology on vegetation greening trends

As illustrated in Figures 4.2 and Figure 4.3, the relative contribution of 2D and 3D building morphology on vegetation greening trends exhibited notable differences between urban and rural settings at both the 250 m and 500 m spatial scales. At 250m scale, in urban areas, the SVF emerged as the most influential variable, contributing 23.60%. Subsequent contributors included the LPI at 20.10%, MBH at 19.00%, BVD at 12.00%, LSI at 11.50%, and ED at 13.30%. FAR and BCR made only negligible contributions to vegetation greening. In rural areas, LSI had the greatest impact on vegetation greening (27.30%). The second and third most influential variables were the SVF (22.80%) and MBH (17.50%), respectively. The contributions of ED, LPI, BVD, FAR, and BCR showed only minor contributions to vegetation greening.

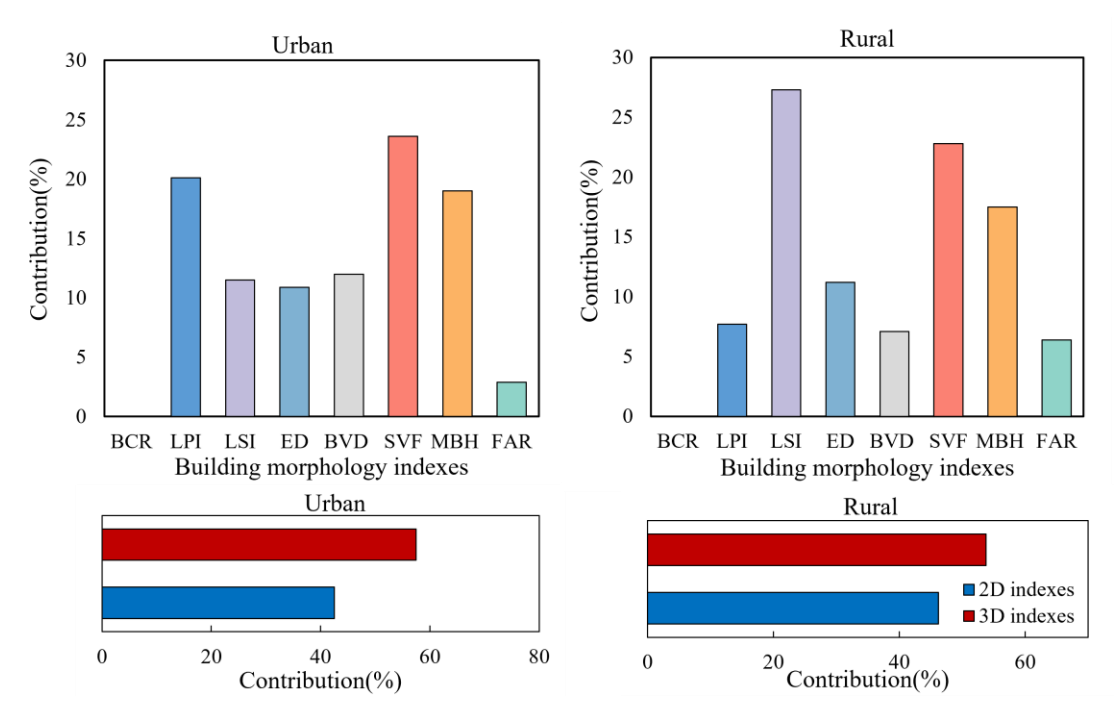


Figure 4.2 Relative contributions (%) of 2D/3D building morphology to vegetation greening trends in urban and rural areas at 250m scale

At the 500m scale within urban environments, SVF was the most significant contributor to vegetation greening, contributing 32.7%, followed by the BCR at 17.2%, MBH at 14.7%, LSI at 12.1%, BVD at 9.5%, LPI at 7.75%, and ED at 5.3%. The influence of FAR was comparatively minor. Similarly, in rural areas, SVF was also the leading factor influencing vegetation greening with a contribution of 39.1%. MBH, LPI, and LSI contributed 16.6%, 12.1%, and 11%, respectively. The relative contributions of other indicators (BCR, ED, BVD, and FAR) were all below 10%.

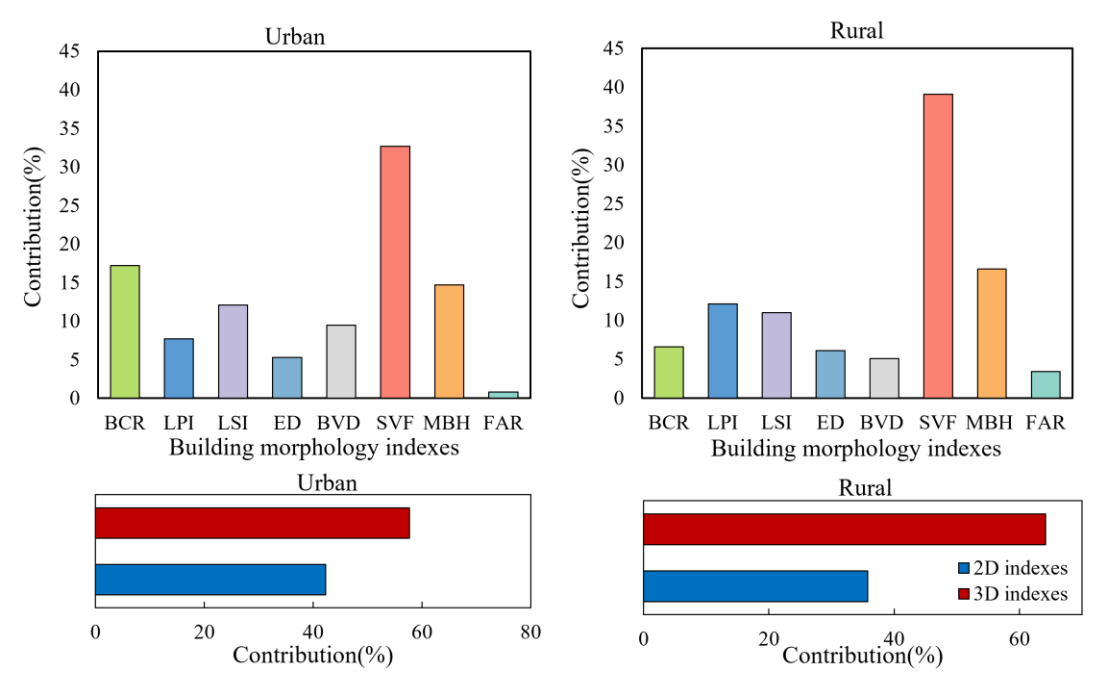


Figure 4.3 Relative contributions (%) of 2D/3D building morphology to vegetation greening trends in urban and rural areas at 500m scale

The 3D building morphology had stronger contributions to vegetation greening than 2D indexes both in 250m and 500m scales. This pattern was more profound in urban areas at the 250m scale. The relative contributions of 2D and 3D building morphology to greening were 42.5% and 57.5% in urban areas, respectively. In rural areas, 2D building morphological indicators accounted for 46.20% of the contribution to greening, while 3D building morphology metrics contributed 53.8%. However, at the 500m scale, the phenomenon that 3D building morphology contributes more than 2D building morphology was more profound in rural areas. In rural areas, 2D and 3D building morphology indicators accounted for 35.8% and 64.2% of total morphology contribution to greening, respectively. In urban areas, 2D building morphological indicators accounted for 42.30% of the total morphology contribution to greening, while 3D indicators occupied 57.7% of the total morphology contribution to greening.

4.2.3.2 The marginal effect of 2D/3D building morphology on vegetation greening trends

To investigate the nonlinear influence of individual building morphology indicators on vegetation greening, we further examined their marginal effects in urban and rural contexts, as illustrated in Figures 4.4 and 4.5, respectively. The marginal effects derived from the BRT model reveal how variations in 2D and 3D building morphology indicators influence vegetation greening. SVF, LPI, MBH, and ED displayed similar marginal effect trends in both urban and rural contexts. The effect of SVF on greening transitioned from negative to positive at 0.82 in urban and 0.88 in rural areas. This implies that sky visibility of around 80% supports vegetation development. LPI had a positive effect on vegetation greening below 15 in urban and below 5 in rural areas but became negative beyond these values. MBH shifted from a negative to a slightly positive influence at 35 m (urban) and 12 m (rural). ED showed a positive impact up to 0.037 m/m² in urban and 0.006 m/m² in rural areas, with a negative effect thereafter. The marginal curves of BVD and LSI exhibited distinct patterns across urban and rural environments. In urban settings, BVD exhibited a positive influence on vegetation greening when values were below 3 m³/m², turned negative between 3 m³/m² and 12 m³/m², and became negligible beyond 12 m³/m². This suggests that maintaining BVD within 0.1-1.3 m³/m² represents the optimal range for promoting vegetation development in urban settings. In rural areas, BVD exhibited a negative effect on greening when lower than 0.1 m³/m² and shifted to a

positive influence when surpassing 1.3 m³/m². Therefore, for rural areas, the favorable conditions for greening occur when BVD values are maintained within the 0.1-1.3 m³/m² range. LSI transitioned from negative to positive influences on greening when exceeding 2.2 in urban areas. In rural areas, the positive effect emerged at 1.05, peaked at 1.2, and became negative when LSI exceeded 3.65. LSI quantifies the geometric complexity of building forms. A higher landscape shape index (LSI) value reflects greater irregularity and complexity in building geometry. Therefore, a moderate degree of building shape complexity is favorable for vegetation greening (2.2–3.3 times the geometric complexity of a square in urban areas and 1.05–3.65 times in rural areas). Exceeding these levels is likely to constrain vegetation growth. The impacts of FAR and BCR on greening were minimal across both urban and rural settings.

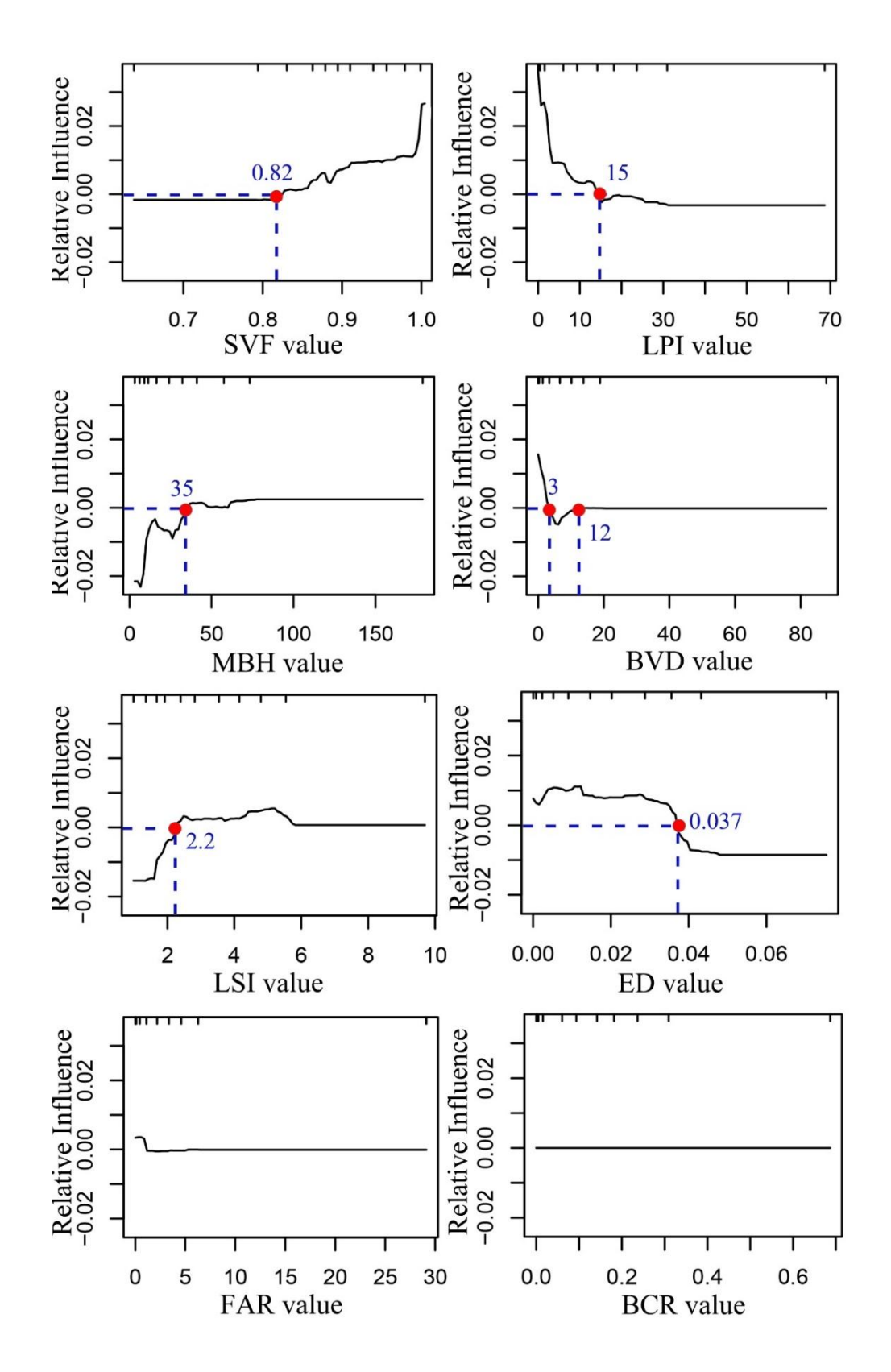


Figure 4.4 The marginal effect of 2D/3D building morphology on the vegetation greening in urban areas at 250m scale

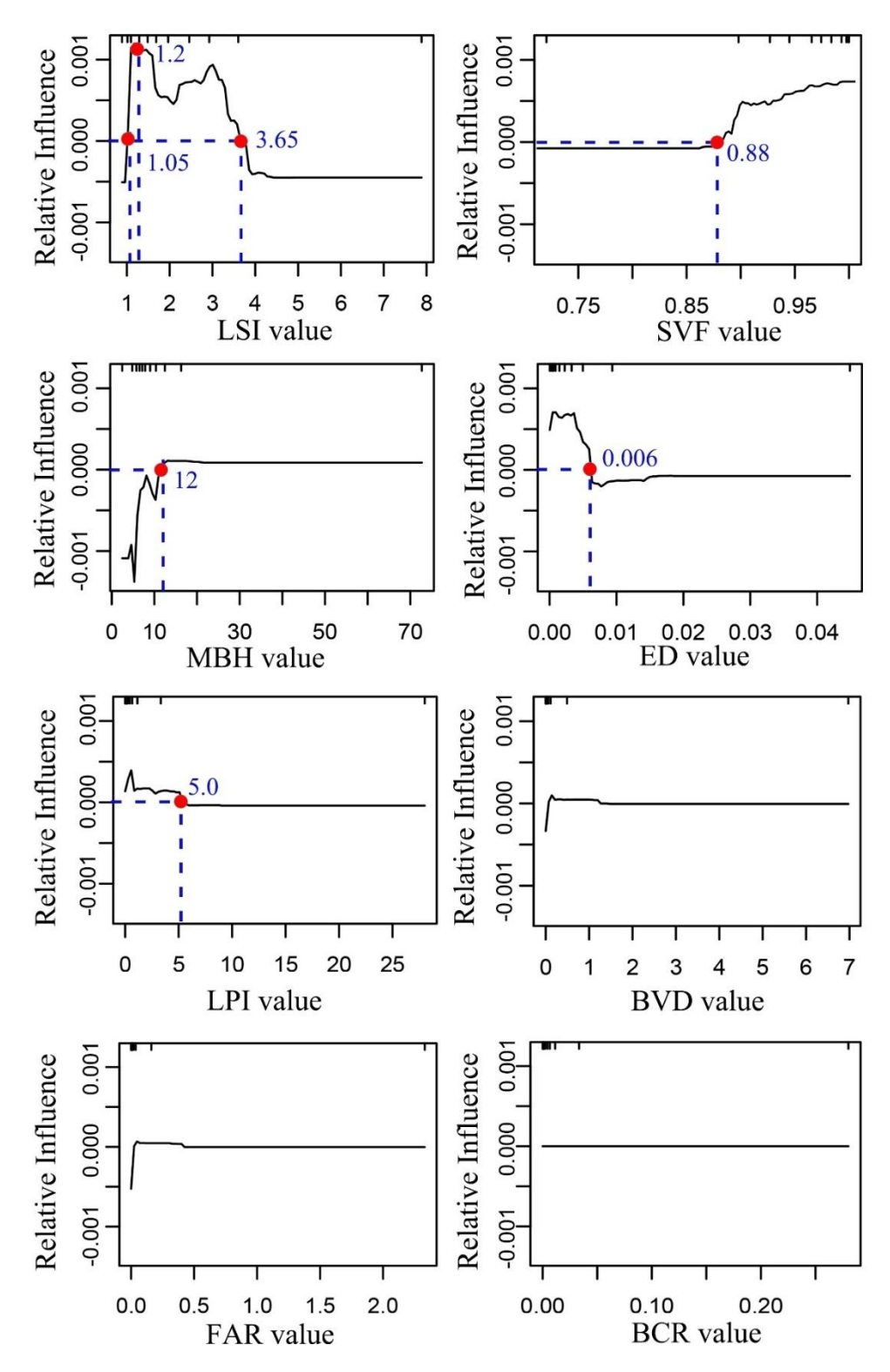


Figure 4.5 The marginal effect of 2D/3D building morphology on vegetation greening in rural areas at 250m scale

The marginal effects of 2D and 3D building morphology on greening at 500m scale in

urban areas are presented in Figure 4.6. The marginal effect of SVF shifted from negative influence to positive influence at the threshold of 0.84. The larger the SVF, the stronger its positive impact on vegetation greening. BCR showed a positive effect on greening when it was smaller than 0.3 and then presented a negative impact on vegetation greening. MBH initially showed a negative effect and transformed to a positive effect at the breakpoint of 11m and eventually tended towards having no impact on vegetation greening. LSI presented a negative impact before reaching the threshold of 9.5 and becomes positive once this threshold is exceeded, indicating that more complex building morphologies benefit vegetation greening. The influence of BVD on vegetation greening transitions from a positive effect to having negligible impact. The marginal effect of LPI transitioned from positive to neutral upon reaching a threshold of 0.025, indicating that greater fragmentation in the built landscape promotes vegetation growth. The influence of ED and FAR on greening is relatively weak, with no clear trends evident.

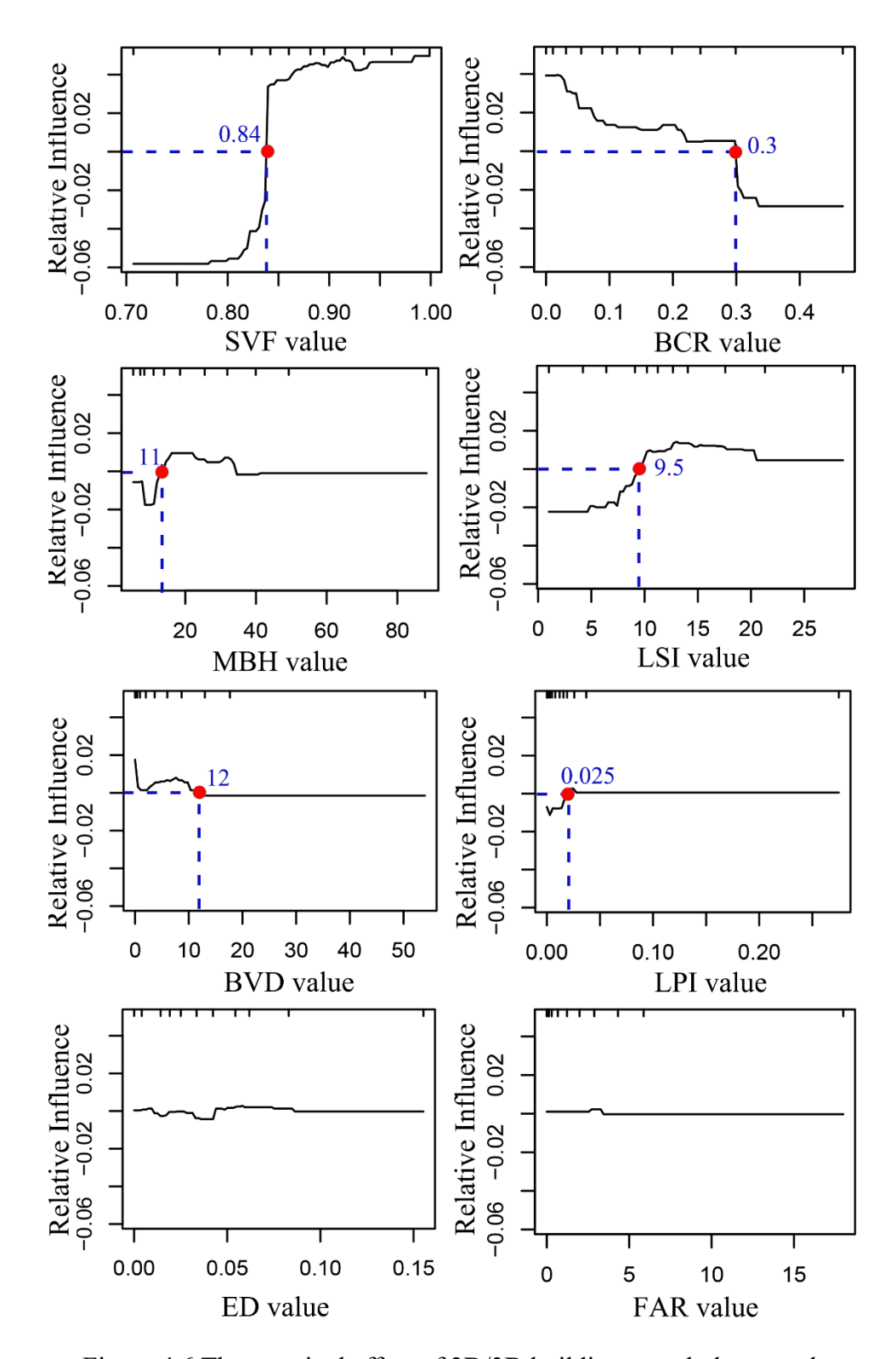


Figure 4.6 The marginal effect of 2D/3D building morphology on the vegetation greening in urban areas at 500m scale

The marginal effects curve of 2D/3D building morphology on greening at 500m scale in rural areas is presented in Figure 4.7. The marginal effects of SVF and MBH displayed similar trends in contrast to urban areas. Specifically, in rural areas, SVF shifted from a negative impact on vegetation growth to a positive effect at a threshold of 0.92. The larger the SVF, the stronger its positive impact on vegetation greening. MBH initially presented a negative effect and when its value exceeded 13m, it appeared to have no impact on vegetation greening. The marginal effects of LPI, LSI, and BCR exhibit opposite trends compared to urban areas. LPI first showed a positive effect on vegetation greening when its value was below 0.005, and after this value, the LPI tended to not affect vegetation greening. LSI has undergone a transition from a positive effect to a negative effect at the threshold of 12. This indicates that in rural areas, simpler building shapes and lower degrees of building fragmentation are more conducive to promoting vegetation growth. BCR illustrated a transition from a negative impact to a slight positive impact. An appropriate layout of building density may be more conducive to promoting vegetation growth.

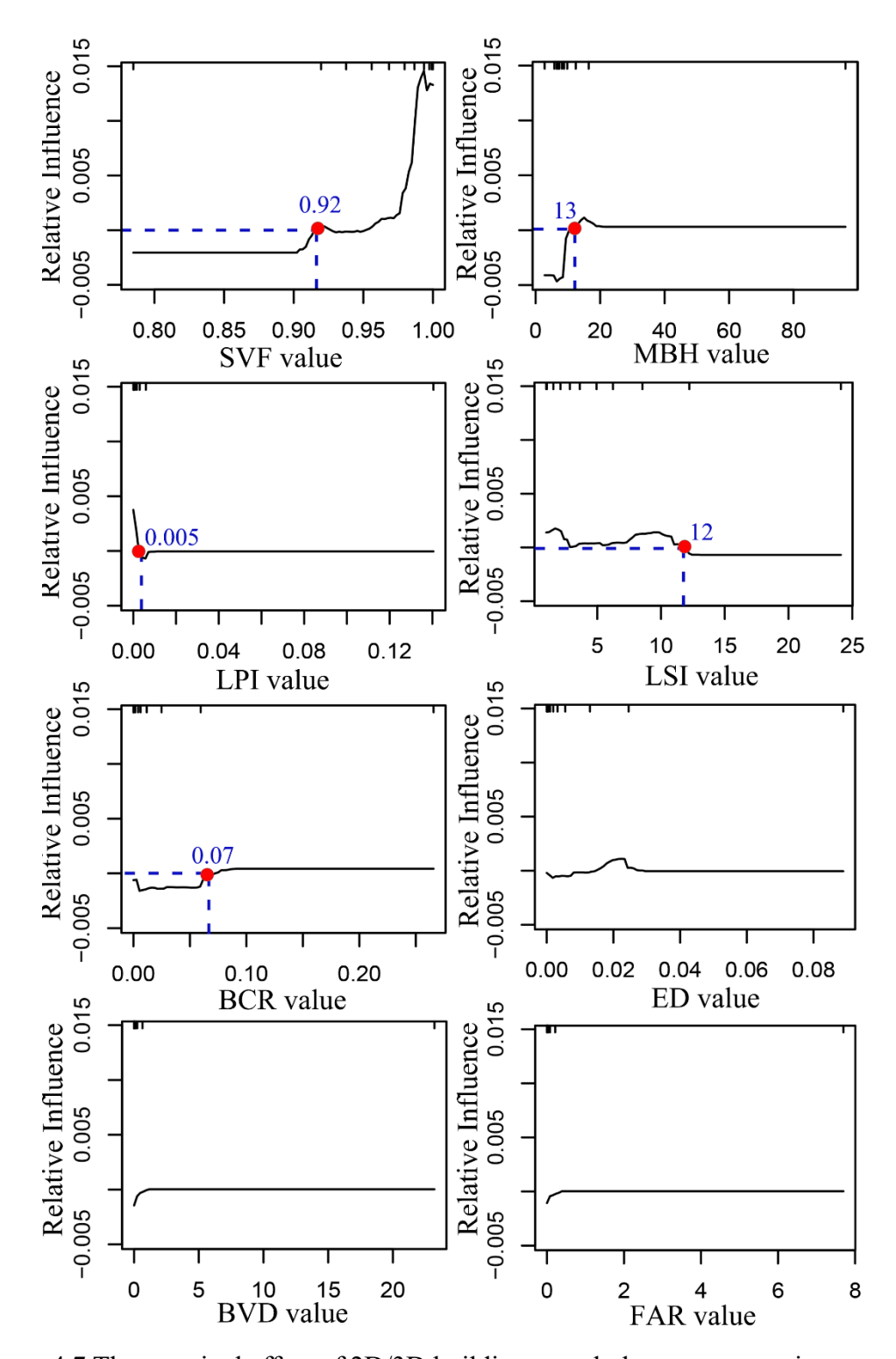


Figure 4.7 The marginal effect of 2D/3D building morphology on vegetation greening in rural areas at 500m scale

4.3 Discussion

4.3.1 The complexity of building morphology - vegetation greening relationship

While previous research has primarily focused on the relationship between vegetation greening and factors such as CO₂ fertilization (Keenan et al., 2013; Ukkola et al., 2016), climate change (Keenan and Riley, 2018; Nemani et al., 2003), land cover/land use transitions (Shen et al., 2023), and nitrogen deposition (Greaver et al., 2016), our study emphasizes the significant role of 2D and 3D building morphology. By employing Pearson correlation analysis and the BRT model, we provide robust evidence that building morphology is closely linked to vegetation growth dynamics. A relatively low but significant correlation was found. This finding indicates that 2D and 3D building morphology may have a moderate relationship with vegetation growth, but it represents only one of several contributing factors. Other environmental and anthropogenic variables also play critical roles. Nonetheless, further investigation into the impact of urban morphological features on vegetation greening remains essential for developing a more holistic understanding of the drivers behind greening dynamics.

Hong Kong is a typical compact city, with high-rise, high-density buildings and extremely limited land for green space in a subtropical climate zone. Existing research conducted in Hong Kong mostly focused on green space dynamics induced by urbanization (Chau and Law, 2023; Feng and Zeng, 2022; Wan and Shen, 2015), climate factors for green space conditions (Feng et al., 2023), and the influence of

green space on microclimate and human health (Li et al., 2023; Wang et al., 2016). Considerable studies have explored the relationship between slope, soil quality, and features of green space on vegetation growth conditions and generally found that the plants in green areas often suffer from substantial growth challenges because of the overcrowded ground (Jim, 1998; Tian et al., 2012). However, few have reported the impact of 2D and 3D building morphology on vegetation greening in Hong Kong. In contrast, our study addresses this research gap by investigating the influencing mechanisms of the 2D/3D building environment on vegetation greening, offering a new insight to understanding vegetation greening drivers. Therefore, this study expands the current research framework on the drivers of vegetation greening but also provides practical insights into the affecting elements of vegetation greening in densely packed urban environments like Hong Kong.

Our findings implied that the impact of 3D building morphology indexes on greening was stronger than 2D indexes. 3D indexes had a more essential impact on the urban climate environment than 2D building morphology was also proved by Cao et al. (Cao et al., 2021). Therefore, the consideration of vertical building morphology in the urban climate and vegetation greening analysis should be highlighted and more 3D building morphology indexes should be developed for urban climate studies in the future. An interesting phenomenon observed was that, based on arguments from previous related studies, the BCR was expected to affect vegetation greening trends. However, our results showed that despite being a key morphological indicator, BCR

appeared to have little to no measurable impact on vegetation greening. Also, the impact of 3D building morphology indicators on greening is greater than 2D indicators (Figure 4.2). A possible explanation for this finding could be the inclusion of 3D indicators in the regression model. These indicators provide a more detailed description of building morphology features. Our results point out the importance of incorporating an assessment of 3D building morphology on vegetable greening. Given the complexity of the built environment, future urban climate research must address achieving more physically representative visibility for 3D morphological indicators. In addition, we found that the 2D/3D building morphology-vegetation greening relationship is not linear but shows a nonlinear pattern that differs from the monotonic positive or negative correlation suggested by some studies. Several critical thresholds were identified within the building morphology-to-vegetation greening association, such as those where the effect switches from positive to negative as well as those where the effect reaches its maximum. These thresholds yield important insights into the complex connections between building morphology and greening, pointing to significant potential for sustainable urban planning.

In addition, these nonlinear patterns imply that optimal thresholds exist for building morphology indicators that optimize the vegetation greening effect. Marginal curves showed that SVF and LSI shifted from being negative to positive to vegetation greening. These results mean that greater SVF and LSI lead to vegetation greening. SVF denotes sky visibility at a specific site. A higher value of SVF allows more

exposure to solar radiation and can provide efficient atmospheric ventilation (Cao et al., 2021; Chatzipoulka et al., 2018). The effect of LPI and ED was changed from a positive to a negative beyond certain thresholds. The LPI thresholds were 15 (urban) and 5 (rural), while those for ED were 0.037 and 0.006, respectively. LPI is the proportion of the largest building patch and serves as an indicator of spatial connectivity. The concentration of large, continuous built-up areas (LPI>15 in urban areas, LPI>5 in rural areas) could help to reduce vegetation greening. This may be attributed to the fact that larger building clusters can decrease available space for vegetation and hinder air circulation, thereby potentially limiting vegetation greening. ED quantifies the total length of building edges relative to the total area, representing the level of spatial fragmentation of buildings. When ED is below 0.037 m/m² in urban areas and below 0.006 m/m² in rural areas, it would be beneficial for vegetation growth, while greater spatial fragmentation of buildings adversely impacts vegetation greening.

4.3.2 Differences in urban and rural greening mechanism

Our study reveals significant differences in greening trends and their driving factors along the urban-rural gradient. First, rural regions exhibited a greater vegetation greening degree in contrast to urban regions (Table 4.2). Such urban-rural disparities may lead to unequal distribution of ecosystem services provided by vegetation, thereby intensifying climate and ecological risks in urban areas, such as heat hazards, drought risk, and pollution exposure (Coleman et al., 2021; Cueva et al., 2022; Li et

al., 2024). Hence, assessing different patterns of vegetation greening across urban and rural areas, and identifying potential determinants of such difference will be crucial to mitigate climate and ecological issues under the context of rapid urbanization. Second, we observed a significant difference in the influence features of 2D/3D building morphology on vegetation greening along urban-rural gradient. SVF was the most influential factor in urban environments, while LSI had the strongest effect on vegetation greening in rural areas. This observation highlights the critical need to examine urban-rural disparities. Urban-rural differences were also evident in the marginal effects of 2D and 3D building morphology on vegetation greening. Specifically, the turning points of 2D and 3D building morphology indices varied between urban and rural areas, providing valuable insights for context-specific morphological optimization. Additionally, LSI exhibited contrasting effects in urban and rural settings. These phenomena both underline the different influencing factors and characteristics for vegetation greening in urban and rural areas, which should be paid attention to in the future. These findings would provide actionable guidance for sustainable building morphology design and emphasize the importance of differentiated planning strategies across urban and rural contexts.

4.3.3 Policy implications

Investigating the impact of 2D and 3D building morphology on vegetation greening is essential for fostering green, resilient, and sustainable urban environments, thereby contributing to the Sustainable Development Goal (SDG) 11 (Sustainable Cities and

Communities). This study provides evidence that the 2D and 3D building morphology exerted an influence on vegetation growth. Our findings deepen our understanding of the characteristics and extent of building morphology that affected the urban ecosystem. Also, this study provides practical information on optimizing building morphology for the planning of greener cities and urban renewal, particularly in high-density cities similar to Hong Kong.

From the 1999, the Hong Kong government has embarked on massive greening programs, such as the Greening Master Plans (GMPs) raised by the Civil Engineering and Development Department (CEDD). Despite the achievement, current greening strategies and policies in Hong Kong have overlooked the building morphological factors in greening frameworks, which are important for the healthy growth of plants. This study offers valuable insights into the integration of building morphology with greening projects, which would help the local greening program achieve its objective of "right-species-at-the-right-place". Specifically, in the context of green city planning, planners and policymakers can promote greener environments by optimizing building morphology from 2D and 3D perspectives. This study suggests that incorporating metrics such as sky view factor (SVF) and landscape shape index (LSI) into the greening program could district-level planning could complement existing GMPs by optimizing building layout and selecting locations with suitable morphology environments for plants. For example, the relative contribution would provide policymakers with factors to prioritize, while the nonlinear association and

turning points existing in the relationship between 2D/3D building morphology and vegetation greening captured by the BRT method can offer essential information into key nodes for building layout planning. Findings on urban-rural disparities provide a basis for the differentiated optimization of building morphology, contributing to more effective sustainable development practices. Rural areas serve as reserves for future urban expansion so that our findings from urban environments can provide essential references for rural areas poised for urbanization. Specifically, for urban areas, as the SVF is an indispensable element, it is crucial to focus on achieving optimal SVF design through judicious building layout while addressing the developmental needs of the region. For example, according to the marginal effect curve, it is advisable to maintain the SVF above 0.82, as values at or above this threshold can effectively contribute to the greening of vegetation. For rural areas, LSI is the primary consideration. It is optimal to maintain LSI within 1.05-3.65 to exert its positive effect, and when LSI equals 1.2, it has the greatest positive impact on greening in rural areas.

4.3.4 Limitations and future research directions

Despite the valuable insights provided, this study has certain limitations. First, based on data from the Hong Kong Herbarium, more than 3,300 vegetation species have been identified in Hong Kong. Disparities of the response of vegetation greening to building morphology may also exist in various vegetation types. Due to the unavailability of high-resolution vegetation type data in Hong Kong, this study was

unable to account for the potential influence of vegetation types on the response of vegetation greening to 2D/3D building morphology. This limitation restricts us from discovering how the renewal of buildings resulted in changes in greenness. In addition, due to the lack of high-resolution mapping data on building heights, it results in limiting this study to Hong Kong, which restricts the generalizability of the findings. To overcome this limitation, future research should develop long-term, highresolution building height data that capture continuous temporal changes. Second, this study focused on only one representative index of vegetation greenness due to its accuracy and widespread use in vegetation trend analysis (Fan et al., 2023; Zhou et al., 2023). Numerous other indices also can be used to characterize vegetation conditions, such as NDVI, NPP, Gross Primary Productivity (GPP), and the more recently introduced kernel NDVI (kNDVI) (Camps-Valls et al., 2021; Wang et al., 2020; Yuan et al., 2007). Studies on vegetation growth analysis have demonstrated that their results are not always consistent, potentially leading to varying conclusions depending on the index used (Ding et al., 2020; D. Zhou et al., 2023). For this reason, further studies should consider multiple vegetation indices that summarize various ecological features. Third, the classification of urban and rural areas in this study is based on the Global Urban Boundaries (GUB) data only. GUB data provides high precision and accurately classifies urban and rural areas according to the 30m artificial impervious surfaces dataset, which is relevant to our study on building morphology. However, the classification of urban and rural areas can vary substantially depending on the criteria used for classification, e.g., population, gross

domestic product, and nighttime light (Florczyk et al., 2019; Li and Zhou, 2017). Since different kinds of datasets and classifications may show different responses, future research must take multi-dataset integration to achieve a more comprehensive evaluation of urban-rural differences. Fourth, this study combines statistical correlation analysis with machine learning model to assess the response of vegetation greening to 2D/3D building morphology. The combined approach helps mitigate the randomness of results compared to relying on a single method. Although the BRT model has been identified as a powerful method for nonlinear relationship detection, the "black box" characteristics of BRT, such as the absence of statistical significance testing and lack of interpretability may potentially introduce uncertainties to the results. Finally, this study has provided only a preliminary exploration of the nonlinear relationship between 2D/3D building morphology and vegetation greening, however, the mechanism of how these 2D/3D building morphology affects vegetation greening is sophisticated. There is an obvious need to acquire more insights from direct measurement and microclimate simulation to uncover deeper underlying mechanisms.

Chapter 5. Direct and indirect effects between building, green space, and urban thermal environments

5.1 Overview

In this chapter, we present the results and analysis (Section 5.2), and discussion (Section 5.3) part of the direct and indirect influence of 2D/3D buildings and green space on urban thermal environments. Moreover, we provide the spatial patterns of summer LST in Hong Kong (Section 5.2.1), the performances of 2D/3D buildings and green space in explaining LST across different scales (Section 5.2.2), and the direct and indirect influence of 2D/3D building and green space on LST (Section 5.2.3). In the Discussion part, we discuss the necessity of introducing both 3D building and green space information in LST-related analysis (Section 5.3.1), the scale effect exists in the relationship between 2D/3D building, 2D/3D green space, and LST (Section 5.3.2), implications of direct and indirect effects of 2D/3D building and green space on LST (Section 5.3.3), and limitations and future research directions (Section 5.3.4).

5.2 Results

5.2.1 Spatial patterns of summer land surface temperature in Hong Kong

The distribution of LSTs in Hong Kong during the summer across different scales is illustrated in Figure 5.1. The overall summer LST in Hong Kong ranged from 24°C to 61°C, with an average of 47 °C. As the scale increases, the minimum value of LST increases and the maximum value decreases, thus the overall range of LST differences decreases as the scale increases. Furthermore, we observed the significant spatial

heterogeneity in LST across different scales in Hong Kong. The spatial distribution of surface temperatures generally showed a high northwest-southeast trend and a low northeast-southwest trend. The cooler areas were primarily block-shaped and located in regions with dense vegetation and water bodies, such as scenic spots, parks, large lakes, wetlands, rivers, and mountain areas. Notably, these included the Tai Mo Shan Country Park, as well as the Lam Tsuen Country Park, Sai Kung West Country Park, Sai Kung East Country Park, Hong Kong Wetland Park, Tai Lam Chung Reservoir, Plover Cove Reservoir, Shan Pui River, and Lantau Island. The high-temperature regions were primarily observed in the highly developed southeast and northwest zones, characterized by dense constructions and factories.

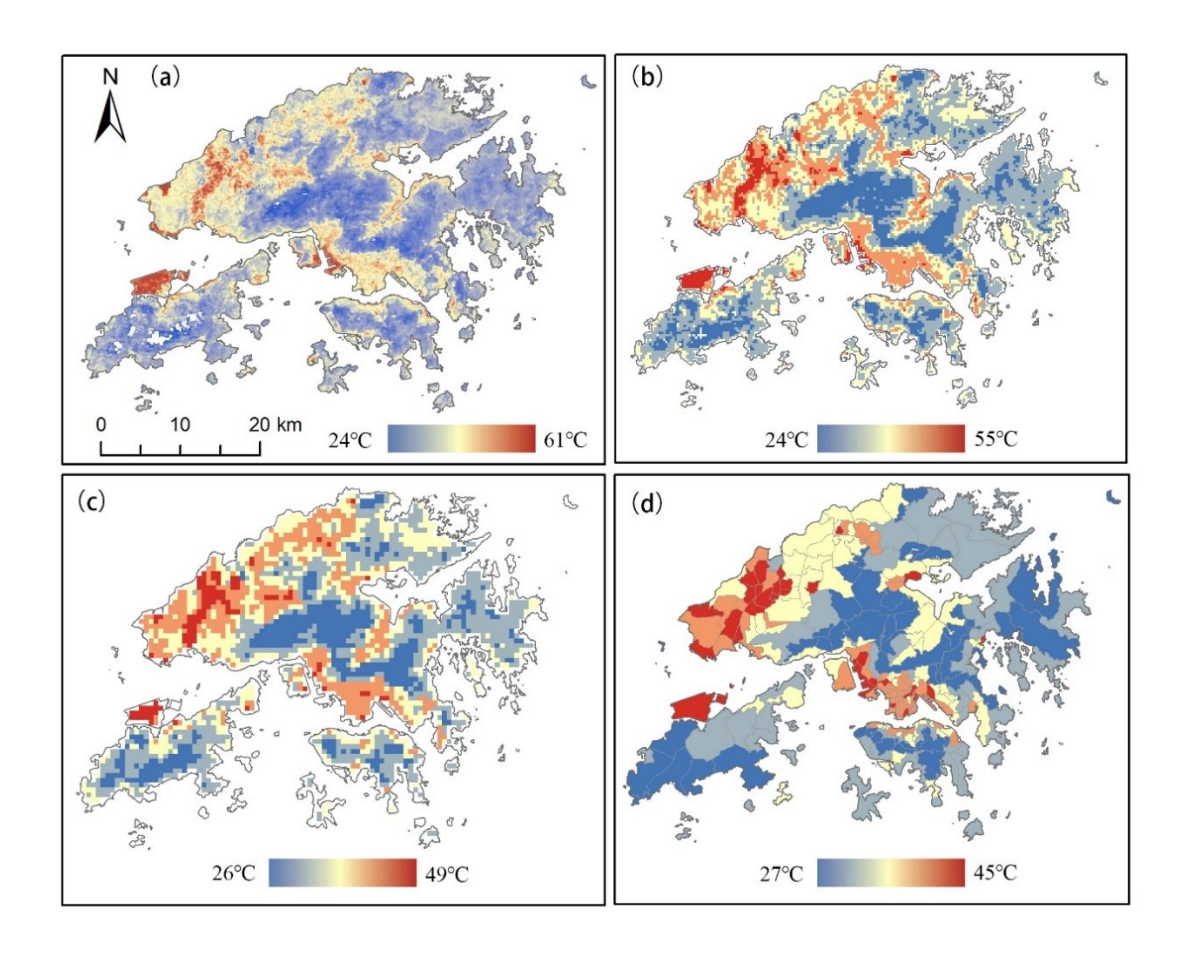


Figure 5.1 Spatial distribution of summer LST in Hong Kong at 100m (a), 300m (b), 600m (c), and district scale (d)

5.2.2 The performances of 2D/3D building and green space in explaining land surface temperature across different scales

It can be observed from Table 5.1, after controlling the Spectral indexes (NDBI, NDVI, and MNDWI) and Terrain and Location (DTM, Slope, and Latitude), the combination of 2D/3D building and green space indexes achieved the best R² across different spatial scales. As the spatial analysis unit size increased, the explanatory power of the regression model also increased. The introduction of 2D/3D building and green space indexes improved 0.027, 0.024, and 0.038 of the explanatory power of the regression model at 300m, 600m, and district scale, respectively.

Specifically, at the 300m scale, from the perspective of comparing buildings and green spaces, regardless of whether in two or three dimensions, the contribution of green spaces to the overall explanatory power is always greater than that of buildings. The 2D green space indexes enhanced the R² of the regression model by 0.008. whereas the 2D building indexes only contributed to a 0.002 increase in explanatory power. The 3D green space indexes improved the explanatory power by 0.014, while 3D building indexes enhanced the R² of the model by 0.01. When combining the 2D/3D green space indexes, there was an enhancement of 0.02 in explanatory power, while 2D/3D building indexes improved the explanatory power by 0.01. From the perspective of 2D and 3D, for both buildings and green spaces, the 3D indexes contributed more to the explanatory power of the regression model compared to the 2D indexes. 3D building indexes improved the R² of the regression model by 0.01, while 2D building indexes enhanced it by 0.002. 3D green space indexes improved the explanatory power by 0.014, while 2D building indexes enhanced it by 0.008. At the 600m scale, in contrast to the 300m scale, the combination of 2D and 3D building and green space indexes contributes less to the overall explanatory power of the model. From the perspective of comparing buildings and green spaces, regardless of whether in two or three dimensions, the contribution of green spaces to the overall explanatory power is always greater than that of buildings. The 2D green space indexes enhanced the explanatory power by 0.006, whereas the 2D building indexes only increased it by 0.002. The 3D green space indexes improved the R² by 0.014,

while 3D building indexes boosted it by 0.011. The combination of 2D/3D green space indexes enhanced the R² by 0.017, while 2D/3D building indexes led to a 0.012 improvement. From the perspective of 2D and 3D, for both buildings and green spaces, the 3D indexes contributed more to the explanatory power of the regression model compared to the 2D indexes. 3D building indexes raised the R² by 0.011, compared to a 0.002 increase from the 2D building indexes. 3D green space indexes improved the R² by 0.014, while 2D building indexes contributed a 0.006 enhancement.

At the district scale, contrary to the analysis results at the pixel level, in both two and three dimensions, the contribution of buildings to enhancing the explanatory power for LST is always greater than that of green spaces. The 2D building indexes enhanced the R² by 0.015, whereas the 2D green space indexes did not contribute to improving the explanatory power. The 3D building indexes contributed a 0.035 increase, while the 3D green space indexes improved R² by 0.013. The combined 2D/3D building indexes led to a 0.035 raise of the R², while 2D/3D green spaces improved the explanatory power by 0.013. From the perspective of 2D and 3D, for both buildings and green spaces, the 3D indexes contributed more to the explanatory power of the regression model compared to the 2D indexes. 3D building indexes improved the R² by 0.035, while 2D building indexes enhanced it by 0.015. 3D green space indexes contributed a 0.013 enhancement of R², while 2D building indexes did not contribute to improving the explanatory power for LST variations.

Table 5.1 Adjusted determinant coefficients (R2) of stepwise multiple linear regression

Scale	300m	600m	District
Controlling factors	0.773	0.824	0.826
Controlling factors + 2D Building	0.775	0.826	0.841
indexes			
Controlling factors + 2D Green space	0.781	0.830	0.826
indexes			
Controlling factors + 3D Building	0.783	0.835	0.861
indexes			
Controlling factors + 3D Green space	0.787	0.838	0.839
indexes			
Controlling factors + 2D/3D Green space	0.793	0.841	0.839
indexes			
Controlling factors + 2D/3D Building	0.783	0.836	0.861
indexes			
Controlling factors + 2D Building and	0.783	0.833	0.841
Green space indexes			
Controlling factors + 2D/3D Building	0.800	0.848	0.864
and Green space indexes			

5.2.3 Direct and indirect effects of 2D/3D building and green space on LST

As shown in Table 5.2, the goodness of fit index (GFI), root mean square error of approximation (RMSEA), root mean square residual (RMR), comparative fit index (CFI), normed fit index (NFI), and non-normed fit index (NNFI) were all meet standard criteria across different scales, which indicated that the model achieved a good fit.

Table 5.2 Evaluation indexes of model fit performance of path analysis at different scales

Scale	GFI	RMSEA	RMR	CFI	NFI	NNFI
Standard	>0.9	< 0.1	< 0.05	>0.9	>0.9	>0.9
300m	1	0.000	0.005	1	1	1
600m	1	0.000	0.005	1	1	1
District	1	0.000	0.013	1	1	1

The results of path analysis at 300m were shown in Figure 5.2, on the one hand, terrain had a negative influence on LST, with a standardized coefficient of -0.297 (R²=0.638). 3D building information, 2D green space information, and 3D green space information also exhibited a negative impact on LST, characterized by a standardized coefficient of -0.243, -0.252, and -0.176 (R²=0.638), respectively. 2D building information showed a positive influence on LST, with a standardized coefficient of 0.457 (R²=0.638). On the other hand, terrain also impacts LST by influencing the 2D building information, 3D building information, 2D green space information, and 3D green space information. Specifically, terrain had negative effects on 2D building information, and 3D building information, characterized by a standardized coefficient of -0.429 (R²=0.184) and -0.269 (R²=0.072). Terrain had positive effects on 2D green space information and 3D green space information, with standardized coefficients of 0.307 (R²=0.432) and 0.239 (R²=0.122). Also, the path analysis illustrated that the 2D/3D building information can affect the 2D/3D green space information. 2D building information negatively affected 2D green space information, with a standardized coefficient of -0.519 and an R² of 0.432. Similarly, 2D building information also had a negative impact on 3D green space information,

evidenced by a standardized coefficient of -0.194 and an R^2 of 0.122. 3D building information had a slight positive effect on both 2D green space information and 3D green space information, evidenced by standardized coefficients of 0.077 (R^2 =0.432) and 0.031 (R^2 =0.122).

Overall, terrain, 2D building information, and 3D building information can both directly and indirectly affect the LST (Table 5.3). The total effect of terrain on LST was -0.615, comprising a direct effect of -0.297 and an indirect effect of -0.318. The total effect of 2D building information on LST was 0.622, including a direct effect of 0.457 and an indirect effect of 0.165. Similarly, the total effect of 3D building information on LST was -0.268, with a direct effect of -0.243 and an indirect effect of -0.025. 2D and 3D green space information only have direct effects, which are -0.252 and -0.176, respectively.

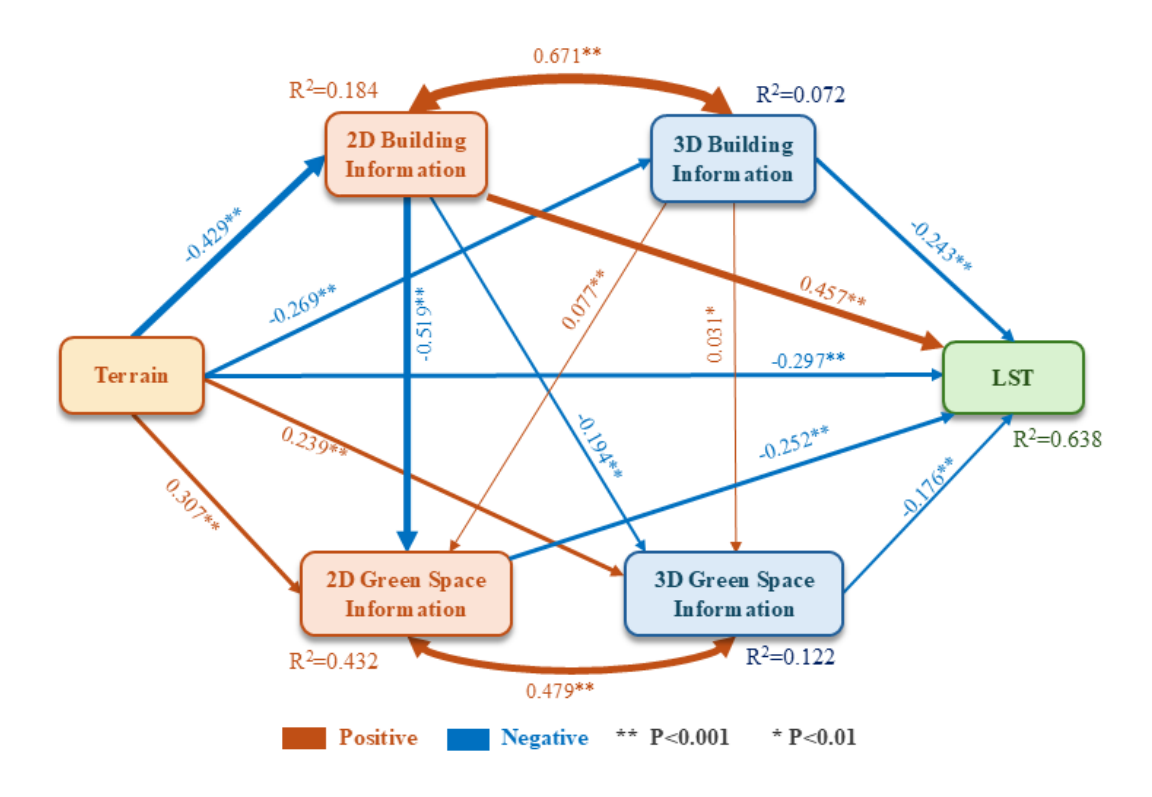


Figure 5.2 Path analysis of the terrain, 2D/3D building/green space, and LST at 300m scale

Figure 5.3 presented the results of path analysis at the 600m scale, similar to the results at the 300m scale, the terrain had a negative influence on LST, with a standardized coefficient of -0.292 (R²=0.691), while the coefficient decreased compared to 300m results. 3D building information, 2D green space information, and 3D green space information also exhibited a negative impact on LST, characterized by a standardized coefficient of -0.263, -0.154, and -0.230 (R²=0.691), respectively. 2D building information showed the strongest direct positive impact on LST, with a standardized coefficient of 0.566 (R²=0.691). Also, terrain impacted LST by influencing the 2D building information, 3D building information, 2D green space information, and 3D green space information. Specifically, terrain had negative effects on 2D building information, and 3D building information, characterized by

standardized coefficients of -0.493 (R²=0.243) and -0.327 (R²=0.107). Terrain had positive effects on 2D green space information and 3D green space information, with standardized coefficients of 0.312 (R²=0.480) and 0.279 (R²=0.142). The 2D/3D building information can affect the 2D/3D green space information at the 600m scale. 2D building information negatively affected 2D green space information, with a standardized coefficient of -0.545 and an R² of 0.480. Similarly, 2D building information also had a negative impact on 3D green space information, evidenced by a standardized coefficient of -0.198 and an R² of 0.142. These values are higher than those observed at the 300m scale in terms of both the coefficients and the R² values. 3D building information only had a significant positive impact on 2D green space with a standardized coefficient of 0.080 (R²=0.480). 3D building information did not have a significant impact on 3D green space information at 600m scale.

Terrain, along with 2D and 3D building information, influences LST both directly and indirectly at 600m scale (Table 5.3). Specifically, the terrain has a total effect of -0.657 on LST, split between a direct effect of -0.292 and an indirect effect of -0.365. Meanwhile, 2D building information contributes a total effect of 0.695 on LST, with a direct effect of 0.566 and an indirect effect of 0.129. In contrast, 3D building information has a lesser overall impact, totaling -0.275, consisting of a direct effect of -0.263 and an indirect effect of -0.012. Both 2D and 3D green space information exerts only direct effects on LST, measuring -0.154 and -0.230, respectively.

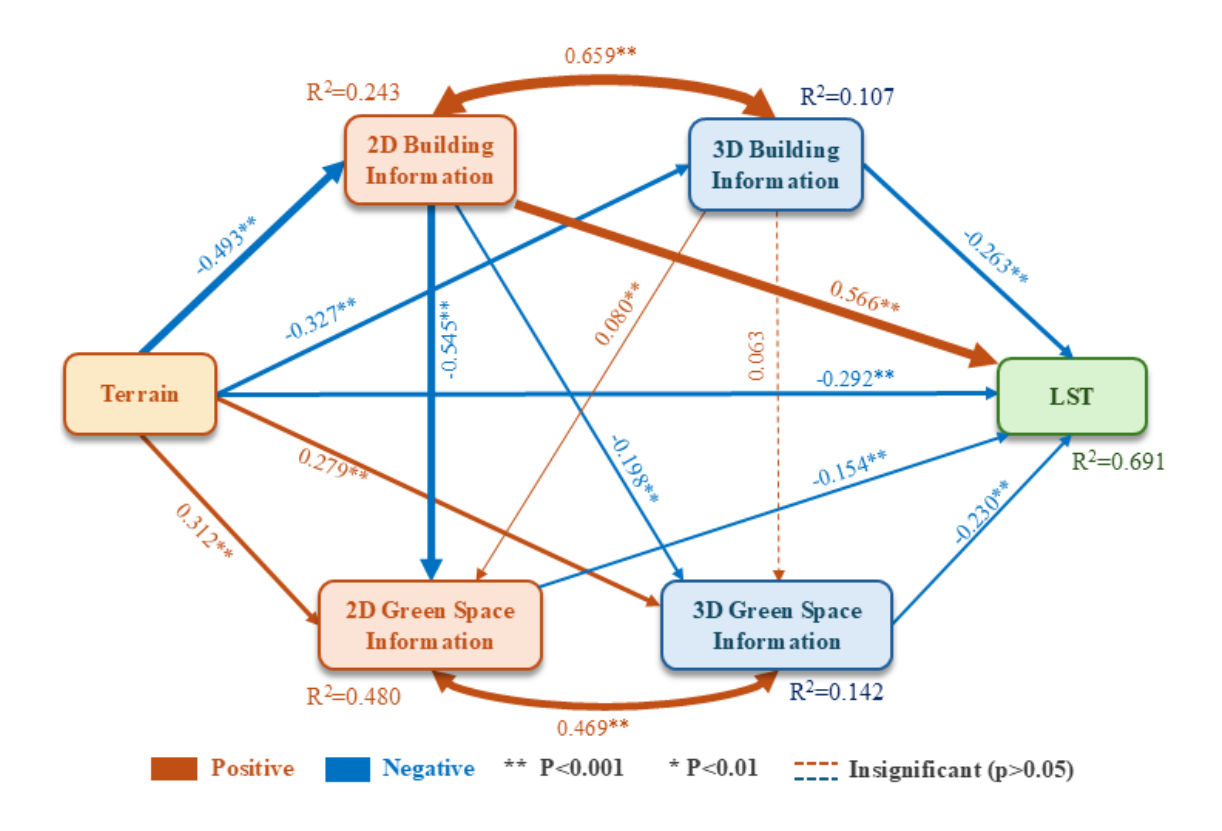


Figure 5.3 Path analysis of the terrain, 2D/3D building/green space, and LST at 600m scale

As illustrated in Figure 5.4, at the district scale, terrain showed a weaker negative influence on LST than pixel scales, with a standardized coefficient of -0.225 (R²=0.741). The negative impact of 3D building information and 2D green space information on LST is amplified at larger scales, as indicated by standardized coefficients of -0.514 and -0.676 (R²=0.741), respectively. The impact of 3D green space on LST was not significant. The positive effect of 2D building information on LST was diminished at the district scale compared to pixel scales, with a standardized coefficient of 0.323 (R²=0.741). Meanwhile, terrain also significantly influenced the 2D building information, 3D building information, 2D green space information, and 3D green space information. To be specific, the terrain had stronger negative effects

on 2D building information and 3D building information, characterized by standardized coefficients of -0.602 (R²=0.360) and -0.470 (R²=0.218). Terrain had positive effects on 2D green space information and 3D green space information, with standardized coefficients of 0.468 (R²=0.772) and 0.571 (R²=0.478). The 2D building information only can affect the 2D green space information at the district scale. 2D building information negatively affected 2D green space information, with a standardized coefficient of -0.501 (R²=0.772). The influence of 2D building information on 3D green space and the influence of 3D building on 2D/3D green space was not significant.

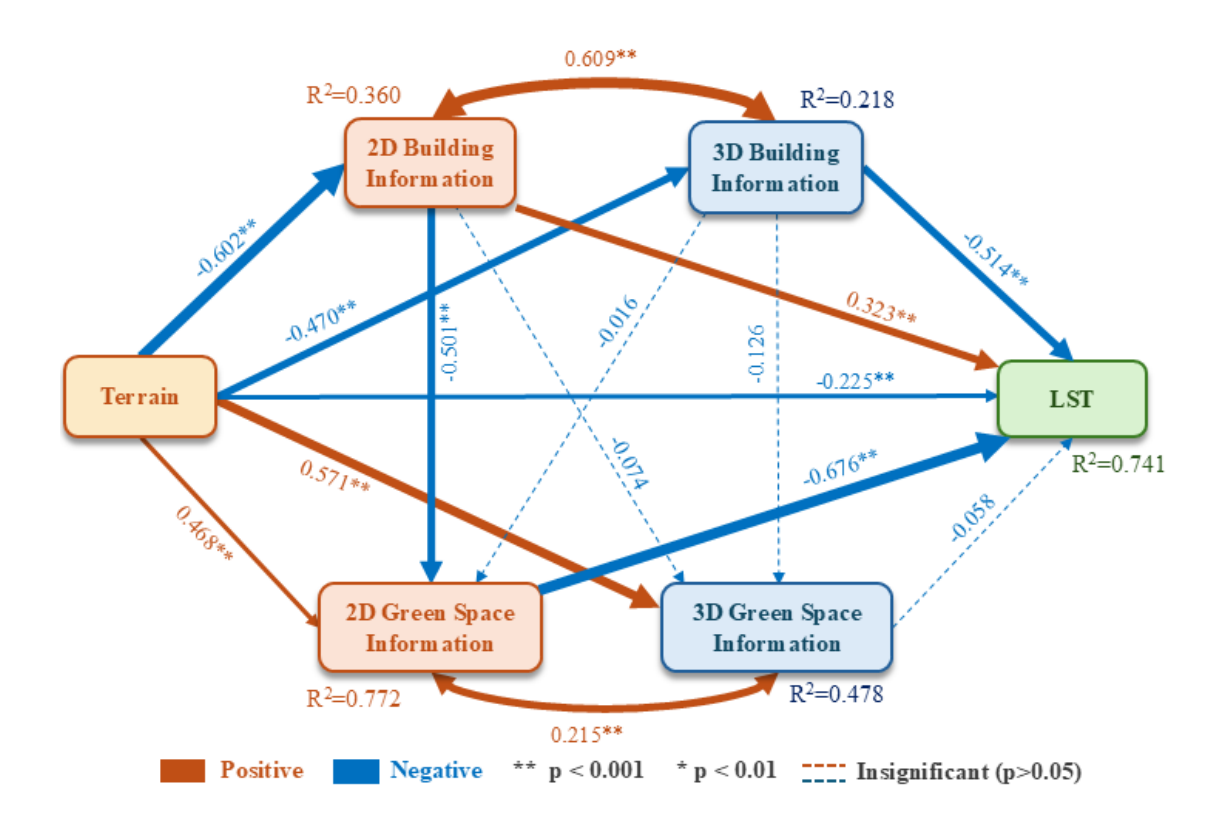


Figure 5.4 Path analysis of the terrain, 2D/3D building/green space, and LST at district scale

Generally, terrain and 2D buildings affected LST both directly and indirectly at the

district scale (Table 5.3). Specifically, the terrain has a total effect of -0.698 on LST, including a direct effect of -0.225 and indirect effects of -0.473. 2D building contributes a total effect of 0.662 on LST, with a direct effect of 0.323 and an indirect effect of 0.339. In contrast, 3D building and 2D green space exert only direct effects on LST, measuring -0.514 and -0.676, respectively. 3D green space had no significant impact on LST on the district scale.

Table 5.3 Summary of the direct and indirect effects of variables on LST

Scale	Variable	Direct effect	Indirect effect	Total effect
	2D building	0.457**	0.165**	0.622**
	information			
	3D building	-0.243**	-0.025**	-0.268**
	information			
300m	2D green space	-0.252**	-	-0.252**
	information			
	3D green space	-0.176**	-	-0.176**
	information			
	Terrain	-0.297**	-0.318**	-0.615**
	2D building	0.566**	0.129**	0.695**
	information			
	3D building	-0.263**	-0.012**	-0.275**
	information			
600m	2D green space	-0.154**	-	-0.154**
	information			
	3D green space	-0.230**	-	-0.230**
	information			
	Terrain	-0.292**	-0.365**	-0.657**
	2D building	0.323**	0.339**	0.662**
	information			
	3D building	-0.514**	-	-0.514**
	information			
District	2D green space	-0.676**	-	-0.676**
	information			
	3D green space	-0.058	-	-0.058
	information			
	Terrain	-0.225**	-0.473**	-0.698**

5.3 Discussion

5.3.1 The necessity of introducing both 2D/3D building and green space morphology indexes in LST-related analysis

Although several studies have emphasized the importance of 2D/3D building and green space morphology in influencing LST variation and mitigation (Chen et al., 2020; Peng et al., 2017), they failed to explicitly quantify the relative contributions of these morphological factors when compared to other basic determinants of LST. This study demonstrates that the combination of 2D/3D building and green space morphology significantly increases the explained variance for LST variation. This study found that 3D building and green space indexes contributed more to explanations of LST variation than 2D indicators at multiple scales. This contrasts with the finding of Xu et al. (2021) (Xu et al., 2024), which reported that 2D morphology indexes significantly influence LST. One plausible explanation for this difference might be the fact that this study included controlling factors in the regression model, while Xu's study only considered morphology indexes. This could lead to bias or uncertainty in the results. Importantly, unlike Xu's study, which took into account only the 3D building morphology indexes, this study includes both 3D building and green space indexes, enhancing the insights into how these two indexes influence LST. 3D building is significantly correlated with urban ventilation and the reception and emission of solar radiation (Li and Hu, 2022; Tian et al., 2019). The evaporative cooling effects of 3D green spaces also can significantly influence LST

(Yuan et al., 2021). We also found that 3D green space indexes are more helpful in enhancing the explanatory power of LST in contrast to 3D building indexes. However, due to the lack of high-resolution green space height data, limited research has investigated the impact of 3D green space indicators on LST and urban climates (Chen et al., 2024). Considering both 2D and 3D impacts of buildings and vegetation on LST can enhance our understanding of its underlying mechanisms and strengthen the link between urban morphology and microclimatic knowledge.

5.3.2 Scale-effect in the relationship between 2D/3D building, 2D/3D green space, and LST

This study explored the performances of 2D/3D buildings and green spaces in enhancing the explanation of LST variations, as well as their direct and indirect effects at different scales. Significant scale effects in the relationship between 2D/3D buildings, 2D/3D green spaces, and LST were observed. Scale effects on LST-influencing factors have also been reported in previous research (Chen et al., 2023; Q. Wu et al., 2019; Xiao et al., 2022; Yang et al., 2020). These imply that planning and strategies for effective mitigation of heat problems need a scale-based approach, as the leading factors may vary with the scale change.

Our finding demonstrated that spatial scales significantly affect the regression model performance, and the relative importance of explanatory variables, and influence the degree of explanatory variables. First, as the spatial scale increases, the explanatory power of all variables for LST also increases. This indicates that interactions at

smaller scales are more complex compared to coarser scales. Second, at pixel scales, green spaces contribute more to enhancing the explanatory power of LST than buildings. However, at the district scale, buildings contribute more to improving LST explanatory power than green spaces. The combination of 2D/3D buildings and green spaces exhibits the strongest capability for enhancing LST explanation on the district scale. We speculate that this might be because green space indexes better help explain LST changes at finer scales, while buildings are more effective in explaining LST variations at coarser scales. Third, the direct and indirect effects of 2D/3D building and green space on LST also varied across different scales. The total effect of terrain on LST increased with scale, primarily due to the increase in indirect effects as the scale enlarges, while the direct effects decreased with increasing scale. The total and direct effects of 2D building features on LST first increased and then decreased, while the indirect effects followed a reverse pattern, decreasing first and increasing thereafter. The total and direct effects of 3D buildings on LST exhibited an upward trend as the scale increased, whereas the indirect effects showed a downward trend. This is primarily due to the insignificance of the influence of 3D buildings on 2D green spaces and 3D green spaces at 600m and district scale. The direct effect of 2D green spaces is greatest at the district scale and smallest at the 600m scale. The direct effect of 3D green spaces on LST shows an increasing trend at the pixel scale but has an insignificant impact on the district scale. These scale effects help guide LST mitigation strategies at different scales. For instance, when planning green spaces at the 300m scale and district level, the focus should be on increasing the 2D area. At the 600m scale, the canopy height characteristics of green spaces become more important.

Across all scales, it is crucial to reduce the coverage of buildings and increase their vertical height.

5.3.3 Implications of direct and indirect effects of 2D/3D building and green space on LST

Unlike previous studies that only considered the effect of 2D/3D buildings and green spaces on thermal environments, this study also considered the potential indirect effects between 2D/3D buildings and 2D/3D green spaces. Additionally, we have considered the potential impact of terrain on 2D/3D buildings and green spaces. Our analysis proved that the terrain not only directly affects LST but also further modulates LST by influencing the distribution of 2D/3D buildings and green spaces. This suggests that terrain plays a complex role in urban climate management, both directly affecting LST and indirectly shaping the landscape patterns. In future urban planning processes, due consideration can be given to placing suitable buildings in areas with slightly higher elevations or slopes, while increasing the height and volume of the buildings. In addition, in mountainous or uneven terrain, the implementation of vertical gardens or terraced green spaces can be used to increase the overall green space.

Furthermore, our results showed that at the 300m and 600m scale, both 2D and 3D building features can significantly influence 2D/3D green spaces. Thus, the distribution of buildings and the strategic placement of green spaces must be

considered in the planning process. In densely built-up areas, increasing the canopy height of green space, implementing green roofs, white roofs, and vertical greening can help to cool down the LST. On the district scale, the impact of 2D building on 3D green space, and 3D building on 2D/3D green space was insignificant. Only the 2D building feature can significantly impact the 2D green space. Therefore, the expansion of the building footprint can be minimized by increasing building heights on a regional scale. This approach not only reduces the warming effect of 2D building structures but also capitalizes on the cooling effect of 3D building features. Moreover, it can reduce the negative effects of 2D building structures on green space coverage, thereby increasing green spaces and fully utilizing its cooling potential.

5.3.4 Limitations and future research directions

There are some limitations in this study. First, given that the heat-related issues are most severe in the summer, our analysis focused only on summer LST in Hong Kong. However, LST exhibits substantial seasonal variation and morphology variables may influence LST differently across seasons. Therefore, investigating the seasonal variation of LST and their response to 2D/3D building and green space indexes is a necessary direction for future research. Second, due to the availability and spatial coverage of LiDAR data, our study was restricted to the high-density city of Hong Kong, which hinders the transferability and generalizability of our study to national or global scales. Additionally, micro-scale studies (less than 100m) are limited due to the scarcity of in situ measurement data. Future research would benefit from integrating

remote sensing data and in situ measurement data to enhance the analysis perspectives. Another limitation is that although we selected several indicators of 2D/3D buildings and green spaces that significantly impact LST based on previous studies, numerous other potential indicators were not considered. Moreover, while this study conducted a multi-scale analysis by selecting 300m, 600m, and district level as analysis scales, this study still has not completely overcome the modifiable areal unit problem (MAUP). MAUP refers to the statistical bias that occurs in spatial analysis when data are aggregated across varying spatial scales (Fotheringham and Wong, 1991; Wu, 2004). The different spatial scales selection can lead to varying research findings although the same analysis is applied to the same data. A wider range of spatial scale analysis should be considered in future studies to enhance the robustness of the observed relationship. Last, this research was based on static data analysis, without considering the change of LST and morphology indexes. Therefore, this study failed to consider dynamic interactions between 2D/3D buildings and 2D/3D green spaces and their dynamic impact on LST due to a lack of multi-year 3D building and green space height data. Fully detangling the dynamic interactions among 2D/3D buildings, 2D/3D green spaces, and LST through the use of dynamic data remains one of the key challenges for future research.

Chapter 6. Conclusions

In this research, the analysis of the interaction between buildings, green space, and urban thermal environments in a high-density city of Hong Kong was conducted. The study concentrates its explorations on the following two aspects: (1) Impacts of 2D/3D building morphology on vegetation greening across the urban-rural gradient, and (2) Direct and indirect influence of 2D/3D building and green space features on urban thermal environments at various spatial scales.

In examining the impact of 2D/3D building morphology on vegetation greening, we developed an analytical framework to investigate the response of vegetation greening to 2D/3D building morphology in Hong Kong, using the Pearson correlation method and the BRT model. Overall, between 2010 and 2020, our analysis identified a significant trend of vegetation greening in Hong Kong, characterized by a mean slope of 0.0024 and greening observed in approximately 69.10% of the total area. Significant uneven trends were shown across urban and rural areas. Although the correlation between building morphology and vegetation greening was relatively low, it remained statistically significant. 3D building morphology exhibited a significantly greater influence on vegetation greening compared to 2D building morphology. Moreover, the influence of 2D/3D building morphology on greening presented a notable urban-rural difference and was highly nonlinear. SVF exerted the greatest influence in urban areas, while LSI had the most significant impact in rural areas. SVF, MBH, LPI, and ED showed similar marginal patterns across urban and rural areas, but their effect directions changed at different thresholds. SVF and MBH

transitioned from negative to positive impacts, while LPI and ED exhibited the opposite trend. The impact of LSI differed between urban and rural areas, showing a transition from negative to positive effects in rural areas and a nonlinear negative—positive—negative pattern in urban areas. The identified complex relationship enriches the current knowledge of how 2D and 3D building morphological characteristics influence vegetation greening across urban and rural areas, which provides meaningful directions for subsequent research and practical guidance for optimizing building layouts for greener city development.

In the analysis of direct and indirect impacts of 2D/3D building and green space on urban thermal environments, we chose the LST to represent the thermal environments and selected ten 2D/3D building and green space indexes to disentangle the direct and indirect effects of 2D/3D building and green space on LST, using the stepwise regression and path analysis method. Overall, the summer LST in Hong Kong ranged from 24°C to 61°C, with an average of 47 °C. Our study has identified significant spatial heterogeneity and scale differences in summer LST across Hong Kong. We found that after adding spectral indexes and terrain as the controlling factors, 2D/3D buildings and green spaces can still effectively enhance the explanatory power of LST variations. Particularly at the district scale, it can increase explanatory power by 0.038. Furthermore, the explanatory power of 3D indicators surpasses that of 2D indicators. At the pixel scale, green spaces demonstrate greater explanatory power than buildings, while at the district scale, buildings exhibit higher explanatory power

than green spaces. Importantly, our analysis demonstrated terrain, 2D/3D building, and 2D/3D green space not only directly impacted LST but also indirectly influenced LST through their interactions. Terrain exerted a direct negative effect on LST and simultaneously played a stronger indirect negative effect by influencing 2D/3D buildings and green spaces, with the total negative effect ranging from -0.698 to -0.615. 2D buildings not only had a positive effect on LST but also enhanced LST further by affecting 2D/3D green spaces. 3D buildings have a negative impact on LST and, at the pixel scale, increase their negative effect by influencing 2D/3D green spaces. 2D/3D building 2D and 3D green spaces have a negative effect on LST, with the impact of 3D green space not being significant at the district scale. By reexamining the interactions between buildings and green spaces from both 2D and 3D perspectives, this research enhances the current understanding of urban thermal environment mechanisms provides insights for thermal problem mitigation, and guides natural-based solutions.

References

- Adelia, A., Yuan, C., Liu, L., Shan, R., 2019. Effects of urban morphology on anthropogenic heat dispersion in tropical high-density residential areas. Energy and Buildings 186, 368–383.
- Aflaki, A., Mirnezhad, M., Ghaffarianhoseini, Amirhosein, Ghaffarianhoseini, Ali, Omrany, H., Wang, Z.-H., Akbari, H., 2017. Urban heat island mitigation strategies: A state-of-the-art review on Kuala Lumpur, Singapore and Hong Kong. Cities 62, 131–145. https://doi.org/10.1016/j.cities.2016.09.003
- Alexander, C., 2021. Influence of the proportion, height and proximity of vegetation and buildings on urban land surface temperature. International Journal of Applied Earth Observation and Geoinformation 95, 102265.
- Antrop, M., 2004. Landscape change and the urbanization process in Europe.

 Landscape and Urban Planning, Development of European Landscapes 67, 9–

 26. https://doi.org/10.1016/S0169-2046(03)00026-4
- Asgarian, A., Amiri, B.J., Sakieh, Y., 2015. Assessing the effect of green cover spatial patterns on urban land surface temperature using landscape metrics approach.

 Urban Ecosyst 18, 209–222. https://doi.org/10.1007/s11252-014-0387-7
- Azhdari, A., Soltani, A., Alidadi, M., 2018. Urban morphology and landscape structure effect on land surface temperature: Evidence from Shiraz, a semi-arid city. Sustainable cities and society 41, 853–864.

- Bai, Y., Wang, W., Liu, M., Xiong, X., Li, S., 2024. Impact of urban greenspace on the urban thermal environment: A case study of Shenzhen, China. Sustainable

 Cities and Society 112, 105591. https://doi.org/10.1016/j.scs.2024.105591
- Ballantyne, A., Smith, W., Anderegg, W., Kauppi, P., Sarmiento, J., Tans, P.,
 Shevliakova, E., Pan, Y., Poulter, B., Anav, A., Friedlingstein, P., Houghton,
 R., Running, S., 2017. Accelerating net terrestrial carbon uptake during the
 warming hiatus due to reduced respiration. Nature Clim Change 7, 148–152.
 https://doi.org/10.1038/nclimate3204
- Baniya, B., Tang, Q., Pokhrel, Y., Xu, X., 2019. Vegetation dynamics and ecosystem service values changes at national and provincial scales in Nepal from 2000 to 2017. Environmental Development 32, 100464.
- Barducci, A., Pippi, I., 1996. Temperature and emissivity retrieval from remotely sensed images using the "Grey body emissivity" method. IEEE Transactions on Geoscience and Remote Sensing 34, 681–695.

 https://doi.org/10.1109/36.499748
- Basu, T., Das, A., 2023. Urbanization induced degradation of urban green space and its association to the land surface temperature in a medium-class city in India. Sustainable Cities and Society 90, 104373.
 https://doi.org/10.1016/j.scs.2022.104373
- Belgiu, M., Drăgut, L., 2016. Random forest in remote sensing: A review of

- applications and future directions. ISPRS Journal of Photogrammetry and Remote Sensing 114, 24–31. https://doi.org/10.1016/j.isprsjprs.2016.01.011
- Berger, C., Rosentreter, J., Voltersen, M., Baumgart, C., Schmullius, C., Hese, S., 2017. Spatio-temporal analysis of the relationship between 2D/3D urban site characteristics and land surface temperature. Remote Sensing of Environment 193, 225–243. https://doi.org/10.1016/j.rse.2017.02.020
- Bowler, D.E., Buyung-Ali, L., Knight, T.M., Pullin, A.S., 2010. Urban greening to cool towns and cities: A systematic review of the empirical evidence.

 Landscape and Urban Planning 97, 147–155.

 https://doi.org/10.1016/j.landurbplan.2010.05.006
- Byomkesh, T., Nakagoshi, N., Dewan, A.M., 2012. Urbanization and green space dynamics in Greater Dhaka, Bangladesh. Landscape Ecol Eng 8, 45–58. https://doi.org/10.1007/s11355-010-0147-7
- Camps-Valls, G., Campos-Taberner, M., Moreno-Martínez, Á., Walther, S., Duveiller, G., Cescatti, A., Mahecha, M.D., Muñoz-Marí, J., García-Haro, F.J., Guanter, L., 2021. A unified vegetation index for quantifying the terrestrial biosphere.

 Science Advances 7, eabc7447.
- Canedoli, C., Crocco, F., Comolli, R., Padoa-Schioppa, E., 2018. Landscape fragmentation and urban sprawl in the urban region of Milan. Landscape Research 43, 632–651. https://doi.org/10.1080/01426397.2017.1336206

- Cao, Q., Luan, Q., Liu, Y., Wang, R., 2021. The effects of 2D and 3D building morphology on urban environments: A multi-scale analysis in the Beijing metropolitan region. Building and Environment 192, 107635.

 https://doi.org/10.1016/j.buildenv.2021.107635
- Chakraborty, T., Qian, Y., 2024. Urbanization exacerbates continental-to regional-scale warming. One Earth 7, 1387–1401.
- Chang, Q., Xiao, X., Doughty, R., Wu, X., Jiao, W., Qin, Y., 2021. Assessing variability of optimum air temperature for photosynthesis across site-years, sites and biomes and their effects on photosynthesis estimation. Agricultural and Forest Meteorology 298–299, 108277.

 https://doi.org/10.1016/j.agrformet.2020.108277
- Chau, N.L., Law, M.S.M., 2023. Impacts of seasonality and urbanization on groundcover community: a case study on the soil slopes of Hong Kong. Urban Ecosystems 26, 1113–1129.
- Chen, A., Yao, L., Sun, R., Chen, L., 2014a. How many metrics are required to identify the effects of the landscape pattern on land surface temperature? Ecological Indicators 45, 424–433.

 https://doi.org/10.1016/j.ecolind.2014.05.002
- Chen, A., Yao, X.A., Sun, R., Chen, L., 2014b. Effect of urban green patterns on surface urban cool islands and its seasonal variations. Urban forestry & urban

- greening 13, 646-654.
- Chen, C., Bagan, H., Yoshida, T., Borjigin, H., Gao, J., 2022. Quantitative analysis of the building-level relationship between building form and land surface temperature using airborne LiDAR and thermal infrared data. Urban Climate 45, 101248.
- Chen, C., Li, D., Keenan, T.F., 2021. Enhanced surface urban heat islands due to divergent urban-rural greening trends. Environ. Res. Lett. 16, 124071. https://doi.org/10.1088/1748-9326/ac36f8
- Chen, J., Zhan, W., Du, P., Li, L., Li, J., Liu, Z., Huang, F., Lai, J., Xia, J., 2022.

 Seasonally disparate responses of surface thermal environment to 2D/3D urban morphology. Building and Environment 214, 108928.

 https://doi.org/10.1016/j.buildenv.2022.108928
- Chen, S., Wong, N.H., Zhang, W., Ignatius, M., 2023. The impact of urban morphology on the spatiotemporal dimension of estate-level air temperature: A case study in the tropics. Building and Environment 228, 109843.
- Chen, X., Wang, H., Yang, J., 2024. Effect of green blue spaces on the urban thermal environment: A field study in Hong Kong. Urban Climate 55, 101912. https://doi.org/10.1016/j.uclim.2024.101912
- Chen, Y., Wu, J., Yu, K., Wang, D., 2020. Evaluating the impact of the building density and height on the block surface temperature. Building and

- Environment 168, 106493. https://doi.org/10.1016/j.buildenv.2019.106493
- Chen, Y., Yang, J., Yu, W., Ren, J., Xiao, X., Xia, J.C., 2023. Relationship between urban spatial form and seasonal land surface temperature under different grid scales. Sustainable Cities and Society 89, 104374.

 https://doi.org/10.1016/j.scs.2022.104374
- Cheung, P.K., Nice, K.A., Livesley, S.J., 2022. Irrigating urban green space for cooling benefits: the mechanisms and management considerations. Environ.

 Res.: Climate 1, 015001. https://doi.org/10.1088/2752-5295/ac6e7c
- Chiang, Y.-C., Liu, H.-H., Li, D., Ho, L.-C., 2023. Quantification through deep learning of sky view factor and greenery on urban streets during hot and cool seasons. Landscape and Urban Planning 232, 104679.
- Coleman, C.J., Yeager, R.A., Riggs, D.W., Coleman, N.C., Garcia, G.R., Bhatnagar, A., Pope, C.A., 2021. Greenness, air pollution, and mortality risk: A U.S. cohort study of cancer patients and survivors. Environment International 157, 106797. https://doi.org/10.1016/j.envint.2021.106797
- Cuerdo-Vilches, T., Díaz, J., López-Bueno, J.A., Luna, M., Navas, M., Mirón, I., Linares, C., 2023. Impact of urban heat islands on morbidity and mortality in heat waves: Observational time series analysis of Spain's five cities. Science of the Total Environment 890, 164412.
- Cueva, J., Yakouchenkova, I.A., Fröhlich, K., Dermann, A.F., Dermann, F., Köhler,

- M., Grossmann, J., Meier, W., Bauhus, J., Schröder, D., Sardemann, G., Thomas, C., Carnicero, A.R., Saha, S., 2022. Synergies and trade-offs in ecosystem services from urban and peri-urban forests and their implication to sustainable city design and planning. Sustainable Cities and Society 82, 103903. https://doi.org/10.1016/j.scs.2022.103903
- Daramola, M.T., Balogun, I.A., 2019. Analysis of the urban surface thermal condition based on sky-view factor and vegetation cover. Remote Sensing Applications: Society and Environment 15, 100253.
- De'ath, G., 2007. Boosted Trees for Ecological Modeling and Prediction. Ecology 88, 243–251. https://doi.org/10.1890/0012-9658(2007)88[243:BTFEMA]2.0.CO;2
- Ding, Z., Peng, J., Qiu, S., Zhao, Y., 2020. Nearly half of global vegetated area experienced inconsistent vegetation growth in terms of greenness, cover, and productivity. Earth's Future 8, e2020EF001618.
- Du, H., Cai, W., Xu, Y., Wang, Z., Wang, Y., Cai, Y., 2017. Quantifying the cool island effects of urban green spaces using remote sensing Data. Urban Forestry & Urban Greening 27, 24–31. https://doi.org/10.1016/j.ufug.2017.06.008
- Efroymson, M.A., 1960. Multiple regression analysis. Mathematical methods for digital computers 191–203.
- Esper, J., Torbenson, M., Büntgen, U., 2024. 2023 summer warmth unparalleled over the past 2,000 years. Nature 631, 94–97. https://doi.org/10.1038/s41586-024-

- Estoque, R.C., Murayama, Y., Myint, S.W., 2017. Effects of landscape composition and pattern on land surface temperature: An urban heat island study in the megacities of Southeast Asia. Science of The Total Environment 577, 349–359. https://doi.org/10.1016/j.scitotenv.2016.10.195
- Ezimand, K., Azadbakht, M., Aghighi, H., 2021. Analyzing the effects of 2D and 3D urban structures on LST changes using remotely sensed data. Sustainable Cities and Society 74, 103216. https://doi.org/10.1016/j.scs.2021.103216
- Fan, C., Myint, S., 2014. A comparison of spatial autocorrelation indices and landscape metrics in measuring urban landscape fragmentation. Landscape and Urban Planning 121, 117–128.
- Fan, F., Xiao, C., Feng, Z., Yang, Y., 2023. Impact of human and climate factors on vegetation changes in mainland southeast asia and yunnan province of China. Journal of Cleaner Production 415, 137690. https://doi.org/10.1016/j.jclepro.2023.137690
- FENG, X., ZENG, Z., 2022. Natural Driving Forces of Vegetation Cover

 Characteristics and Change Trends in the Guangdong-Hong Kong-Macao

 Greater Bay Area. Ecology and Environment 31, 1713.
- Feng, X., Zeng, Z., He, M., 2023. A 20-year vegetation cover change and its response to climate factors in the Guangdong-Hong Kong-Macao Greater Bay Area

- under the background of climate change. Frontiers in Ecology and Evolution 10, 1080734.
- Ferguson, G., Woodbury, A.D., 2007. Urban heat island in the subsurface.

 Geophysical Research Letters 34. https://doi.org/10.1029/2007GL032324
- Florczyk, A., Melchiorri, M., Corbane, C., Schiavina, M., Pesaresi, M., Panagiotis, P., Sabo, F., Freire, S., Ehrlich, D., Kemper, T., Tommasi, P., Airaghi, D., Zanchetta, L., 2019. Description of the GHS Urban Centre Database 2015. https://doi.org/10.2760/037310
- Fotheringham, A.S., Wong, D.W., 1991. The modifiable areal unit problem in multivariate statistical analysis. Environment and planning A 23, 1025–1044.
- Founda, D., Santamouris, M., 2017. Synergies between Urban Heat Island and Heat
 Waves in Athens (Greece), during an extremely hot summer (2012). Scientific
 reports 7, 1–11.
- Frolking, S., Mahtta, R., Milliman, T., Esch, T., Seto, K.C., 2024. Global urban structural growth shows a profound shift from spreading out to building up.

 Nat Cities 1–12. https://doi.org/10.1038/s44284-024-00100-1
- Fu, C., Chen, C., Fu, Z., 2025. Seasonal Spatiotemporal Dynamics and Gradients of the Urban Heat Island Effect in Subtropical Furnace Megacity. Sustainability 17. https://doi.org/10.3390/su17073238
- Galdies, C., Lau, H.S., 2020. Urban Heat Island Effect, Extreme Temperatures and

- Climate Change: A Case Study of Hong Kong SAR, in: Leal Filho, W., Nagy, G.J., Borga, M., Chávez Muñoz, P.D., Magnuszewski, A. (Eds.), Climate Change, Hazards and Adaptation Options: Handling the Impacts of a Changing Climate. Springer International Publishing, Cham, pp. 369–388. https://doi.org/10.1007/978-3-030-37425-9 20
- GALLO, K.P., TARPLEY, J.D., 1996. The comparison of vegetation index and surface temperature composites for urban heat-island analysis. International Journal of Remote Sensing 17, 3071–3076.

 https://doi.org/10.1080/01431169608949128
- Gillespie, A., Rokugawa, S., Matsunaga, T., Cothern, J.S., Hook, S., Kahle, A.B.,
 1998. A temperature and emissivity separation algorithm for Advanced

 Spaceborne Thermal Emission and Reflection Radiometer (ASTER) images.

 IEEE Transactions on Geoscience and Remote Sensing 36, 1113–1126.

 https://doi.org/10.1109/36.700995
- Giridharan, R., Emmanuel, R., 2018. The impact of urban compactness, comfort strategies and energy consumption on tropical urban heat island intensity: A review. Sustainable cities and society 40, 677–687.
- Giridharan, R., Ganesan, S., Lau, S.S.Y., 2004. Daytime urban heat island effect in high-rise and high-density residential developments in Hong Kong. Energy and Buildings 36, 525–534. https://doi.org/10.1016/j.enbuild.2003.12.016

- Giridharan, R., Lau, S.S.Y., Ganesan, S., Givoni, B., 2007. Urban design factors influencing heat island intensity in high-rise high-density environments of Hong Kong. Building and Environment 42, 3669–3684. https://doi.org/10.1016/j.buildenv.2006.09.011
- Gong, F.-Y., Zeng, Z.-C., Zhang, F., Li, X., Ng, E., Norford, L.K., 2018. Mapping sky, tree, and building view factors of street canyons in a high-density urban environment. Building and Environment 134, 155–167.
- Gong, P., Li, X., Wang, J., Bai, Y., Chen, B., Hu, T., Liu, X., Xu, B., Yang, J., Zhang, W., 2020. Annual maps of global artificial impervious area (GAIA) between 1985 and 2018. Remote Sensing of Environment 236, 111510.
- Greaver, T.L., Clark, C.M., Compton, J.E., Vallano, D., Talhelm, A.F., Weaver, C.P., Band, L.E., Baron, J.S., Davidson, E.A., Tague, C.L., 2016. Key ecological responses to nitrogen are altered by climate change. Nature Climate Change 6, 836–843.
- Guo, G., Wu, Z., Chen, Y., 2019. Complex mechanisms linking land surface temperature to greenspace spatial patterns: Evidence from four southeastern Chinese cities. Science of The Total Environment 674, 77–87. https://doi.org/10.1016/j.scitotenv.2019.03.402
- Guo, G., Wu, Z., Xiao, R., Chen, Y., Liu, X., Zhang, X., 2015. Impacts of urban biophysical composition on land surface temperature in urban heat island

- clusters. Landscape and Urban Planning 135, 1–10.
- Guo, L., Du, S., Sun, W., Fan, D., Wu, Y., 2025. Multi-scale impact of urban building function and 2D/3D morphology on urban heat island effect: a case study in Shanghai, China. Energy and Buildings 115719.

 https://doi.org/10.1016/j.enbuild.2025.115719
- Guo, Y., Gasparrini, A., Armstrong, B.G., Tawatsupa, B., Tobias, A., Lavigne, E.,
 Coelho, M. de S.Z.S., Pan, X., Kim, H., Hashizume, M., Honda, Y., Guo, Y.L.L., Wu, C.-F., Zanobetti, A., Schwartz, J.D., Bell, M.L., Scortichini, M.,
 Michelozzi, P., Punnasiri, K., Li, S., Tian, L., Garcia, S.D.O., Seposo, X.,
 Overcenco, A., Zeka, A., Goodman, P., Dang, T.N., Dung, D.V., Mayvaneh, F.,
 Saldiva, P.H.N., Williams, G., Tong, S., 2017. Heat Wave and Mortality: A
 Multicountry, Multicommunity Study. Environmental Health Perspectives
 125, 087006. https://doi.org/10.1289/EHP1026
- Haaland, C., Van Den Bosch, C.K., 2015. Challenges and strategies for urban greenspace planning in cities undergoing densification: A review. Urban Forestry & Urban Greening 14, 760–771. https://doi.org/10.1016/j.ufug.2015.07.009
- Haberl, H., Erb, K.H., Krausmann, F., Gaube, V., Bondeau, A., Plutzar, C., Gingrich, S., Lucht, W., Fischer-Kowalski, M., 2007. Quantifying and mapping the human appropriation of net primary production in earth's terrestrial ecosystems. Proc. Natl. Acad. Sci. U.S.A. 104, 12942–12947.
 https://doi.org/10.1073/pnas.0704243104

- Han, D., An, H., Wang, F., Xu, X., Qiao, Z., Wang, M., Sui, X., Liang, S., Hou, X.,
 Cai, H., 2022. Understanding seasonal contributions of urban morphology to
 thermal environment based on boosted regression tree approach. Building and
 Environment 226, 109770.
- Han, S., Hou, H., Estoque, R.C., Zheng, Y., Shen, C., Murayama, Y., Pan, J., Wang,
 B., Hu, T., 2023. Seasonal effects of urban morphology on land surface
 temperature in a three-dimensional perspective: A case study in Hangzhou,
 China. Building and Environment 228, 109913.
 https://doi.org/10.1016/j.buildenv.2022.109913
- Han, W., 2023. Analyzing the scale dependent effect of urban building morphology on land surface temperature using random forest algorithm. Scientific Reports 13, 19312.
- Handayani, H.H., Estoque, R.C., Murayama, Y., 2018. Estimation of built-up and green volume using geospatial techniques: A case study of Surabaya,

 Indonesia. Sustainable cities and society 37, 581–593.
- He, C., Liu, Z., Gou, S., Zhang, Q., Zhang, J., Xu, L., 2019. Detecting global urban expansion over the last three decades using a fully convolutional network.

 Environ. Res. Lett. 14, 034008. https://doi.org/10.1088/1748-9326/aaf936
- He, Y., Liu, Z., Ng, E., 2022. Parametrization of irregularity of urban morphologies for designing better pedestrian wind environment in high-density cities A

- wind tunnel study. Building and Environment 226, 109692. https://doi.org/10.1016/j.buildenv.2022.109692
- He, Y., Wang, Z., Wong, H.M., Chen, G., Ren, C., Luo, M., Li, Y., Lee, T., Chan, P.W., Ho, J.Y., Ng, E., 2023. Spatial-temporal changes of compound temperature-humidity extremes in humid subtropical high-density cities: An observational study in Hong Kong from 1961 to 2020. Urban Climate 51, 101669.
 https://doi.org/10.1016/j.uclim.2023.101669
- Hecht, R., Meinel, G., Buchroithner, M.F., 2008. Estimation of urban green volume based on single-pulse LiDAR data. IEEE Transactions on Geoscience and Remote Sensing 46, 3832–3840.
- Heinl, M., Hammerle, A., Tappeiner, U., Leitinger, G., 2015. Determinants of urban-rural land surface temperature differences A landscape scale perspective.

 Landscape and Urban Planning 134, 33–42.

 https://doi.org/10.1016/j.landurbplan.2014.10.003
- Ho, J.Y., Shi, Y., Lau, K.K., Ng, E.Y., Ren, C., Goggins, W.B., 2023. Urban heat island effect-related mortality under extreme heat and non-extreme heat scenarios: A 2010–2019 case study in Hong Kong. Science of The Total Environment 858, 159791.
- Hu, L., Wendel, J., 2019. Analysis of urban surface morphologic effects on diurnal thermal directional anisotropy. ISPRS Journal of Photogrammetry and Remote

- Sensing 148, 1–12.
- Hu, Y., Dai, Z., Guldmann, J.-M., 2020. Modeling the impact of 2D/3D urban indicators on the urban heat island over different seasons: A boosted regression tree approach. Journal of Environmental Management 266, 110424. https://doi.org/10.1016/j.jenvman.2020.110424
- Hua, J., Zhang, X., Ren, C., Shi, Y., Lee, T.-C., 2021. Spatiotemporal assessment of extreme heat risk for high-density cities: A case study of Hong Kong from 2006 to 2016. Sustainable Cities and Society 64, 102507.
 https://doi.org/10.1016/j.scs.2020.102507
- Huang, S., Wang, S., Gan, Y., Wang, C., Horton, D.E., Li, C., Zhang, X., Niyogi, D., Xia, J., Chen, N., 2024. Widespread global exacerbation of extreme drought induced by urbanization. Nature Cities 1, 597–609.
- Huang, X., Wang, Y., 2019. Investigating the effects of 3D urban morphology on the surface urban heat island effect in urban functional zones by using high-resolution remote sensing data: A case study of Wuhan, Central China. ISPRS Journal of Photogrammetry and Remote Sensing 152, 119–131.
 https://doi.org/10.1016/j.isprsjprs.2019.04.010
- Huete, A., Didan, K., Miura, T., Rodriguez, E.P., Gao, X., Ferreira, L.G., 2002.

 Overview of the radiometric and biophysical performance of the MODIS vegetation indices. Remote sensing of environment 83, 195–213.

- IPCC, I.P. on C.C., 2021. Climate Change 2021: The Physical Science Basis (No. AR6 WGI). IPCC, Geneva, Switzerland.
- Ji, L., Laouadi, A., Shu, C., Gaur, A., Lacasse, M., Wang, L. (Leon), 2022. Evaluating approaches of selecting extreme hot years for assessing building overheating conditions during heatwaves. Energy and Buildings 254, 111610.
 https://doi.org/10.1016/j.enbuild.2021.111610
- Ji, Y., Zhan, W., Du, H., Wang, S., Li, L., Xiao, J., Liu, Z., Huang, F., Jin, J., 2023.
 Urban-rural gradient in vegetation phenology changes of over 1500 cities
 across China jointly regulated by urbanization and climate change. ISPRS
 Journal of Photogrammetry and Remote Sensing 205, 367–384.
 https://doi.org/10.1016/j.isprsjprs.2023.10.015
- Jia, S., Wang, Y., 2021. Effect of heat mitigation strategies on thermal environment, thermal comfort, and walkability: A case study in Hong Kong. Building and Environment 201, 107988. https://doi.org/10.1016/j.buildenv.2021.107988
- Jia, S., Wang, Y., Liang, T.C., Weng, Q., Yoo, C., Chen, W., Ding, X., 2024.
 Multiscale estimation of the cooling effect of urban greenspace in subtropical and tropical cities. Urban Forestry & Urban Greening 98, 128390.
 https://doi.org/10.1016/j.ufug.2024.128390
- Jia, W., Zhao, S., 2020. Trends and drivers of land surface temperature along the urban-rural gradients in the largest urban agglomeration of China. Science of

- The Total Environment 711, 134579. https://doi.org/10.1016/j.scitotenv.2019.134579
- Jia, W., Zhao, S., Liu, S., 2018. Vegetation growth enhancement in urban environments of the Conterminous United States. Global Change Biology 24, 4084–4094. https://doi.org/10.1111/gcb.14317
- Jia, W., Zhao, S., Zhang, X., Liu, S., Henebry, G.M., Liu, L., 2021. Urbanization imprint on land surface phenology: The urban–rural gradient analysis for Chinese cities. Global Change Biology 27, 2895–2904.
 https://doi.org/10.1111/gcb.15602
- Jiang, R., Li, W., Lu, X.X., Xie, J., Zhao, Y., Li, F., 2021. Assessment of temperature extremes and climate change impacts in Singapore, 1982–2018. Singapore Journal of Tropical Geography 42, 378–396. https://doi.org/10.1111/sjtg.12384
- Jiao, L., Xu, G., Xiao, F., Liu, Y., Zhang, B., 2017. Analyzing the Impacts of Urban Expansion on Green Fragmentation Using Constraint Gradient Analysis. The Professional Geographer 69, 553–566.
 https://doi.org/10.1080/00330124.2016.1266947
- Jim, C.Y., 1998. Impacts of intensive urbanization on trees in Hong Kong.

 Environmental Conservation 25, 146–159.
- Jimenez-Munoz, J.C., Cristobal, J., Sobrino, J.A., Soria, G., Ninyerola, M., Pons, X., 2009. Revision of the Single-Channel Algorithm for Land Surface

- Temperature Retrieval From Landsat Thermal-Infrared Data. IEEE Transactions on Geoscience and Remote Sensing 47, 339–349. https://doi.org/10.1109/TGRS.2008.2007125
- Kamal, A., Abidi, S.M.H., Mahfouz, A., Kadam, S., Rahman, A., Hassan, I.G., Wang,
 L.L., 2021. Impact of urban morphology on urban microclimate and building energy loads. Energy and Buildings 253, 111499.
 https://doi.org/10.1016/j.enbuild.2021.111499
- Ke, X., Men, H., Zhou, T., Li, Z., Zhu, F., 2021. Variance of the impact of urban green space on the urban heat island effect among different urban functional zones:

 A case study in Wuhan. Urban Forestry & Urban Greening 62, 127159.
- Keenan, T.F., Hollinger, D.Y., Bohrer, G., Dragoni, D., Munger, J.W., Schmid, H.P., Richardson, A.D., 2013. Increase in forest water-use efficiency as atmospheric carbon dioxide concentrations rise. Nature 499, 324–327.
- Keenan, T.F., Riley, W.J., 2018. Greening of the land surface in the world's cold regions consistent with recent warming. Nature Climate Change 8, 825–828.
- Khoshnoodmotlagh, S., Daneshi, A., Gharari, S., Verrelst, J., Mirzaei, M., Omrani, H., 2021. Urban morphology detection and it's linking with land surface temperature: A case study for Tehran Metropolis, Iran. Sustainable Cities and Society 74, 103228. https://doi.org/10.1016/j.scs.2021.103228
- Kong, F., Yin, H., James, P., Hutyra, L.R., He, H.S., 2014. Effects of spatial pattern of

- greenspace on urban cooling in a large metropolitan area of eastern China.

 Landscape and urban planning 128, 35–47.
- Kong, L., Lau, K.K.-L., Yuan, C., Chen, Y., Xu, Y., Ren, C., Ng, E., 2017. Regulation of outdoor thermal comfort by trees in Hong Kong. Sustainable Cities and Society 31, 12–25. https://doi.org/10.1016/j.scs.2017.01.018
- Koprowska, K., Łaszkiewicz, E., Kronenberg, J., 2020. Is urban sprawl linked to green space availability? Ecological Indicators 108, 105723. https://doi.org/10.1016/j.ecolind.2019.105723
- Kotharkar, R., Dongarsane, P., Keskar, R., 2023. Determining influence of urban morphology on air temperature and heat index with hourly emphasis. Building and Environment 233, 110044.
- Lan, Y., Zhan, Q., 2017. How do urban buildings impact summer air temperature? The effects of building configurations in space and time. Building and Environment 125, 88–98. https://doi.org/10.1016/j.buildenv.2017.08.046
- Lau, K.K.-L., Chung, S.C., Ren, C., 2019. Outdoor thermal comfort in different urban settings of sub-tropical high-density cities: An approach of adopting local climate zone (LCZ) classification. Building and Environment 154, 227–238.
- Lau, K.K.-L., Ren, C., Shi, Y., Zheng, V., Yim, S., Lai, D., 2015. Determining the optimal size of local climate zones for spatial mapping in high-density cities.

 Presented at the Proceedings of the 9th International Conference on Urban

- Climate jointly with 12th Symposium on the Urban Environment, Toulouse, France, pp. 20–24.
- Levermore, G., Parkinson, J., Lee, K., Laycock, P., Lindley, S., 2018. The increasing trend of the urban heat island intensity. Urban Climate 24, 360–368. https://doi.org/10.1016/j.uclim.2017.02.004
- Li, B., Cheng, C., 2024. Quantifying the impact of buildings on land surface temperature: Intrinsic structure and extrinsic morphology. Building and Environment 259, 111680.
- Li, B., Liu, Y., Xing, H., Meng, Y., Yang, G., Liu, X., Zhao, Y., 2022. Integrating urban morphology and land surface temperature characteristics for urban functional area classification. Geo-Spatial Information Science 25, 337–352.
- Li, D., Sun, T., Liu, M., Yang, L., Wang, L., Gao, Z., 2015. Contrasting responses of urban and rural surface energy budgets to heat waves explain synergies between urban heat islands and heat waves. Environmental Research Letters 10, 054009.
- Li, D., Wu, S., Liang, Z., Li, S., 2020. The impacts of urbanization and climate change on urban vegetation dynamics in China. Urban Forestry & Urban Greening 54, 126764. https://doi.org/10.1016/j.ufug.2020.126764
- Li, F., Zheng, W., Wang, Y., Liang, J., Xie, S., Guo, S., Li, X., Yu, C., 2019. Urban

 Green Space Fragmentation and Urbanization: A Spatiotemporal Perspective.

- Forests 10, 333. https://doi.org/10.3390/f10040333
- Li, G., Cao, Y., Fang, C., Sun, S., Qi, W., Wang, Z., He, S., Yang, Z., 2025. Global urban greening and its implication for urban heat mitigation. Proc. Natl. Acad. Sci. U.S.A. 122, e2417179122. https://doi.org/10.1073/pnas.2417179122
- Li, H., Li, Y., Wang, T., Wang, Z., Gao, M., Shen, H., 2021. Quantifying 3D building form effects on urban land surface temperature and modeling seasonal correlation patterns. Building and Environment 204, 108132. https://doi.org/10.1016/j.buildenv.2021.108132
- Li, H., Wu, J., 2004. Use and misuse of landscape indices. Landscape ecology 19, 389–399.
- Li, J., Song, C., Cao, L., Zhu, F., Meng, X., Wu, J., 2011. Impacts of landscape structure on surface urban heat islands: A case study of Shanghai, China. Remote sensing of environment 115, 3249–3263.
- Li, L., Zha, Y., 2020. Population exposure to extreme heat in China: Frequency, intensity, duration and temporal trends. Sustainable Cities and Society 60, 102282. https://doi.org/10.1016/j.scs.2020.102282
- Li, Long, Zhan, W., Ju, W., Peñuelas, J., Zhu, Z., Peng, S., Zhu, X., Liu, Z., Zhou, Y., Li, J., Lai, J., Huang, F., Yin, G., Fu, Y., Li, M., Yu, C., 2023. Competition between biogeochemical drivers and land-cover changes determines urban greening or browning. Remote Sensing of Environment 287, 113481.

- https://doi.org/10.1016/j.rse.2023.113481
- Li, N., Zhao, F., Chen, S., Li, C., Wang, Y., Ma, Y., Chen, L., 2024. Indirect non-linear effects of landscape patterns on vegetation growth in Kunming City. npj Urban Sustain 4, 30. https://doi.org/10.1038/s42949-024-00165-w
- Li, X., Li, W., Middel, A., Harlan, S.L., Brazel, A.J., Turner Ii, B., 2016. Remote sensing of the surface urban heat island and land architecture in Phoenix, Arizona: Combined effects of land composition and configuration and cadastral–demographic–economic factors. Remote Sensing of Environment 174, 233–243.
- Li, X., Zhou, W., Ouyang, Z., 2013. Relationship between land surface temperature and spatial pattern of greenspace: What are the effects of spatial resolution?

 Landscape and Urban Planning 114, 1–8.

 https://doi.org/10.1016/j.landurbplan.2013.02.005
- Li, X., Zhou, W., Ouyang, Z., Xu, W., Zheng, H., 2012. Spatial pattern of greenspace affects land surface temperature: evidence from the heavily urbanized Beijing metropolitan area, China. Landscape ecology 27, 887–898.
- Li, X., Zhou, Y., 2017. Urban mapping using DMSP/OLS stable night-time light: a review. International Journal of Remote Sensing 38, 6030–6046. https://doi.org/10.1080/01431161.2016.1274451
- Li, X., Gong, P., Zhou, Y., Wang, J., Bai, Y., Chen, B., Hu, T., Xiao, Y., Xu, B., Yang,

- J., Liu, X., Cai, W., Huang, H., Wu, T., Wang, X., Lin, P., Li, Xun, Chen, J., He, C., Li, Xia, Yu, L., Clinton, N., Zhu, Z., 2020. Mapping global urban boundaries from the global artificial impervious area (GAIA) data. Environ. Res. Lett. 15, 094044. https://doi.org/10.1088/1748-9326/ab9be3
- Li, Yilun, Ouyang, W., Yin, S., Tan, Z., Ren, C., 2023. Microclimate and its influencing factors in residential public spaces during heat waves: An empirical study in Hong Kong. Building and Environment 236, 110225. https://doi.org/10.1016/j.buildenv.2023.110225
- Li, Y., Schubert, S., Kropp, J.P., Rybski, D., 2020. On the influence of density and morphology on the Urban Heat Island intensity. Nat Commun 11, 2647. https://doi.org/10.1038/s41467-020-16461-9
- Li, Yizhen, Zhang, X., Xia, C., 2023. Towards a greening city: How does regional cooperation promote urban green space in the Guangdong-Hong Kong-Macau Greater Bay Area? Urban Forestry & Urban Greening 86, 128033. https://doi.org/10.1016/j.ufug.2023.128033
- Li, Z., Hu, D., 2022. Exploring the relationship between the 2D/3D architectural morphology and urban land surface temperature based on a boosted regression tree: A case study of Beijing, China. Sustainable Cities and Society 78, 103392. https://doi.org/10.1016/j.scs.2021.103392
- Li, Z., Sun, F., Wang, H., Wang, T., Feng, Y., 2024. Detecting the interactions between

- vegetation greenness and drought globally. Atmospheric Research 304, 107409. https://doi.org/10.1016/j.atmosres.2024.107409
- Liao, W., Hong, T., Heo, Y., 2021. The effect of spatial heterogeneity in urban morphology on surface urban heat islands. Energy and Buildings 244, 111027.
- Lin, J., Qiu, S., Tan, X., Zhuang, Y., 2023. Measuring the relationship between morphological spatial pattern of green space and urban heat island using machine learning methods. Building and Environment 228, 109910. https://doi.org/10.1016/j.buildenv.2022.109910
- Liu, L., Zhang, Y., 2011. Urban Heat Island Analysis Using the Landsat TM Data and ASTER Data: A Case Study in Hong Kong. Remote Sensing 3, 1535–1552. https://doi.org/10.3390/rs3071535
- Liu, M., Hu, Y.-M., Li, C.-L., 2017. Landscape metrics for three-dimensional urban building pattern recognition. Applied Geography 87, 66–72.
- Liu, Z., Anderson, B., Yan, K., Dong, W., Liao, H., Shi, P., 2017. Global and regional changes in exposure to extreme heat and the relative contributions of climate and population change. Sci Rep 7, 43909. https://doi.org/10.1038/srep43909
- Liu, Z., Zhou, Y., Feng, Z., 2023. Response of vegetation phenology to urbanization in urban agglomeration areas: A dynamic urban–rural gradient perspective.
 Science of The Total Environment 864, 161109.
 https://doi.org/10.1016/j.scitotenv.2022.161109

- Logan, T.M., Zaitchik, B., Guikema, S., Nisbet, A., 2020. Night and day: The influence and relative importance of urban characteristics on remotely sensed land surface temperature. Remote Sensing of Environment 247, 111861. https://doi.org/10.1016/j.rse.2020.111861
- Luo, Y., Sun, W., Yang, K., Zhao, L., 2021. China urbanization process induced vegetation degradation and improvement in recent 20 years. Cities 114, 103207. https://doi.org/10.1016/j.cities.2021.103207
- Luyssaert, S., Jammet, M., Stoy, P.C., Estel, S., Pongratz, J., Ceschia, E., Churkina, G., Don, A., Erb, K., Ferlicoq, M., 2014. Land management and land-cover change have impacts of similar magnitude on surface temperature. Nature Climate Change 4, 389–393.
- Mahtta, R., Mahendra, A., Seto, K.C., 2019. Building up or spreading out? Typologies of urban growth across 478 cities of 1 million+. Environ. Res. Lett. 14, 124077. https://doi.org/10.1088/1748-9326/ab59bf
- Maimaitiyiming, M., Ghulam, A., Tiyip, T., Pla, F., Latorre-Carmona, P., Halik, Ü., Sawut, M., Caetano, M., 2014. Effects of green space spatial pattern on land surface temperature: Implications for sustainable urban planning and climate change adaptation. ISPRS Journal of Photogrammetry and Remote Sensing 89, 59–66. https://doi.org/10.1016/j.isprsjprs.2013.12.010
- Masoudi, M., Tan, P.Y., 2019. Multi-year comparison of the effects of spatial pattern

- of urban green spaces on urban land surface temperature. Landscape and Urban Planning 184, 44–58. https://doi.org/10.1016/j.landurbplan.2018.10.023
- Masoudi, M., Tan, P.Y., Fadaei, M., 2021. The effects of land use on spatial pattern of urban green spaces and their cooling ability. Urban Climate 35, 100743.
- Masoudi, M., Tan, P.Y., Liew, S.C., 2019. Multi-city comparison of the relationships between spatial pattern and cooling effect of urban green spaces in four major Asian cities. Ecological Indicators 98, 200–213. https://doi.org/10.1016/j.ecolind.2018.09.058
- Masselot, P., Mistry, M.N., Rao, S., Huber, V., Monteiro, A., Samoli, E., Stafoggia,
 M., de'Donato, F., Garcia-Leon, D., Ciscar, J.-C., Feyen, L., Schneider, A.,
 Katsouyanni, K., Vicedo-Cabrera, A.M., Aunan, K., Gasparrini, A., 2025.
 Estimating future heat-related and cold-related mortality under climate
 change, demographic and adaptation scenarios in 854 European cities. Nature
 Medicine. https://doi.org/10.1038/s41591-024-03452-2
- Nahlik, M.J., Chester, M.V., Pincetl, S.S., Eisenman, D., Sivaraman, D., English, P., 2017. Building Thermal Performance, Extreme Heat, and Climate Change. Journal of Infrastructure Systems 23, 04016043.
 https://doi.org/10.1061/(ASCE)IS.1943-555X.0000349
- Nemani, R.R., Keeling, C.D., Hashimoto, H., Jolly, W.M., Piper, S.C., Tucker, C.J., Myneni, R.B., Running, S.W., 2003. Climate-driven increases in global

- terrestrial net primary production from 1982 to 1999. science 300, 1560–1563.
- Ng, E., Chen, L., Wang, Y., Yuan, C., 2012. A study on the cooling effects of greening in a high-density city: An experience from Hong Kong. Building and Environment 47, 256–271. https://doi.org/10.1016/j.buildenv.2011.07.014
- Nichol, J.E., Fung, W.Y., Lam, K., Wong, M.S., 2009. Urban heat island diagnosis using ASTER satellite images and 'in situ' air temperature. Atmospheric Research 94, 276–284. https://doi.org/10.1016/j.atmosres.2009.06.011
- Nor, A.N.M., Corstanje, R., Harris, J.A., Brewer, T., 2017. Impact of rapid urban expansion on green space structure. Ecological Indicators 81, 274–284. https://doi.org/10.1016/j.ecolind.2017.05.031
- Oke, T.R., 1982. The energetic basis of the urban heat island. Quarterly journal of the royal meteorological society 108, 1–24.
- Oliveira, S., Andrade, H., Vaz, T., 2011. The cooling effect of green spaces as a contribution to the mitigation of urban heat: A case study in Lisbon. Building and environment 46, 2186–2194.
- Ouyang, W., Ren, G., Tan, Z., Li, Y., Ren, C., 2024. Natural shading vs. artificial shading: A comparative analysis of their cooling efficacy in extreme hot weather. Urban Climate 55, 101870.

 https://doi.org/10.1016/j.uclim.2024.101870
- Ouyang, Z., Sciusco, P., Jiao, T., Feron, S., Lei, C., Li, F., John, R., Fan, P., Li, X.,

- Williams, C.A., 2022. Albedo changes caused by future urbanization contribute to global warming. Nature communications 13, 3800.
- Pearson, K., 1908. On a mathematical theory of determinantal inheritance, from suggestions and notes of the late WFR Weldon. Biometrika 6, 80–93.
- Peng, F., Wong, M.S., Ho, H.C., Nichol, J., Chan, P.W., 2017. Reconstruction of historical datasets for analyzing spatiotemporal influence of built environment on urban microclimates across a compact city. Building and Environment 123, 649–660. https://doi.org/10.1016/j.buildenv.2017.07.038
- Peng, W., Yuan, X., Gao, W., Wang, R., Chen, W., 2021. Assessment of urban cooling effect based on downscaled land surface temperature: A case study for Fukuoka, Japan. Urban Climate 36, 100790.

 https://doi.org/10.1016/j.uclim.2021.100790
- Pouteau, R., Rambal, S., Ratte, J.-P., Gogé, F., Joffre, R., Winkel, T., 2011.

 Downscaling MODIS-derived maps using GIS and boosted regression trees:

 The case of frost occurrence over the arid Andean highlands of Bolivia.

 Remote Sensing of Environment 115, 117–129.

 https://doi.org/10.1016/j.rse.2010.08.011
- Qiao, Z., Han, X., Wu, C., Liu, L., Xu, X., Sun, Z., Sun, W., Cao, Q., Li, L., 2020.

 Scale effects of the relationships between 3D building morphology and urban heat island: A case study of provincial capital cities of mainland China.

- Complexity 2020, 9326793.
- Qin, Z., Karnieli, A., Berliner, P., 2001. A mono-window algorithm for retrieving land surface temperature from Landsat TM data and its application to the Israel-Egypt border region. International Journal of Remote Sensing 22, 3719–3746. https://doi.org/10.1080/01431160010006971
- Rawson, H.M., Begg, J.E., Woodward, R.G., 1977. The effect of atmospheric humidity on photosynthesis, transpiration and water use efficiency of leaves of several plant species. Planta 134, 5–10. https://doi.org/10.1007/BF00390086
- Reba, M., Seto, K.C., 2020. A systematic review and assessment of algorithms to detect, characterize, and monitor urban land change. Remote Sensing of Environment 242, 111739. https://doi.org/10.1016/j.rse.2020.111739
- Ren, C., Cai, M., Li, X., Shi, Y., See, L., 2020. Developing a rapid method for 3-dimensional urban morphology extraction using open-source data. Sustainable Cities and Society 53, 101962. https://doi.org/10.1016/j.scs.2019.101962
- Ren, Y., Deng, L.-Y., Zuo, S.-D., Song, X.-D., Liao, Y.-L., Xu, C.-D., Chen, Q., Hua, L.-Z., Li, Z.-W., 2016. Quantifying the influences of various ecological factors on land surface temperature of urban forests. Environmental Pollution 216, 519–529. https://doi.org/10.1016/j.envpol.2016.06.004
- Rhee, J., Park, S., Lu, Z., 2014. Relationship between land cover patterns and surface temperature in urban areas. GIScience & Remote Sensing 51, 521–536.

- Rogan, J., Wright, T.M., Cardille, J., Pearsall, H., Ogneva-Himmelberger, Y.,
 Riemann, R., Riitters, K., Partington, K., 2016. Forest fragmentation in

 Massachusetts, USA: a town-level assessment using Morphological spatial
 pattern analysis and affinity propagation. GIScience & Remote Sensing 53,
 506–519. https://doi.org/10.1080/15481603.2016.1141448
- Ru, J., Zhou, Y., Hui, D., Zheng, M., Wan, S., 2018. Shifts of growing-season precipitation peaks decrease soil respiration in a semiarid grassland. Global Change Biology 24, 1001–1011. https://doi.org/10.1111/gcb.13941
- Russo, S., Dosio, A., Graversen, R.G., Sillmann, J., Carrao, H., Dunbar, M.B., Singleton, A., Montagna, P., Barbola, P., Vogt, J.V., 2014. Magnitude of extreme heat waves in present climate and their projection in a warming world. Journal of Geophysical Research: Atmospheres 119, 12,500-12,512. https://doi.org/10.1002/2014JD022098
- Salvati, A., Monti, P., Roura, H.C., Cecere, C., 2019. Climatic performance of urban textures: Analysis tools for a Mediterranean urban context. Energy and Buildings 185, 162–179.
- Serbin, S.P., Singh, A., Desai, A.R., Dubois, S.G., Jablonski, A.D., Kingdon, C.C., Kruger, E.L., Townsend, P.A., 2015. Remotely estimating photosynthetic capacity, and its response to temperature, in vegetation canopies using imaging

- spectroscopy. Remote Sensing of Environment, Special Issue on the Hyperspectral Infrared Imager (HyspIRI) 167, 78–87. https://doi.org/10.1016/j.rse.2015.05.024
- Shahmohamadi, P., Che-Ani, A.I., Etessam, I., Maulud, K.N.A., Tawil, N.M., 2011.

 Healthy Environment: The Need to Mitigate Urban Heat Island Effects on

 Human Health. Procedia Engineering, 2nd International Building Control

 Conference 20, 61–70. https://doi.org/10.1016/j.proeng.2011.11.139
- Shahtahmassebi, A.R., Li, C., Fan, Y., Wu, Y., Gan, M., Wang, K., Malik, A., Blackburn, G.A., 2021. Remote sensing of urban green spaces: A review.

 Urban Forestry & Urban Greening 57, 126946.
- Shen, C., Hou, H., Zheng, Y., Murayama, Y., Wang, R., Hu, T., 2022. Prediction of the future urban heat island intensity and distribution based on landscape composition and configuration: A case study in Hangzhou. Sustainable Cities and Society 83, 103992. https://doi.org/10.1016/j.scs.2022.103992
- Shen, F., Yang, L., Zhang, L., Guo, M., Huang, H., Zhou, C., 2023. Quantifying the direct effects of long-term dynamic land use intensity on vegetation change and its interacted effects with economic development and climate change in jiangsu, China. Journal of Environmental Management 325, 116562.
- Shi, Y., Ren ,Chao, Zheng ,Yingsheng, and Ng, E., 2016. Mapping the urban microclimatic spatial distribution in a sub-tropical high-density urban

- environment. Architectural Science Review 59, 370–384. https://doi.org/10.1080/00038628.2015.1105195
- Siddique, S., Uddin, Md.M., 2022. Green space dynamics in response to rapid urbanization: Patterns, transformations and topographic influence in Chattogram city, Bangladesh. Land Use Policy 114, 105974. https://doi.org/10.1016/j.landusepol.2022.105974
- Šímová, P., Gdulová, K., 2012. Landscape indices behavior: A review of scale effects.

 Applied Geography 34, 385–394.

 https://doi.org/10.1016/j.apgeog.2012.01.003
- Sobrino, J.A., Jiménez-Muñoz, J.C., Paolini, L., 2004. Land surface temperature retrieval from LANDSAT TM 5. Remote Sensing of Environment 90, 434–440. https://doi.org/10.1016/j.rse.2004.02.003
- Song, J., Chen, W., Zhang, J., Huang, K., Hou, B., Prishchepov, A.V., 2020. Effects of building density on land surface temperature in China: Spatial patterns and determinants. Landscape and Urban Planning 198, 103794.
- Streule, M., Karaman, O., Sawyer, L., Schmid, C., 2020. Popular Urbanization:

 Conceptualizing Urbanization Processes Beyond Informality. International

 Journal of Urban and Regional Research 44, 652–672.

 https://doi.org/10.1111/1468-2427.12872
- Taleghani, M., 2018. Outdoor thermal comfort by different heat mitigation strategies-

- A review. Renewable and Sustainable Energy Reviews 81, 2011–2018. https://doi.org/10.1016/j.rser.2017.06.010
- Tan, K.W., 2006. A greenway network for singapore. Landscape and Urban Planning 76, 45–66. https://doi.org/10.1016/j.landurbplan.2004.09.040
- Tan, P.Y., Ismail, M.R.B., 2015. The effects of urban forms on photosynthetically active radiation and urban greenery in a compact city. Urban Ecosyst 18, 937–961. https://doi.org/10.1007/s11252-015-0461-9
- Tan, P.Y., Wang, J., Sia, A., 2013. Perspectives on five decades of the urban greening of Singapore. Cities 32, 24–32. https://doi.org/10.1016/j.cities.2013.02.001
- Tan, Z., Lau, K.K.-L., Ng, E., 2017. Planning strategies for roadside tree planting and outdoor comfort enhancement in subtropical high-density urban areas.Building and Environment 120, 93–109.
- Tan, Z., Lau, K.K.-L., Ng, E., 2016. Urban tree design approaches for mitigating daytime urban heat island effects in a high-density urban environment. Energy and Buildings 114, 265–274. https://doi.org/10.1016/j.enbuild.2015.06.031
- The Hong Kong Observatory, 2016. The Hong Kong Observatory.
- Tian, L., Chen, J., Yu, S., 2013. How has Shenzhen been heated up during the rapid urban build-up process? Landscape and Urban Planning 115, 18–29. https://doi.org/10.1016/j.landurbplan.2013.03.009
- Tian, Y., Tsendbazar, N.-E., Van Leeuwen, E., Fensholt, R., Herold, M., 2022. A

- global analysis of multifaceted urbanization patterns using Earth Observation data from 1975 to 2015. Landscape and Urban Planning 219, 104316. https://doi.org/10.1016/j.landurbplan.2021.104316
- Tian, Y., Zhou, W., Qian, Y., Zheng, Z., Yan, J., 2019. The effect of urban 2D and 3D morphology on air temperature in residential neighborhoods. Landscape Ecol 34, 1161–1178. https://doi.org/10.1007/s10980-019-00834-7
- Tian Yuhong, Jim C. Y., Tao Yan, 2012. Challenges and Strategies for Greening the Compact City of Hong Kong. Journal of Urban Planning and Development 138, 101–109. https://doi.org/10.1061/(ASCE)UP.1943-5444.0000076
- Tuholske, C., Caylor, K., Funk, C., Verdin, A., Sweeney, S., Grace, K., Peterson, P.,
 Evans, T., 2021. Global urban population exposure to extreme heat. Proc. Natl.
 Acad. Sci. U.S.A. 118, e2024792118.
 https://doi.org/10.1073/pnas.2024792118
- Turner, M.G., O'Neill, R.V., Gardner, R.H., Milne, B.T., 1989. Effects of changing spatial scale on the analysis of landscape pattern. Landscape Ecol 3, 153–162. https://doi.org/10.1007/BF00131534
- Ukkola, A.M., Prentice, I.C., Keenan, T.F., Van Dijk, A.I., Viney, N.R., Myneni, R.B., Bi, J., 2016. Reduced streamflow in water-stressed climates consistent with CO2 effects on vegetation. Nature Climate Change 6, 75–78.
- Wan, C., Shen, G.Q., 2015. Salient attributes of urban green spaces in high density

- cities: The case of Hong Kong. Habitat International 49, 92-99.
- Wang, C., Wang, Z.-H., Kaloush, K.E., Shacat, J., 2021. Cool pavements for urban heat island mitigation: A synthetic review. Renewable and Sustainable Energy Reviews 146, 111171.
- Wang, D., Lau, K.K.-L., Ruby, H., Wong, S.Y., Kwok, T.C., Woo, J., 2016.

 Neighbouring green space and all-cause mortality in elderly people in Hong

 Kong: a retrospective cohort study. The Lancet 388, S82.
- Wang, P., Gu, C., Yang, H., Wang, H., 2022. The multi-scale structural complexity of urban morphology in China. Chaos, Solitons & Fractals 164, 112721. https://doi.org/10.1016/j.chaos.2022.112721
- Wang, Q., Peng, L.L.H., Jiang, W., Yin, S., Feng, N., Yao, L., 2024. Urban form affects the cool island effect of urban greenery via building shadows. Building and Environment 254, 111398. https://doi.org/10.1016/j.buildenv.2024.111398
- Wang, R., Gamon, J.A., Emmerton, C.A., Springer, K.R., Yu, R., Hmimina, G., 2020.Detecting intra-and inter-annual variability in gross primary productivity of aNorth American grassland using MODIS MAIAC data. Agricultural andForest Meteorology 281, 107859.
- Wang, W., Zhou, W., Ng, E.Y.Y., Xu, Y., 2016. Urban heat islands in Hong Kong: statistical modeling and trend detection. Natural Hazards 83, 885–907. https://doi.org/10.1007/s11069-016-2353-6

- Wang, X., Li, B., Liu, Y., Yang, Y., Fu, X., Shen, R., Xu, W., Yao, L., 2024. Trends and attributions of the long-term thermal comfort across the urban–rural gradient in major Chinese cities. Applied Geography 164, 103221. https://doi.org/10.1016/j.apgeog.2024.103221
- Wang, Y., Berardi, U., Akbari, H., 2016. Comparing the effects of urban heat island mitigation strategies for Toronto, Canada. Energy and buildings 114, 2–19.
- Wang, Z., Zhou, R., Rui, J., Yu, Y., 2025a. Revealing the impact of urban spatial morphology on land surface temperature in plain and plateau cities using explainable machine learning. Sustainable Cities and Society 118, 106046.
- Wang, Z., Zhou, R., Yu, Y., 2025b. The impact of urban morphology on land surface temperature under seasonal and diurnal variations: marginal and interaction effects. Building and Environment 112673.
- Wong, L.P., Alias, H., Aghamohammadi, N., Aghazadeh, S., Nik Sulaiman, N.M., 2017. Urban heat island experience, control measures and health impact: A survey among working community in the city of Kuala Lumpur. Sustainable Cities and Society 35, 660–668. https://doi.org/10.1016/j.scs.2017.09.026
- Wong, N.H., Yu, C., 2005. Study of green areas and urban heat island in a tropical city. Habitat International 29, 547–558.

 https://doi.org/10.1016/j.habitatint.2004.04.008
- Wright, S., 1934. The method of path coefficients. The annals of mathematical

- statistics 5, 161–215.
- Wu, B., Huang ,Hailan, and Wang, Y., 2024. Quantifying spatial patterns of urban building morphology in the China's Guangdong-Hong Kong-Marco greater bay area. International Journal of Digital Earth 17, 2392832. https://doi.org/10.1080/17538947.2024.2392832
- Wu, J., 2004. Effects of changing scale on landscape pattern analysis: scaling relations. Landscape ecology 19, 125–138.
- Wu, Q., Tan, J., Guo, F., Li, H., Chen, S., 2019. Multi-Scale Relationship between
 Land Surface Temperature and Landscape Pattern Based on Wavelet
 Coherence: The Case of Metropolitan Beijing, China. Remote Sensing 11.
 https://doi.org/10.3390/rs11243021
- Wu, S., Chen, B., An, J., Lin, C., Gong, P., 2024. The interplay of cloud cover and 3D urban structures reduces human access to sunlight. Nature Cities 1, 686–694. https://doi.org/10.1038/s44284-024-00120-x
- Wu, W.-B., Ma, J., Meadows, M.E., Banzhaf, E., Huang, T.-Y., Liu, Y.-F., Zhao, B.,
 2021. Spatio-temporal changes in urban green space in 107 Chinese cities
 (1990–2019): The role of economic drivers and policy. International Journal of
 Applied Earth Observation and Geoinformation 103, 102525.
 https://doi.org/10.1016/j.jag.2021.102525
- Wu, W.-B., Yu, Z.-W., Ma, J., Zhao, B., 2022. Quantifying the influence of 2D and 3D

- urban morphology on the thermal environment across climatic zones.

 Landscape and Urban Planning 226, 104499.

 https://doi.org/10.1016/j.landurbplan.2022.104499
- Wu, Y., Che, Y., Liao, W., Liu, X., 2025. The impact of urban morphology on land surface temperature across urban-rural gradients in the Pearl River Delta,

 China. Building and Environment 267, 112215.
- Wu, Z., Chen, R., Meadows, M.E., Sengupta, D., Xu, D., 2019. Changing urban green spaces in Shanghai: trends, drivers and policy implications. Land Use Policy 87, 104080. https://doi.org/10.1016/j.landusepol.2019.104080
- Xiao, R., Cao, W., Liu, Y., Lu, B., 2022. The impacts of landscape patterns spatiotemporal changes on land surface temperature from a multi-scale perspective: A case study of the Yangtze River Delta. Science of The Total Environment 821, 153381.
- Xu, C., Chen, G., Huang, Q., Su, M., Rong, Q., Yue, W., Haase, D., 2022. Can improving the spatial equity of urban green space mitigate the effect of urban heat islands? An empirical study. Science of The Total Environment 841, 156687. https://doi.org/10.1016/j.scitotenv.2022.156687
- Xu, F., Chi, G., 2019. Spatiotemporal variations of land use intensity and its driving forces in China, 2000–2010. Reg Environ Change 19, 2583–2596. https://doi.org/10.1007/s10113-019-01574-9

- Xu, J., Jin, Y., Ling, Y., Sun, Y., Wang, Y., 2025. Exploring the seasonal impacts of morphological spatial pattern of green spaces on the urban heat island.Sustainable Cities and Society 106352.
- Xu, Y., Ren, C., Ma, P., Ho, J., Wang, W., Lau, K.K.-L., Lin, H., Ng, E., 2017. Urban morphology detection and computation for urban climate research. Landscape and urban planning 167, 212–224.
- Xu, Y., Yang, J., Zheng, Y., Li, W., 2024. Impacts of two-dimensional and three-dimensional urban morphology on urban thermal environments in high-density cities: A case study of Hong Kong. Building and Environment 252, 111249. https://doi.org/10.1016/j.buildenv.2024.111249
- Yang, C., Kui, T., Zhou, W., Fan, J., Pan, L., Wu, W., Liu, M., 2023. Impact of refined 2D/3D urban morphology on hourly air temperature across different spatial scales in a snow climate city. Urban Climate 47, 101404.
- Yang, C., Zhao, S., 2022. Urban vertical profiles of three most urbanized Chinese cities and the spatial coupling with horizontal urban expansion. Land Use Policy 113, 105919. https://doi.org/10.1016/j.landusepol.2021.105919
- Yang, J., Huang, X., 2021. The 30 m annual land cover dataset and its dynamics in China from 1990 to 2019. Earth Syst. Sci. Data 13, 3907–3925. https://doi.org/10.5194/essd-13-3907-2021
- Yang, J., Sun, J., Ge, Q., Li, X., 2017. Assessing the impacts of urbanization-

- associated green space on urban land surface temperature: A case study of Dalian, China. Urban Forestry & Urban Greening 22, 1–10. https://doi.org/10.1016/j.ufug.2017.01.002
- Yang, J., Yang, Y., Sun, D., Jin, C., Xiao, X., 2021. Influence of urban morphological characteristics on thermal environment. Sustainable Cities and Society 72, 103045. https://doi.org/10.1016/j.scs.2021.103045
- Yang, J., Zhan, Y., Xiao, X., Xia, J.C., Sun, W., Li, X., 2020. Investigating the diversity of land surface temperature characteristics in different scale cities based on local climate zones. Urban Climate 34, 100700.
- Yao, L., 2024. Assessment of long time-series greening signatures across the urban–rural gradient in Chinese cities. Ecological Indicators 160, 111826.
- Yao, L., Li, T., Xu, M., Xu, Y., 2020. How the landscape features of urban green space impact seasonal land surface temperatures at a city-block-scale: An urban heat island study in Beijing, China. Urban Forestry & Urban Greening 52, 126704.
- Yee, M., Kaplan, J.O., 2022. Drivers of urban heat in Hong Kong over the past 116 years. Urban Climate 46, 101308. https://doi.org/10.1016/j.uclim.2022.101308
- Yin, C., Yuan, M., Lu, Y., Huang, Y., Liu, Y., 2018. Effects of urban form on the urban heat island effect based on spatial regression model. Science of the Total Environment 634, 696–704.

- Yu, X., Liu, Y., Zhang, Z., Xiao, R., 2021. Influences of buildings on urban heat island based on 3D landscape metrics: an investigation of China's 30 megacities at micro grid-cell scale and macro city scale. Landscape Ecol 36, 2743–2762. https://doi.org/10.1007/s10980-021-01275-x
- Yuan, B., Zhou, L., Dang, X., Sun, D., Hu, F., Mu, H., 2021. Separate and combined effects of 3D building features and urban green space on land surface temperature. Journal of Environmental Management 295, 113116.
- Yuan, B., Zhou, L., Hu, F., Wei, C., 2024. Effects of 2D/3D urban morphology on land surface temperature: Contribution, response, and interaction. Urban Climate 53, 101791. https://doi.org/10.1016/j.uclim.2023.101791
- Yuan, C., Adelia, A.S., Mei, S., He, W., Li, X.-X., Norford, L., 2020. Mitigating intensity of urban heat island by better understanding on urban morphology and anthropogenic heat dispersion. Building and Environment 176, 106876.
- Yuan, W., Liu, S., Zhou, Guangsheng, Zhou, Guoyi, Tieszen, L.L., Baldocchi, D., Bernhofer, C., Gholz, H., Goldstein, A.H., Goulden, M.L., 2007. Deriving a light use efficiency model from eddy covariance flux data for predicting daily gross primary production across biomes. Agricultural and Forest Meteorology 143, 189–207.
- Yue, W., Liu, X., Zhou, Y., Liu, Y., 2019. Impacts of urban configuration on urban heat island: An empirical study in China mega-cities. Science of The Total

- Environment 671, 1036–1046. https://doi.org/10.1016/j.scitotenv.2019.03.421
- Zahid Iqbal, Q.M., Chan, A.L.S., 2016. Pedestrian level wind environment assessment around group of high-rise cross-shaped buildings: Effect of building shape, separation and orientation. Building and Environment 101, 45–63. https://doi.org/10.1016/j.buildenv.2016.02.015
- Zeng, P., Sun, F., Liu, Y., Tian, T., Wu, J., Dong, Q., Peng, S., Che, Y., 2022. The influence of the landscape pattern on the urban land surface temperature varies with the ratio of land components: Insights from 2D/3D building/vegetation metrics. Sustainable Cities and Society 78, 103599.
- Zeng, Z., Piao, S., Li, L.Z., Zhou, L., Ciais, P., Wang, T., Li, Y., Lian, X.U., Wood,
 E.F., Friedlingstein, P., 2017. Climate mitigation from vegetation biophysical
 feedbacks during the past three decades. Nature Climate Change 7, 432–436.
- Zhang, J., Li, Z., Wei, Y., Hu, D., 2022. The impact of the building morphology on microclimate and thermal comfort-a case study in Beijing. Building and Environment 223, 109469.
- Zhang, L., Yang, L., Zohner, C.M., Crowther, T.W., Li, M., Shen, F., Guo, M., Qin, J., Yao, L., Zhou, C., 2022. Direct and indirect impacts of urbanization on vegetation growth across the world's cities. Sci. Adv. 8, eabo0095.
 https://doi.org/10.1126/sciadv.abo0095
- Zhang, L., Yuan, C., 2023. Multi-scale climate-sensitive planning framework to

- mitigate urban heat island effect: A case study in Singapore. Urban Climate 49, 101451. https://doi.org/10.1016/j.uclim.2023.101451
- Zhang, Q., Zhou, D., Xu, D., Rogora, A., 2022. Correlation between cooling effect of green space and surrounding urban spatial form: Evidence from 36 urban green spaces. Building and Environment 222, 109375.
 https://doi.org/10.1016/j.buildenv.2022.109375
- Zhang, S., Jia, W., Zhu, H., You, Y., Zhao, C., Gu, X., Liu, M., 2023. Vegetation growth enhancement modulated by urban development status. Science of The Total Environment 883, 163626.

 https://doi.org/10.1016/j.scitotenv.2023.163626
- Zhang, Z., Luan, W., Yang, J., Guo, A., Su, M., Tian, C., 2023. The influences of 2D/3D urban morphology on land surface temperature at the block scale in Chinese megacities. Urban Climate 49, 101553. https://doi.org/10.1016/j.uclim.2023.101553
- Zhao, J., Chen, S., Jiang, B., Ren, Y., Wang, H., Vause, J., Yu, H., 2013. Temporal trend of green space coverage in China and its relationship with urbanization over the last two decades. Science of The Total Environment 442, 455–465. https://doi.org/10.1016/j.scitotenv.2012.10.014
- Zhao, S., Liu, S., Zhou, D., 2016. Prevalent vegetation growth enhancement in urban environment. Proc. Natl. Acad. Sci. U.S.A. 113, 6313–6318.

- https://doi.org/10.1073/pnas.1602312113
- Zheng, Y., Ren, C., Shi, Y., Yim, S.H.L., Lai, D.Y.F., Xu, Y., Fang, C., Li, W., 2023.
 Mapping the spatial distribution of nocturnal urban heat island based on Local
 Climate Zone framework. Building and Environment 234, 110197.
 https://doi.org/10.1016/j.buildenv.2023.110197
- Zheng, Y., Ren, C., Xu, Y., Wang, R., Ho, J., Lau, K., Ng, E., 2018. GIS-based mapping of Local Climate Zone in the high-density city of Hong Kong. Urban Climate 24, 419–448. https://doi.org/10.1016/j.uclim.2017.05.008
- Zhou, B., Rybski, D., Kropp, J.P., 2017. The role of city size and urban form in the surface urban heat island. Scientific reports 7, 4791.
- Zhou, D., Zhang, L., Hao, L., Sun, G., Xiao, J., Li, X., 2023. Large discrepancies among remote sensing indices for characterizing vegetation growth dynamics in Nepal. Agricultural and Forest Meteorology 339, 109546.
- Zhou, L., Gong, Y., López-Carr, D., Huang, C., 2024. A critical role of the capital green belt in constraining urban sprawl and its fragmentation measurement.

 Land Use Policy 141, 107148.

 https://doi.org/10.1016/j.landusepol.2024.107148
- Zhou, L., Hu, F., Wang, B., Wei, C., Sun, D., Wang, S., 2022a. Relationship between urban landscape structure and land surface temperature: Spatial hierarchy and interaction effects. Sustainable Cities and Society 80, 103795.

- https://doi.org/10.1016/j.scs.2022.103795
- Zhou, L., Yuan, B., Hu, F., Wei, C., Dang, X., Sun, D., 2022b. Understanding the effects of 2D/3D urban morphology on land surface temperature based on local climate zones. Building and Environment 208, 108578.
- Zhou, W., Huang, G., Cadenasso, M.L., 2011. Does spatial configuration matter?

 Understanding the effects of land cover pattern on land surface temperature in urban landscapes. Landscape and urban planning 102, 54–63.
- Zhou, W., Wang, J., Cadenasso, M.L., 2017. Effects of the spatial configuration of trees on urban heat mitigation: A comparative study. Remote Sensing of Environment 195, 1–12. https://doi.org/10.1016/j.rse.2017.03.043
- Zhou, W., Yu, W., Yao, Y., Jing, C., 2023. Understanding the indirect impacts of urbanization on vegetation growth using the Continuum of Urbanity framework. Science of The Total Environment 899, 165693.
- Zhou, X., Wang, Y.-C., 2011. Spatial–temporal dynamics of urban green space in response to rapid urbanization and greening policies. Landscape and Urban Planning 100, 268–277. https://doi.org/10.1016/j.landurbplan.2010.12.013